REMARKS/ARGUMENTS

Entry of the amendment and reconsideration of the present application is respectfully requested. Claims 1, and 5 are pending, and under examination. No new matter has been added.

Rejections under 35 U.S.C. §112, 1st Paragraph – Enablement:

Claims 1 and 5 were rejected under 35 U.S.C. §112, 1st paragraph for lack of enablement.

The Action asserts that the specification fails to teach how to use the isolated polypeptide of SEQ ID NO: 4 in a plant or the agronomic benefit of the isolated polypeptide, and further that the specification does not provide guidance regarding any use of the isolated polypeptide of SEQ ID NO: 4 and polypeptides having at least 95% sequence identity thereto.

Applicant respectfully disagrees. As noted in the Action, modulating RuvB expression levels provides the means to modulate the efficiency with which nucleic acids of interest are incorporated into the genomes of a target plant cell (page 3, lines 20-22).

Further guidance for the use of the polypeptide of SEQ ID NO: 4 and polypeptides having at least 95% sequence identity thereto is found, for example, on page 24, lines 12-19:

> "In particular, the polynucleotides and *polypeptides* of the present invention *can be expressed temporally or spatially, e.g., at developmental stages, in tissues, and/or in quantities, which are uncharacteristic of non-recombinantly engineered plants*. Thus the present invention provides utility in such exemplary applications as in the control of homologous recombination efficiency or transformation efficiency in plants." [emphasis added]

On page 25, lines 10 – 13:

> The proteins of the present invention can be employed in assays for enzyme agonists or antagonists of enzyme function, or for use as immunogens or

antigens to obtain *antibodies specifically immunoreactive with a protein of the present invention*. Such antibodies can be used in *assays for expression levels...*" [emphasis added]

Therefore, the specification has provided guidance on the use of the polypeptide of SEQ ID NO: 4 and polypeptides having 95% sequence identity thereto, for example the use of the polypeptides to modulate homologous recombination and/or transformation efficiency in plants. As defined on page 10, lines 16-23, the term "isolated" encompasses materials (*e.g.*, polypeptides) which have been altered by deliberate human intervention to a composition and/or placed at a location in the cell not native to a material found in that environment.

The specification also provides guidance on the use of the polypeptide of SEQ ID NO: 4 and polypeptides having 95% sequence identity thereto to create antibodies *specifically immunoreactive* to SEQ ID NO: 4 or polypeptides having 95% sequence identity thereto. Contrary to the assertion of the Action, not just any protein can be used as an immunogen for the purpose of generating antibodies specifically immunoreactive to the polypeptides of the invention; therefore, this use does have a specific biological activity.

Applicant provides Appendix A, comprising information RuvB activity and the function of homologous recombination in plants. Appendix A provides information on homologous recombination and RuvB in plants. RuvB homologues have been identified in *Arabidopsis thaliana*, At5g22330 and At5g67630. The three-dimensional crystal structure of RuvB from bacteria has been solved, (Putnam *et al.*, 2001 JMB 311:297-310), further characterizing the function of domains, such as the Walker boxes. Qui *et al.* (1998 JBC 273:27786-27793) reported the identification of a human homologue of RuvB, noting in the 2nd paragraph of page 27786, that the extensive presence of bacterial RecA (involved in the same process as RuvB & RuvC) homologues across many eukaryotes suggests that "the machinery involved in recombination is highly conserved among all organisms from bacteria to man". Pang *et al.* (1993 Nucl. Acids Res. 21:1647-1653) showed that two cDNAs from *A.*

thaliana could complement *E. coli* ruvC mutants. Shalev *et al.* (1999 PNAS 96:7398-7402) showed stimulation of homologous recombination in plants transformed with bacterial RuvC, suggesting that the other homologous recombination components are not only present, but capable of interacting with the bacterial homologues.

Therefore, it is respectfully submitted that sufficient guidance is presented in the specification and claims as originally filed to enable one of skill in the art to make and use the polypeptides of SEQ ID NO: 4, and polypeptides having 95% sequence identity to SEQ ID NO:4. It is respectfully requested that the rejection of claims 1 and 5 under 35 U.S.C. §112, 1st paragraph for lack of enablement be withdrawn.

CONCLUSION

Applicant has fully responded to the Office Action issued January 26, 2005 and respectfully requests consideration of the response submitted herein. Applicant believes the response overcomes all of the rejections in the Action, such that the application is now in condition for allowance and hereby request early notification of the same. The Office is invited to call the Applicants' representative in order to expedite prosecution and allowance of the application.

Respectfully submitted,

Virginia Dress
Agent for Applicant(s)
Registration No. 48,243

PIONEER HI-BRED INTERNATIONAL, INC.
Corporate Intellectual Property
7100 N.W. 62nd Avenue
P.O. Box 1000
Johnston, Iowa 50131-1000
Phone: (515) 270-4192
Facsimile: (515) 334-6883

doi:10.1006/jmbi.2001.4852 available online at http://www.idealibrary.com on IDEAL J. Mol. Biol. (2001) 311, 297–310

JMB

Structure and Mechanism of the RuvB Holliday Junction Branch Migration Motor

Christopher D. Putnam[1], Sheila B. Clancy[1], Hiro Tsuruta[2] Susana Gonzalez[3], James G. Wetmur[3] and John A. Tainer[1]*

[1]*Department of Molecular Biology, Skaggs Institute for Chemical Biology, The Scripps Research Institute, MB 4 10550 North Torrey Pines Rd La Jolla, CA 92037, USA*

[2]*Stanford Synchrotron Radiation Laboratory/Stanford Linear Accelerator Center Stanford University, P.O. Box 4349, MS 69, Stanford CA 94309-0210, USA*

[3]*Department of Microbiology Box 1124, Mount Sinai School of Medicine, New York NY 10029-6574, USA*

**Corresponding author*

The RuvB hexamer is the chemomechanical motor of the RuvAB complex that migrates Holliday junction branch-points in DNA recombination and the rescue of stalled DNA replication forks. The 1.6 Å crystal structure of *Thermotoga maritima* RuvB together with five mutant structures reveal that RuvB is an ATPase-associated with diverse cellular activities (AAA+-class ATPase) with a winged-helix DNA-binding domain. The RuvB-ADP complex structure and mutagenesis suggest how AAA+-class ATPases couple nucleotide binding and hydrolysis to interdomain conformational changes and asymmetry within the RuvB hexamer implied by the crystallographic packing and small-angle X-ray scattering in solution. ATP-driven domain motion is positioned to move double-stranded DNA through the hexamer and drive conformational changes between subunits by altering the complementary hydrophilic protein-protein interfaces. Structural and biochemical analysis of five motifs in the protein suggest that ATP binding is a strained conformation recognized both by sensors and the Walker motifs and that intersubunit activation occurs by an arginine finger motif reminiscent of the GTPase-activating proteins. Taken together, these results provide insights into how RuvB functions as a motor for branch migration of Holliday junctions.

Keywords: AAA+-class ATPases; arginine finger; branch migration; Holliday junction; recombination

Introduction

Recombination is a general DNA repair pathway in eukaryotes and prokaryotes. Growing evidence suggests that one of the major functions of recombination is to restart replication forks that have been stalled due to DNA damage that may occur from 15% to 50% of the time, and may be more important in bacteria than the recombinational repair of double-stranded DNA (dsDNA) breaks.[1] The central, four-stranded recombination intermediate formed in both these repair processes is the Holliday junction, which can be generated by RecA and RecA homologs in dsDNA break repair[2] and in a RecA-independent fashion from replication forks.[3] Rapid migration of the Holliday junction in bacteria through heterologous DNA regions is performed by the RuvAB DNA translocase,[4–6] which is also implicated in the repair of stalled replication forks.[7]

The genes of the *ruv* locus operate late in recombination, and cells with mutations in these genes are sensitive to DNA damage, forming non-septate, multinucleate filaments that arise from covalently crosslinked chromosomes.[8] The RuvA protein forms symmetric tetramers and binds to one face of the Holliday junction.[9] The RuvB ATPase assembles into functional homohexameric rings and is the chemomechanical device that drives branch migration in the presence of RuvA.[10–11] The RuvC dimer resolves Holliday junctions by symmetrically nicking the Holliday junction at the crossover point. *In vivo* and *in vitro* data indicate that the RuvABC proteins function coordinately. RuvB, which has low affinity for Holliday junctions,[12–13]

Abbreviations used: dsDNA, double-stranded DNA; AAA, ATPases associated with diverse cellular activities; TIP49, TBP interaction protein of ~49 kDa; EM, electron microscopy; SAXS, small angle X-ray scattering; ss, single-stranded; PK, pyruvate kinase; LDH, lactate dehydrogenase.

E-mail address of the corresponding author: jat@scripps.edu

0022-2836/01/020297–14 $35.00/0

is targeted to opposite sides of the RuvA/Holliday junction complex through protein-protein interactions.[14] *In vivo*, RuvC functions only in the presence of RuvAB,[15] and can form a RuvABC/Holliday junction complex.[16] Thus, an RuvABC branch migration/resolution complex likely exists, similar to co-fractionating mammalian branch migration and resolution complexes.[17,18]

Structural studies of RuvB were undertaken to decipher the molecular basis for chemomechanical energy transduction and the mechanism of branch migration by the hexameric RuvB ATPases. Biochemical and structural studies of specific mutant RuvBs were pursued to probe specific mechanisms by which RuvB adopts different nucleotide-driven conformational changes. The RuvB structural results presented here provide insights into the structures of the archeal and eukaryotic TIP49 paralogs involved in chromatin remodeling and DNA repair.[19,20] Together, these results provide the framework for a detailed structural understanding of how RuvB converts chemical energy into the driving force behind branch migration of Holliday junctions formed during DNA recombination and DNA replication.

Results and Discussion

Structure of the RuvB subunit

Thermotoga maritima RuvB was crystallized in the space group $P6_5$ from active enzyme overexpressed in *Escherichia coli*,[21] and the structure of RuvB was determined to 1.6 Å resolution by multiple isomorphous replacement (Table 1). Electron density maps for the wild-type protein and the five active-site mutant structures were clear from Gln17 to Pro329, except for a disordered gap between Ile131 and Asp147. The RuvB subunit is made up of three sequential domains, which assemble into a fairly flat, triangular molecule ~25–35 Å thick and ~50 Å on each side (Figure 1(a)), and forms a helix with six subunits per turn through crystal packing. The N-terminal ATPase domain, domain I, represents about half of the protein and consists of a central five-stranded, all parallel β-sheet with the topology β5-β1-β4-β3-β2 that is surrounded by eight α-helices. The smaller, all-helical domain II (α9-11), and the mixed α-β C-terminal domain III (α13-17, β6-7), both pack against the C-terminal edges of the β-sheet of domain I. These three domains are linked by extended loops, which, although ordered in these crystal structures, could allow motion between the domains.

An ADP molecule binds at the interface of RuvB domains I and II (Figure 1(a)). The location of ADP within the RuvB structure immediately suggests that nucleotide binding states drive conformational changes between RuvB domains. Structural analysis and sequence conservation identify four motifs at the domain I-II boundary (Walker A, Walker B, sensor 1, and sensor 2) likely to be important in nucleotide-driven conformational changes of the

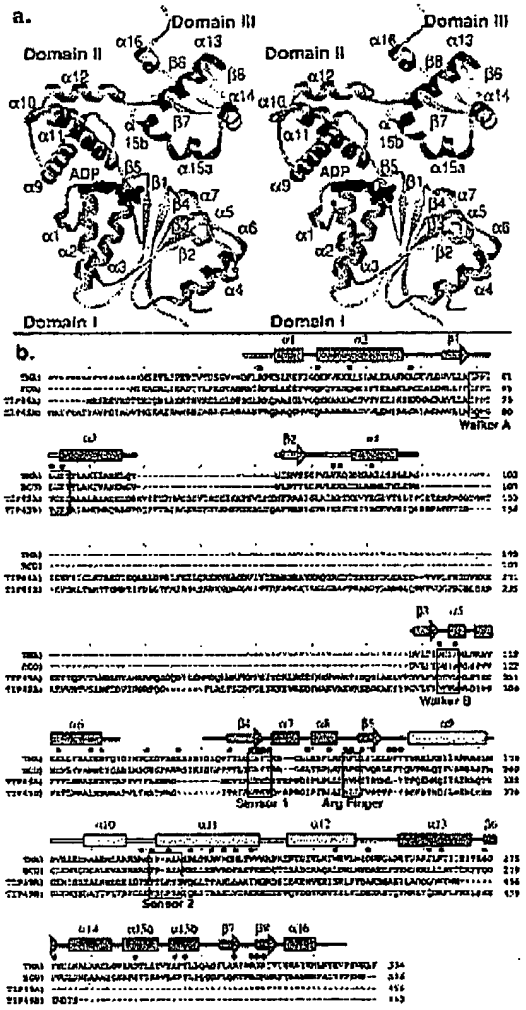

Figure 1. RuvB fold, domain assembly, functional motifs and ADP-binding position. (a) Each of the three RuvB structural domains is generated sequentially from the amino acid sequence, with an ADP molecule bound at the interface between the AAA+-class ATPase domains I (blue) and II (gold). The winged-helix domain III (green) is "masked" in these domain conformations, suggesting that DNA binding is induced only upon relative motion of the different domains. (b) Sequence alignment of *T. maritima* (TMA), *E. coli* (ECO) RuvB, *H. sapiens* TIP49a (TIP49A), and *H. sapiens* TIP49b (TIP49B) proteins displayed with the *T. maritima* secondary structure assignment. Gaps in the sequence are displayed as dashes. Red residues are absolutely conserved across an additional 15 different bacterial RuvB sequences. Red dots above the sequence represent strong and moderate dominant negative mutations isolated in the *E. coli* RuvB protein.[24] Sequence alignments were generated by the program SEQUOIA (CM Bruns, http://www.scripps.edu/~bruns/sequoia.html).

Table 1. *T. martima* RuvB crystallographic parameters and refinement statistics

Parameters	Native	Lys64Arg	Ala156Ser	Thr158Val	Arg170Ala	Pro216Gly		
Space group	$P6_5$	$P6_5$	$P6_5$	$P6_5$	$P6_5$	$P6_5$		
Beamline	SSRL 9-1	APS 14BMC	SSRL 9-1	ALS 5.0.2	SSRL 7-1	SSRL 7-1		
Wavelength (Å)	0.98	1.00	0.97	1.10	1.08	1.08		
Cell *a,b,c* (Å)	86.9, 86.9, 81.6	86.6, 86.6, 81.4	86.7, 86.7, 81.4	86.6, 86.6, 81.6	86.6, 86.6, 82.4	86.2, 86.2, 82.2		
Resolution (Å)	20-1.6/1.63-1.60	20-1.8/1.86-1.80	20-2.0/2.07-2.00	30-1.9/1.97-1.90	35-1.8/1.86-1.80	99-1.7/1.76-1.70		
Completeness (%)	99.0/99.0	89.5/79.8	99.1/91.4	99.2/97.6	97.4/83.5	98.1/94.6		
Reflections								
Observed	210,740	77,808	81,462	87,639	94,671	336,037		
Unique	43,763	29,025	23,654	26,948	31,816	37,484		
R_{sym} (%)[a]	7.1/46.0	5.8/36.6	7.7/41.0	3.6/12.6	5.7/49.0	4.4/33.2		
I/σ	29.4/3.1	23.6/2.7	18.4/3.4	23.6/8.2	17.1/1.5	27.0/2.6		
Mosaicity	0.7	1.4	0.4	0.3	0.2	0.4		
Refinement								
Resolution limits	20-1.6	20-1.8	20-2.0	20-1.9	20-1.9	20-1.7		
R_{cryst} (%)	23.4	23.4	21.6	22.6	21.6	22.0		
R_{free} (%)	25.3	26.6	25.0	24.9	25.0	25.6		
Parameters	$K_2Pt(CN)_4$	$K_2Pt(SCN)_4$	K_1AuBr_6	$AuCl_3$	K_2IrCl_6	K_2PtCl_6	K_2PtCl_4	SeMet
Concentration (mM)	1	1	1	1	1	1	0.1	-
Soaking time (hours)	4	1.5	21	2	24	6	2	-
Beamline	SSRL 9-1	SSRL 9-1	SSRL 9-1	SSRL 9-1	SSRL 9-1	SSRL 9-1	SSRL 9-1	SSRL 7-1
Wavelength (Å)	0.98	0.98	0.98	0.98	0.98	0.98	0.98	1.08
Resolution (Å)	3.8	2.0	2.9	3.2	2.1	2.0	2.3	1.95
Completeness (%)	99.6	100.0	95.7	99.1	99.5	100.0	99.4	98.2
Reflections								
Observed	201,526	181,430	22,701	24,777	83,921	313,379	47,868	62,398
Unique	32,506	23,865	7607	5773	20,532	23,775	15,438	25,243
R_{sym} (%)[a]	6.3	6.6	7.9	8.2	6.9	10.7	5.8	6.2
I/σ	33.4	34.6	16.4	25.9	25.1	37.1	22.0	16.2
Phasing[b]								
Number of sites	1	7	4	9	4	5	2	6
Resolution (Å)	2.5	2.5	2.5	3.2	2.5	2.5	2.5	2.5
R_{Cullis}								
Isomorphous	0.82	0.72	0.92	0.77	0.90	0.86	0.93	0.82
Anomalous	0.73	0.69	0.97	0.91	0.93	0.86	0.99	0.99
rms f/E_{lack}	1.12	1.57	0.72	1.39	0.75	0.95	0.65	1.11

[a] $R_{sym} = \Sigma_i|I_i - \langle I\rangle|\Sigma\langle I\rangle$ for all reflections (no σ cutoff).
[b] R_{Cullis}; rms f/E_{lack}, root-mean-square heavy atom F/isomorphous lack of closure error (phasing power).

protein structure (Figure 1(b)). The structures of domains I and II demonstrate that RuvB shares a common fold with the AAA+-super class of ATPases, named from an acronym of ATPases associated with diverse cellular activities.[22] The AAA+-class of ATPases includes chaperones, proteases, and nucleic acid processing enzymes, and has roles in vesicle fusion, vesicle formation, mitotic spindle formation and cytoskeletal integrity.

Domain III possesses the winged-helix DNA-binding fold, which is a modified form of the helix-turn-helix DNA-binding motif that is observed in many transcriptional regulators and in non-specific DNA-binding proteins such as histone H5 (reviewed by Gajiwala & Burley[23]). However, in the RuvB structure, the recognition helix α15, which lies in the DNA major groove in the canonical binding mode, is broken by the absolutely conserved Pro299 into α15a and α15b (Figure 1(a)). Extensive sequence conservation for domain III residues that possess both structural and potential recognition roles (Figure 1(b)) suggests the importance of this third domain, as does an isolated dominant negative nonsense mutation in *E. coli* RuvB[24] that preserves domains I and II, which pack into the hexamer, but deletes most of domain III.

This three-domain RuvB structure appears to be similar to the *Thermus thermophilus* RuvB structure recently published at 3.2 Å resolution determined independently[25] and a related *T. thermophilus* crystal form solved at 3.6 Å resolution (C.D.P. & J.A.T., unpublished results). This resemblance suggests that the high-resolution RuvB structure presented here is representative of all RuvB branch migration motors.

The RuvB structure furthermore rationalizes the insertions and deletions observed in the archaeal and eukaryotic RuvB homologs, termed TBP interaction protein of ~49 kDa (TIP49).[19,20] TIP49 proteins lack a RuvB-like domain III, but have a ~200 amino acid residue insertion between α3 and β3 (Figure 1(b)). This inserted domain appears to be unique to TIP49 by database searches and, given the ability of TIP49 to hexamerize, could be positioned where domain III sits in the RuvB structure near the C-terminal face of the domain I β-sheet. Thus, we suggest that the TIP49 inserted domain is positioned to function equivalently to RuvB domain III.

Implicated roles for Walker motifs A and B in RuvB conformational change

In addition to driving nucleotide triphosphate hydrolysis,[26] the RuvB structure suggests that conserved Walker A and B motifs may also function in driving conformational changes upon binding ATP. The Walker A motif, also termed the P-loop, is involved in coordination of the triphosphates and presenting the γ-phosphate group for cleavage. The Walker B motif coordinates a divalent metal ion and likely activates the water nucleophile for ATP cleavage. In the ADP-bound complex of RuvB (Figure 2(a)), the two motifs are not aligned appropriately for activating and cleaving ATP. This misalignment may also explain the inability to co-crystallize or soak divalent metals, non-hydrolyzable ATP analogs, or transition-state analogs such as aluminum and beryllium fluoride into this crystal form (data not shown), as these compounds would require a precise alignment of the active site.

Comparison of the Walker A and B motifs in these RuvB structures and in the AMP-PNP bound NSF-D2,[27,28] which possesses active-site geometry consistent with the highly conserved roles of Walker A and B in ATP hydrolysis, suggest that alignment of the motifs would result in local conformational changes that could be propagated into domain motions. Superposition of the central β-sheets in domain I suggests that ATP and/or metal binding may systematically shift α3 by ~3 Å towards the helical N terminus (Figure 3). Additionally, α2 would be shifted in the ATP state toward the protein core, partially accommodating the space left by α3. Combined, these motions would shift the orientation of domain II by ~30° at Walker A (Figure 3), and alter both the position of the winged-helix domain III and the subunit-subunit interface. Thus mutations in Walker A that disrupt normal γ-phosphate positioning, such as the Lys64Arg mutant (Figure 2(c)) whose guanidium group would likely shift the γ-phosphate group. The guanidium group position is constrained by other residues of Walker A (Gly58, Pro59, and Pro60), the β-sheet (Leu56, Ala57, Ala156, and Thr157), and the nucleotide and the conformational changes in both RuvB-like and NSF-D2-like conformations. Additionally, the residues of Walker B that inactivate the ATPase and branch migration activity[29] may impact both the hydrolytic machinery as well as an important sensor of the presence of a γ-phosphate group.

Although it is not possible to rule out that the RuvB/NSF-D2 differences are static variations in family members, the observed misalignment in the ADP-bound complex of RuvB is inconsistent with the conserved roles in an active ATPase site, which are supported by extensive mutagenesis for RuvB.[29,30] In the absence of direct superposition of the central β-sheet for these proteins, the most obvious marker for the misalignment becomes the relative distances between main-chain atoms for the Walker A and B motifs. In the NSF-D2 structure, the C^{α} atom for the Walker A lysine residue (Lys557 in 556-GKT-558) is roughly equidistant (~8.8 Å) from both of the C^{α} atoms of the Walker B carboxylate residues (Asp611 and Asp612 in 661-DDIE-614). For the RuvB structure, the C^{α} atom for the Walker A lysine residue (Lys64 in 63-GKT-65) is much closer to the C^{γ} atom of the first carboxylate group (Asp109 at ~8.8 Å) than the second (Glu110 at ~10.7 Å). This difference is indicative of the systematic shift of α2 along the β-sheet and relates residues of Walker A that bind β and

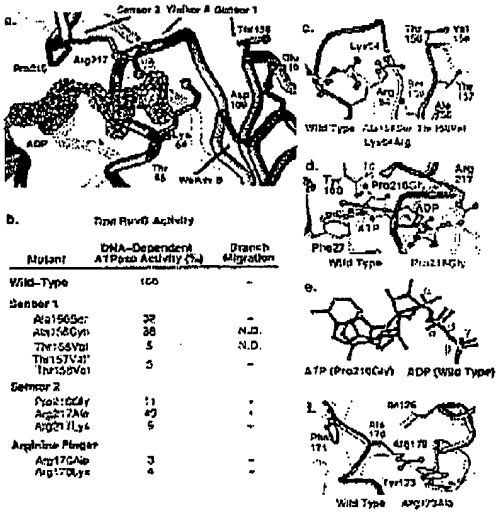

b.

Mutant	DNA-Dependent ATPase Activity (%)	Branch Migration
Wild-Type	100	+
Sensor 1		
Ala156Ser	32	+
Ala156Gln	38	N.D.
Thr158Val	5	N.D.
Thr157Val/Thr158Val	5	-
Sensor 2		
Pro216Gly	11	-
Arg217Ala	40	+
Arg217Lys	5	-
Arginine Finger		
Arg170Ala	3	-
Arg170Lys	4	-

Figure 2. RuvB nucleotide recognition and an implied strained ATP-bound conformation. (a) Details of the nucleotide-binding site reveal that the phosphate groups are coordinated by the Walker A motif (including Lys64 and Thr65) with the ADP moiety contacted by residues of the sensor 2 motif (Pro216 and Arg217). Sensor 1 (Thr158) and Walker B (Asp109 and Glu110) motifs are located near the position of the γ-phosphate group. The isosurface of the simulated annealing omit difference density is shown for ADP, contoured at 3σ (green). (b) Structure-based mutational analysis reveals the importance of ATP hydrolysis in branch migration and the key roles played by sensor 1, sensor 2, and arginine finger in RuvB. Biochemical characterization of the DNA-dependent ATPase activity of RuvB mutants[21] and branch migration of an *in vitro* reconstituted RuvAB-Holliday junction complex.[21,52] Proteins scored as inactive, "-", in branch migration activity are either wholly or substantially compromised, as they showed less than 3% of wild-type activity after an incubation of 60 minutes. (c) Overlay of the wild-type RuvB protein (blue) with structures of the sensor 1 mutations Ala156Ser (yellow), Thr158Val (light blue), and the Walker A mutation Lys64Arg (light brown). (d) Overlay of the sensor 2 mutation Pro216Gly (yellow) with wild-type RuvB, illustrating some of the structural rearrangements required to accommodate the misregistered ATP (Figure 2(c)) in the nucleotide-binding site. (e) Details of ATP binding from the Pro216Gly structure (red) and ADP binding from the wild-type structure (blue) demonstrating the reorientation of the both adenine and ribose moieties and the phosphate misregistration, where the ATP γ-phosphate group binds at the β position and the ATP β-phosphate group binds at the α position. This structure suggests that binding ATP in the appropriate conformation channels binding energy into a strained RuvB conformation. (f) Overlay of the arginine finger mutation Arg170Ala (yellow) with wild-type RuvB, suggesting the dramatic loss of ATPase and branch migration assay are due to loss of the guanidium functionality, as structural perturbations are small.

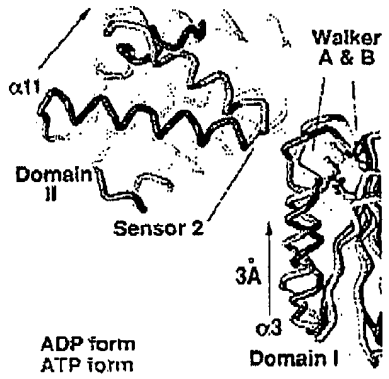

Figure 3. Nucleotide-driven conformational changes in AAA+-class ATPases. Overlay of the ADP bound RuvB domain I (blue) with the AMP-PNP bound N5F-D2 domain I (green) demonstrates the implied ~3 Å shift of α3 upon ATP binding, which aligns Walker A and B motifs (indicated by the conserved lysine residue of Walker A and carboxylate groups of Walker B), to generate an ATP hydrolysis site containing appropriate geometry as observed in N5F-D2. This motion of α3 is linked to a conformational change in domain II, in which the sensor 2 helix rotates dramatically. Comparison of the RuvB structure with other ADP-bound AAA+-class ATPases suggests that this structural rearrangement is the hallmark of this class of proteins.

γ-phosphate groups directly with the catalytic machinery at Walker B.

Roles for sensor motifs and evidence for a strained ATP state

From our RuvB structural and mutational results, we propose that RuvB exists in three distinct states with distinct conformational states during the reaction cycle: ATP-bound, ADP-bound, and empty. Recognition of each of these states is likely *via* two types of detectors that interact either with the ADP moiety or with the ATP γ-phosphate group. In addition to the interaction of the Walker A and B motifs in sensing the ATP-bound state, the sensor 1 and sensor 2 motifs are critical for responding to the nucleotide based on both structural analysis and mutagenesis results (Figure 2(a)-(c)).

Sensor 1 is located on domain I at β4 between the Walker A and B motifs (Figure 2(a)), and appears positioned to distinguish nucleotide diphosphate and triphosphate states by forming a hydrogen bond through the Thr158 side-chain to the ATP γ-phosphate group. The Thr158 side-chain, even when rotated about χ1, is not close enough to form a hydrogen bond to a modeled γ-phosphate group (5.5 Å) in this ADP-complex structure (Figure 2(b)); however, the proposed shift of Walker A and B motifs in response to ATP

binding would bring the Thr158 side-chain into position (~3 Å) for hydrogen bond formation. Significantly, mutation of Thr158 to the isosteric valine inactivates DNA-dependent ATPase activity (Figure 2(b)), even though the mutation does not change the structure of the ADP-bound form of the enzyme (Figure 2(c)). The other absolutely conserved residues in the sensor 1 motif do not appear to sense the ATP state of the enzyme directly, but likely play structural roles. Gly155 packs directly against the hydrophobic core of the protein, and any other residue would possess substantial steric clashes. Ala156 lies underneath Walker A, and residues with large side-chains would disrupt the position of Lys64. Mutation of Ala156 to either serine or cysteine is tolerated (Figure 2(b)), and the structure of the Ala156Ser mutant is undisrupted in the ADP-bound complex (Figure 2(c)); however, this position is strictly conserved as alanine in all bacterial RuvB sequences and could be more problematic, depending on the structural influence of ATP or DNA-dependent rearrangements on this region. Thus, sensor 1 may help distinguish between nucleotide diphosphate and nucleotide triphosphate-bound states of the enzyme.

Sensor 2, located on domain II (Figure 2(a)), packs against the ATPase binding site. Pro216, which is conserved in RuvBs as either proline or methionine, packs directly against the adenine face, and Arg217 forms a charged hydrogen bond to the β-phosphate group. Mutations in both of these sensor 2 residues affects the ATPase activity of the enzyme. The mutation of Arg217 to lysine inhibits ATPase activity, although the Arg217Ala mutant activity is higher (Figure 2(b)). Mutation of Pro216 to glycine shows hindered ATPase activity at low enzyme concentrations (data not shown), but normal ATPase activity at high concentrations (Figure 2(b)). Notably, the crystal structure of this mutant (Figure 2(d)-(e)) reveals that Pro216 is important for preventing alternative nucleotide-binding states from occurring. Thus, the Pro216Gly mutant surprisingly binds ATP, not ADP, as isolated from cells, but the ATP binds non-productively, such that the phosphate groups of the ATP are out of register. The ATP γ-phosphate group binds in the normal β position and the ATP β-phosphate group binds in the normal α position (Figure 2(e)). This out-of-register binding is accommodated by a rearrangement of the binding site that is prevented in the wild-type protein by steric collision between the nucleotide 3′ hydroxyl group and the Pro216 ring. The ADP molecule bound by the wild-type enzyme is in the *anti* conformation, while the ATP molecule in the Pro216Gly is *syn*. Importantly, the altered nucleotide-binding mode in this mutant and its inefficiency at lower protein concentrations suggests that correct positioning of the ATP γ-phosphate group is energetically costly, consistent with the γ-phosphate-induced conformational changes inferred from the structure. Both Pro216 and Arg217 in sensor 2 interact with components of the nucleotide present in both ADP and ATP. Hence, this motif, unlike sensor 1, likely distinguishes between nucleotide-bound and unbound states in addition to enforcing a strained ATP-bound conformational state to prevent non-productive binding.

Although the sensor 2 motif was previously defined only for the highly conserved region,[31] analysis of the RuvB structure suggests that the motif definition should be expanded. The adenosine ring is buried within a pocket and sequestered from solvent by the hydrophobic side-chains of Pro21, Phe27, Ile188, and Pro216. This hydrophobic collapse can be likened to a vise in which domains I and II clamp down on the flat adenine. The polar faces of the ring interact with more polar environments: N-1 and N-3 hydrogen bond to water molecules; the exocyclic N-6 amine hydrogen atom bonds to the Ile28 backbone carbonyl group; and N-7 is oriented towards the Tyr180 hydroxyl and Leu62 backbone carbonyl groups. The ADP 2′ and 3′-hydroxyl groups make no specific protein interactions, and the only specific hydrogen bonding interaction with ADP is through the exocyclic amine group. This lack of specific interactions explains the ability of the *E. coli* and *T. thermophilus* RuvBs to utilize alternative nucleotides including dATP, dCTP, and dTTP.[13,32] The possibility that the more hydrophilic guanine base may prevent the hydrophobic collapse between domains I and II may explain biochemical studies for the *Thermus* RuvB that can hydrolyze GTP and dGTP efficiently, but cannot use these nucleotides for *in vitro* branch migration,[32] as nucleotide binding is decoupled from the hydrophobic collapse.

All three states of the enzyme can be detected through recognition of either the ADP moiety or the γ-phosphate group. The sensor 1 and the Walker A and B motifs respond to the binding of the γ-phosphate group and a divalent cation. This ATP state, as revealed by the alternative nucleotide binding in the Pro216Gly mutant, is likely to exist in a tense or strained conformation with a triggered structural transition (Figure 3). Sensor 2 recognizes the ADP through interaction with the sugar and diphosphate moieties as well as hydrophobic collapse around the ring. These three RuvB conformational states within domains of an individual RuvB subunit provide the chemomechanical force that drives Holliday junction branch migration in the context of an active hexamer.

RuvB hexameric assembly

The crystallographically determined subunit contacts in the helix with six subunits per turn use the same molecular interfaces that are observed in the HslU and NSF-D2 hexameric AAA+-class ATPases.[27,28,33,34] Superimposition of RuvB domain I onto the conserved domain of HslU results in a polar hexamer (Figure 4(a)) that satisfies known constraints, including the two-lobe construction (the large lobe is domains I and II, the small lobe is domain III) and dimensions observed by electron

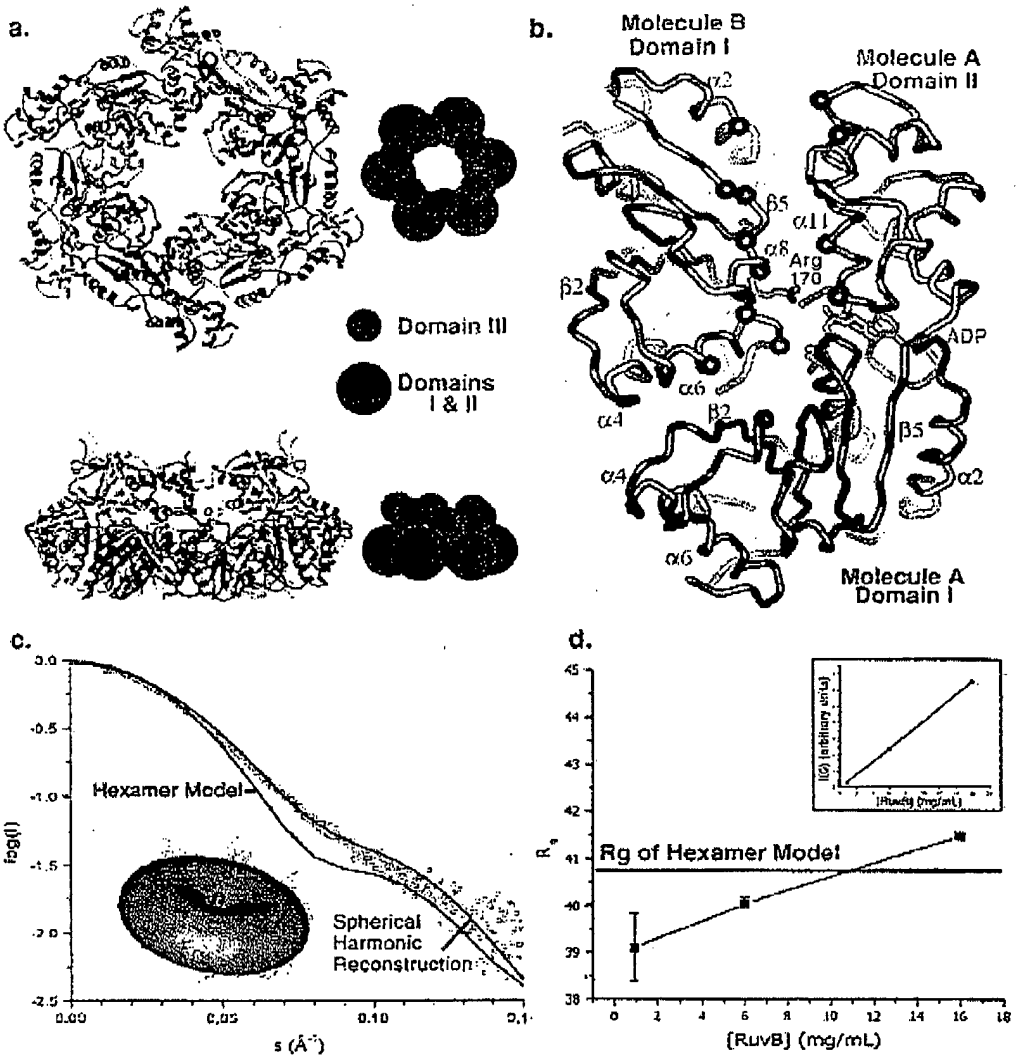

Figure 4. RuvB hexameric interfaces and assembly. (a) The RuvB hexamer assembly generated from the HslU hexamer (PDB code 1DO0[34]) closely resembles EM reconstructions of RuvB hexamers bound to DNA.[35] The large lobe of the polar ring is generated from domains I and II, while the small lobe comprises domain III. (b) Hexameric interface between two adjacent subunits of the RuvB hexamer. The hexameric interface is assembled entirely from domains I and II. Dominant negative mutations[24] along these interfaces are indicated by a red sphere at the amino acid C^{α} position. The side-chain of the arginine finger (green) of molecule B approaches the bound nucleotide (yellow) within the adjacent molecule A. (c) Fit of the *Thermotoga* RuvB hexamer assembly (blue) and a spherical harmonic reconstruction (green) to SAXS data collected from *E. coli* RuvB hexamers at 6 mg/ml. The spherical harmonic reconstruction shown here ($L = 2$, $p3$ symmetry) is representative of the flattened toroids generated *ab initio* from the experimental data. (d) The calculated hexamer radius of gyration (R_g) closely matches the experimentally determined values. Importantly, the forward scattering intensity ($I(0)$) is linear in response to RuvB concentration, indicating that aggregation and hexamer disassembly were not occuring during these SAXS measurements.

microscopy (EM).[35] The entire subunit interface, made up almost entirely by domains I and II, is hydrophilic and possesses extensive shape complementarity (Figure 4(b)). The domain I-domain I interface between adjacent subunits is slightly negatively charged, whereas the domain I-domain II interface is positively charged. The binding of domain I within the cleft formed by domains I and

II of the adjacent subunit (Figure 4(b)) provides a mechanism whereby nucleotide-induced conformational changes between domains I and II can affect the subunit-subunit interactions (Figure 3) and suggest that subunits shift positions during the reaction cycle.

This assembly is also consistent with our experimental small-angle X-ray scattering (SAXS) data measured on solutions of *E. coli* RuvB hexamers (Figure 4(c)). Calculated scattering from the hexamer is similar to the experimental scattering curve (Figure 4(c)). SAXS data provide an overall radius of gyration (R_g) for the particle of ~40 Å (Figure 4(d)) with a maximum intraparticle distance (D_{max}) of ~120 Å, consistent with our hexamer model (Figure 4(d)). Additionally, an *ab initio* spherical harmonic reconstruction, which fits the experimental curve with a small number of parameters,[36] agrees fairly well with the hexamer (Figure 4(c)). SAXS data can exclude packing arrangements that give different radii of gyration and maximum interparticle distances, such as more globular arrangements or asymmetric hexamers that are more elliptical and would have increased maximum intraparticle distances. SAXS cannot provide atomic-resolution details of the interfaces of this prolate ellipsoid model as shown through systematic generation of 64,000 computational perturbations of this hexamer (data not shown); however, there is no reason *a priori* to expect that any computationally generated assembly should be in agreement with these experimental SAXS data. Taken together, the agreement of the hexamer with experimentally determined SAXS data, the similarities to EM reconstructions,[35] the conservation with other hexameric AAA + -class ATPases,[27,28,33,34] and similarities to the crystallographic packing interfaces suggest that this hexamer arrangement is likely to be correct.

Assembly is critical for ATPase activity in RuvB[37,38] and in other AAA + -class ATPases.[22] RuvB is known to be functional as a hexamer and assemble into rings.[35] The fact that ADP-bound RuvB assembles into a helix with six subunits per turn in these crystals rather than a hexameric ring suggests that asymmetry in the RuvB ring arises simply through assembly and that not all subunits of a hexameric ring can exist in an ADP-bound form. Both the RecA and T7gp4 proteins have been observed in helical and ring forms, and these proteins are believed to possess functional asymmetries.[39,40]

Arginine fingers in AAA+-class ATPases

To test the role of the strictly conserved arginine following the Walker A and B motifs in functional hexameric AAA + -class ATPases, Arg170 in RuvB was mutagenized to both alanine and lysine. Both mutants were deficient ATPases and were not activated upon DNA binding like wild-type (Figure 2(b)). These results match the inactivation observed in mutants of the equivalent arginine to leucine and lysine in the AAA + -class ATPase domain of the *E. coli* FtsH ATPase-dependent protease[41] and an arginine to histidine mutation isolated in *E. coli* RuvB.[24] The crystal structure of Arg170Ala lacks any real conformational changes from wild-type (Figure 2(f)), indicating that the defect in the mutant involves loss of the arginine guanidium group.

The hexameric assembly demonstrates that the arginine residue approaches the nucleotide phosphate groups (Figure 4(b)) and may function analogously to arginine fingers identified in the GTPase-activating proteins (GAPs). These arginine residues function to regulate nucleotide hydrolysis by binding the γ-phosphate group within the Ras GTPase switch, which activates GTPase activity by 10^5-fold (reviewed by Noel[42]). Arginine fingers have been implicated in a number of other unrelated NTPases, including Rho GTPases,[43] T7gp4,[40] and F_1-ATPase.[44] In the RuvB hexamer, Arg170 deviates slightly from the position required to facilitate ATP hydrolysis (Figure 4(b)), suggesting that ADP-bound RuvB is not the correct state to activate ATP hydrolysis in the adjacent subunit. In fact, proper arginine geometry for ATP hydrolysis can be observed by modeling in NSF-D2 bound to the non-hydrolyzable ATP analog AMP-PNP,[41] suggesting that ATP binding in one subunit drives ATP hydrolysis in the adjacent molecule. These structural and biochemical results provide a mechanism to explain previous kinetic proposals[38,45] in which ATP is both a substrate and an allosteric effector.

Model for the RuvABC complex

Double-stranded DNA can pass through the center of the RuvB hexamer (Figure 5(a)) that ranges from 25 to 35 Å in diameter. This is in contrast to the unrelated phage T7 gp4 hexameric DNA helicases, where unwinding is believed to be driven by translocation of only a single strand through the center,[40] and would explain why RuvB can translocate along DNA[37] but fails to act as a helicase in the absence of RuvA.[10] Biochemical data also support both strands passing through the center of the hexamer. RuvB appears to be able to migrate through interstrand psoralen crosslinks,[46] and protects about 24 base-pairs of both DNA strands in DNase I footprinting experiments.[47] The 1.5 turns of *B*-DNA within the central channel of the hexamer (Figure 5(a)) are also consistent with the geometry of the RuvA/Holliday junction complex[9] and closely resemble EM reconstructions of RuvB bound to plasmid DNA[35] in which DNA is bound at either end of the hexamer (domain I and domain III) surrounding an interior cavity (the gap between domain II and DNA).

Domain III of RuvB overlays well with other winged-helix domains (Figure 5(b)). Two different DNA-binding modes have been observed for this family of proteins;[23] however, both involve faces of domain III that are not oriented towards the DNA

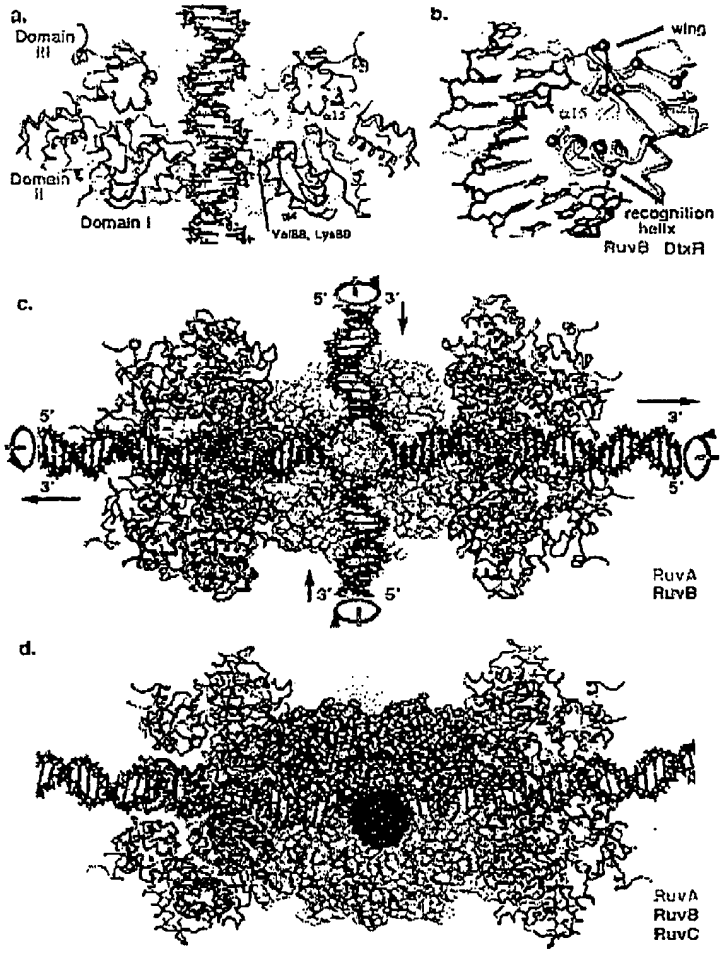

Figure 5. Structurally implied RuvB/DNA and RuvABC/Holliday junction interactions. (a) The structurally implied path of duplex DNA through the RuvB hexamer in Holliday junction branch migration. Domains I (blue) and III (green) are positioned to interact with the DNA (black). The β2-α4 loop forms a tight constriction around the DNA and includes Val88 and Lys89, identified as positions of dominant negative mutations in *E. coli* RuvB,[24] and shown as red balls as are similar mutations in domain III. Topological evidence suggesting that the DNA is melted or underwound[27,38,49] is not illustrated here. (b) Superposition of the domain III of RuvB (green) onto the diphtheria toxin repressor (DtxR)-DNA co-crystal structure (purple, PDB code 1DDN[61]). The DtxR utilizes the canonical mode for winged helix binding in which the recognition helix (α15a and α15b in RuvB) lies in the major groove and the wing contacts DNA phosphate groups. This canonical binding mode[23] is most consistent with the positive charge of the wing and net negative charge of the recognition helix. C^{α} positions of residues critical for RuvB function in this domain[24] are indicated by red balls and, excluding residues involved in the stabilization of the domain, include the positive charges and glycine of the wing and residues of the recognition helix that contact the DNA major groove. Placing this face of the domain against DNA running through the hexamer (a) requires a 60-90° rotation of domain III relative to the AAA+-class ATPase domains I and II. (c) Depiction of the RuvAB/Holliday junction complex shows the RuvB hexamers (dark blue, purple) on either face of the RuvA tetramer (yellow surface, PDB code 1BDX[9]). The orientation of the RuvB hexamer is derived from EM images indicating that the large lobe (domains I and II) face the RuvA hexamer.[14] The rings are rotated so that domain III from one of the RuvB subunits is aligned with the DNA major groove, as suggested by the winged-helix binding mode, and the rings are related by a 2-fold rotation about an axis perpendicular to the page. The direction of the DNA migration and rotation is indicated by arrows in which two duplexes (red and blue) are unwound and recombined in the RuvA tetramer. (d) Depiction of the RuvABC/Holliday junction complex rotated 90° relative to (a) showing the binding of the RuvC dimer to the face of the Holliday junction opposite RuvA. The RuvC dimer (red surface, PDB code 1HJR[62]) is oriented so that the active sites face the phosphodiester backbone and the fit suggests that RuvC should make protein-protein contacts with RuvB, as suggested from biochemical results.[16]

in the hexamer assembly of ADP-bound conformations of RuvB (Figure 5(a)). Thus, unless domain III of RuvB possesses a third, novel binding mode, this domain needs to be reoriented by 60-90° to present the appropriate binding face towards the DNA passing through the central channel of the complex. A canonical winged-helix interaction is supported by both homology and dominant negative mutations (Figure 5(b)), the flexible random-coil linkage between domains II and III, and a ~20° rotation of domain III relative to domains I and II determined by superimposing the *T. maritima* RuvB structure and the *T. thermophilus* RuvB structures ([25]; C.D.P. & J.A.T., unpublished results). If the rearrangement occurs, appropriate domain III orientations may be forced by packing interaction between adjacent domain IIIs that does not occur in the crystal packing.

An ATP-bound state of RuvB modeled from NSF-D2 (Figure 3) would force domain III into closer proximity to DNA, consistent with both gel shift experiments[18] and DNase I footprints in which ATPγS improves the protection of the domain III side of the footprint.[47] Winged-helix domains have been structurally characterized only with dsDNA, and the RuvB structure suggests that RuvB may interact primarily with and translocate along both strands of dsDNA. Paradoxically, the helicase activity of RuvAB possesses a 5′ → 3′ directionality,[10] but has not been characterized independently of RuvA. The resolution of this problem may be that strand specificity in the *in vitro* helicase reaction may be due to differences in the way RuvA presents 5′ and 3′-tailed substrates to the RuvB translocase and not to strand specificity of RuvB itself.

The large face of the RuvB hexamer faces the RuvA tetramer[14] and can be associated with domains I and II from these crystallographic results (Figure 5(c)). This orientation of the RuvB ring places the disordered region between Ile131 and Asp147 onto the RuvA contact region, which forms a crystal contact as a pair of interacting β-hairpins in the *T. thermophilus* crystal form[22] (C.D.P. & J.A.T., unpublished results). Geometric constraints demand that only one or two RuvB subunits interact with the RuvA tetramer at any one time. Interestingly, the RuvB subunit positioned to place the winged-helix domain into the DNA major groove is also the subunit positioned to interact with RuvA. An RuvC dimer fits in the RuvAB/Holliday junction complex (Figure 5(d)) such that the active sites can generate two symmetrical cuts, consistent with genetic and biochemical data indicating that RuvC functions in concert with RuvAB.[15,16]

Structural implications for RuvB-driven DNA translocation and branch migration

Branch migration by the RuvAB complex requires a screw motion of the DNA (Figure 5(c)), which includes both translational and rotational components. The result of this motion is to change the identity of the bases being migrated through a DNA pathway defined by the backbone, but not to move the pathway itself. This restriction makes any proposed RuvAB mechanism different from the proposed single-stranded (ss)DNA migration models in T7gp4, in which simple translation of the DNA can occur along with motion of the backbone positions.[40] Two classes of different, testable models can be proposed for branch migration by RuvAB, both of which are influenced dramatically by the fixed nature of the backbone pathway and cannot be distinguished by current experimental evidence.

The first class of models would involve a fixed RuvAB interaction, in which RuvB molecules remain fixed to RuvA once the complex is formed. In this class of models, only one or two subunits will be in the correct position to perform work during the branch migration reaction due to the fixed DNA backbone pathway. In this scenario, the arginine finger motif may function to prevent wasteful ATP hydrolysis prior to multimer assembly or trigger ATP hydrolysis in the active subunit once conformational changes due to ATP binding have occurred. The topological distortions observed for trapped RuvB-DNA complexes[21,38,49] may arise from distortions in the ATP-bound state of RuvB that are unable to relax without ATP hydrolysis.

The second class of models would provide for a rotating RuvAB interaction, in which RuvB molecules rotate into and out of the active position in response to ATP hydrolysis (Figure 6). Rotation of the RuvB hexamer relative to RuvA could be driven both by interaction with the DNA template and the nature of the RuvAB interface itself. This

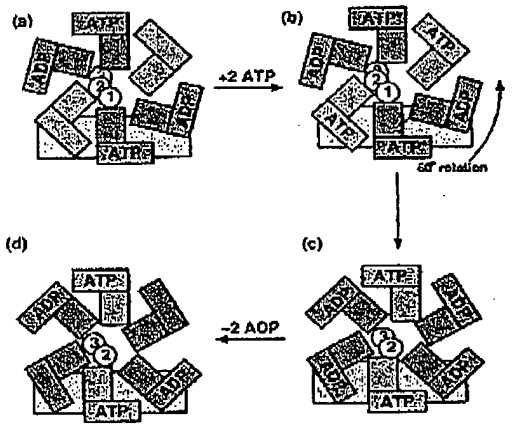

Figure 6. Structurally implied mechanism for branch migration. Illustration of a mechanism for RuvB branch migration involving a rotation of the RuvB hexamer (green, cyan, and blue subunits) relative to the RuvA tetramer (yellow bar). Stepwise migration of the DNA is indicated by motion of the circled numbers through the center of the hexamer, although the fundamental translocation step size is unknown. The 2-fold symmetry of the loading of the nucleotide binding sites is based on pre-steady state kinetics of RuvB, which hydrolyzes two ATP molecules per hexamer.[38,45] The starting state (a) with two ATP and two ADP molecules is inferred from the optimal nucleotide ratio (2 ATPγS:1 ATP) for forming topologically underwound DNA,[21,38,49] equivalent to step (b), and the productive arginine finger geometry observed in the AMP-PNP bound NSF-D2.[41] ATP hydrolysis in step (b) may drive rotation of the RuvB hexamer (c) by opening of the ADP-bound state along DNA as well as through interactions with RuvA. ATP serves as an allosteric effector for ADP release,[45] which may be driven by interface changes between subunits that may be released after rotation (d) or during rotation. Hydrolysis of ATP by RuvB is kinetically rapid and ADP release is slow.[45]

model is also consistent with biochemical data suggesting ATP is both substrate and allosteric effector,[38,45] inducing ADP release in other binding sites, likely due to the influence of ATP-induced domain I-II changes upon the hexamer interface (Figure 4(b)). The orientation of the arginine finger, which likely triggers hydrolysis in the ATP bound form, would be consistent with the required counter-clockwise screwing of DNA through the RuvAB complex (Figure 6). Topological distortions for trapped RuvB-DNA complexes may be due to a symmetry mismatch between the hexameric RuvB ring (60° steps from the six subunits) and DNA (36° steps from the ten base-pairs per turn).

For the rotating RuvAB interaction, RuvA may function as an adenine nucleotide exchange factor, driving ADP/ATP exchange in the bound RuvB molecule and driving RuvB rotation once ATP is hydrolyzed. RuvA improves the ATPase activity of RuvB with and without DNA,[45] increasing the K_m of RuvB for ATP by seven to eight-fold and maximizing the hydrolysis rate at an 8:6 RuvA:RuvB stoichiometry, which is the maximum number of tetramers that can sterically interact with one face of a RuvB hexamer. The isolated C-terminal RuvA domain that binds RuvB inhibits ATP hydrolysis,[50] possibly representing a state in which each RuvB subunit remains bound to a RuvA domain and ATP.

These structural and mutagenesis studies of RuvB suggest in detail how RuvB utilizes the AAA+-class ATPase fold to convert nucleotide binding and hydrolysis to mechanical action in the migration of Holliday junctions. The structural results strongly suggest that domain-domain motions triggered by nucleotide-bound states drives the hexamer subunit-subunit conformational changes. Additionally, the helix formed by the ADP-bound RuvB strongly suggests that asymmetry is key to function of the hexamer, and the arginine finger provides a mechanism to couple sequential hydrolysis between adjacent subunits potentially producing a wave of ATP hydrolysis in the ring. These results can be interpreted in terms of either rotating or fixed RuvAB translocation models, neither of which is clearly distinguishable with current data. These results provide a framework to experimentally address a number of important questions regarding RuvB function, including determination of the step size and the number of nucleotides hydrolyzed per step, elucidation of the atomic structure and the permanency of the RuvAB interaction, and delineation of the functionally relevant nucleotide-loaded states of the hexamer during branch migration.

Experimental Procedures

RuvB expression, mutagenesis, and biochemical characterization

T. maritima RuvB was overexpressed recombinantly in *E. coli* and purified as described.[21] The selenomethionine-incorporated protein was generated by cloning the RuvB expression plasmid into methionine auxotrophic *E. coli* strain B834 (Novagen) followed by expressing in LeMaster's defined medium with methionine replaced with 50 mg/l of D,L-selenomethionine (Sigma). *T. maritima* RuvB mutants were generated performing the QuickChange PCR protocol (Stratagene) on the pET11c expression construct.[21]

RuvB DNA-dependent ATPase activities were measured using a colorimetric assay that detected the release of inorganic phosphate[21] using 5-20 μg of protein per reaction. Branch migration assays utilized *T. maritima* RuvA and Holliday junctions prepared as described.[51,52] Briefly, Holliday junction arms were generated using PCR snapback products and these arms were then annealed at 70°C. Products of RuvAB branch migration for these substrates are heteroduplexes. Importantly, use of mismatches in the Holliday junctions forces the reaction to be energetically disfavored, preventing thermally driven migration of the junctions. Reactions were analyzed using native polyacrylamide gels and were stained with ethidium bromide.

Crystallization and X-ray structure determination

Crystals of RuvB were grown by vapor diffusion in sitting drop plates against 1 M 1,6-hexanediol, 100 mM $CoCl_2$, 100 mM sodium acetate (pH 4.6). Crystals were cryocooled in mother liquor supplemented with 20% (w/v) glycerol. X-ray diffraction data were collected at the Stanford Synchrotron Radiation Laboratory (SSRL), the Advanced Light Source (ALS), and the Advanced Photon Source (APS). Data were processed using Denzo and Scalepack.[53]

One strong initial $K_2Pt(CN)_4$ site was identified through isomorphous and anomalous Pattersons, and other derivative sites were subsequently identified by cross-phasing. Protein phases were generated with MLPHARE in the CCP4 package,[54] and an initial structure was built with Xfit.[55] Refinement was performed with CNS version 1.0[56] by using the maximum-likelihood target function with 10% of the reflections omitted from the refinement for cross-validation testing[57] with manual inspection and rebuilding into σA-weighted $2F_{obs} - F_{calc}$ and $F_{obs} - F_{calc}$ electron density maps with Xfit. The methionine positions of the refined structure were verified through isomorphous difference Fourier maps calculated by using data from the selenomethionine-substituted protein (data not shown).

Identification of ADP in the crystal structure

ADP was identified by examination of the bound nucleotide density and verified with a standard ATP regeneration system in which ATP formation from ADP is linked to NADH oxidation with pyruvate kinase (PK) and lactate dehydrogenase (LDH) and measured spectrophotometrically ($\Sigma_{340} = 6.22\ cm^{-1}\ mM^{-1}$). Typical reaction conditions contained the following: 5 mg of acid-denatured RuvB, 1 mM phosphoenolpyruvate, 250 μM NADH, 20 units of LDH/ml, 40 units of PK/ml, and 5 mM DTT in 200 mM Hepes (pH 7.5). Data from the assay indicate that ~50% of the purified protein was bound to ADP (data not shown).

Small-angle X-ray solution scattering

E. coli RuvB was expressed from the pEAW112 plasmid and isolated by using published protocols.[5] Hexamers were formed by concentration and isolated by gel filtration on a Superose-12 column in 20 mM Tris-HCl (pH 8.0), 50 mM NaCl, 1 mM DTT. Scattering data were collected at the SSRL beamline 4-2. For each concentration, the Guinier region of the small-angle scattering was linear. R_g, D_{max}, and $I(0)$ were derived from experimental data using GNOM.[58] Spherical harmonic reconstructions were generated using SASTA[36,59] and fits of the computational hexamers were calculated through CRYSOL.[60]

Protein Data Bank accession numbers

Coordinates for native RuvB and the Lys64Arg, Ala156Ser, Thr158Val, Arg170Ala, and Pro216Gly mutants have been deposited in the RCSB Protein Data Bank under the entries 1IN4, 1IN6, 1IN5, 1IN8, 1IN7, and 1J7 K, respectively.

Acknowledgments

We thank Karl-Peter Hopfner and Clifford Mol for helpful discussions; Clifford Mol, David Barondeau, and Andrew Arvai for assisting data collection; and Jie Tong for purifying samples of RuvB that initiated the crystallographic efforts. We are indebted to Tom Macke for the computational generation DNA coordinates for Figure 5. We thank the staff at the crystallographic beamlines at SSRL, ALS, and APS for excellent data collection facilities. The pEAW112 plasmid was a kind gift from Michael Cox. This work is based upon research conducted at the Stanford Synchrotron Radiation Laboratory (SSRL), which is funded by the Department of Energy (BES, BER) and the National Institutes of Health (NCRR, NIGMS), the Advanced Light Source (ALS) at Lawrence Berkeley National Laboratory (LBNL), and the Advanced Photon Source (APS) at the Argonne National Laboratory. This work has been funded by the NIH grant CA76431 to J.A.T. and a Howard Hughes Predoctoral Fellowship to C.D.P.

References

1. Cox, M. M., Goodman, M. F., Kreuzer, K. N., Sherratt, D. J., Sandler, S. J. & Marian, K. J. (2000). The importance of repairing stalled replication forks. *Nature*, 404, 37-41.
2. Cox, M. M. (1999). Recombinational DNA repair in bacteria and the RecA protein. *Prog. Nucl. Acid Res. Mol. Biol.* 63, 311-366.
3. Zou, H. & Rothstein, R. (1997). Holliday junctions accumulate in replication mutants via a RecA homolog-independent mechanism. *Cell*, 90, 87-96.
4. Iype, L. E., Inman, R. B. & Cox, M. M. (1995). Blocked RecA protein-mediated DNA strand exchange reactions are reversed by the RuvA and RuvB proteins. *J. Biol. Chem.* 270, 19473-19480.
5. Iype, L. E., Wood, E. A., Inman, R. B. & Cox, M. M. (1994). RuvA and RuvB proteins facilitate the bypass of heterologous DNA insertions during RecA protein-mediated DNA strand exchange. *J. Biol. Chem.* 269, 24967-24978.
6. Adams, D. E. & West, S. C. (1996). Bypass of DNA heterologies during RuvAB-mediated three- and four-strand branch migration. *J. Mol. Biol.* 263, 582-596.
7. Seigneur, M., Bidnenko, V., Ehrlich, S. D. & Michel, B. (1998). RuvAB acts at arrested replication forks. *Cell*, 95, 419-430.
8. Ishioka, K., Fukuoh, A., Iwasaki, H., Nakata, A. & Shinagawa, H. (1998). Abortive recombination in *Escherichia coli ruv* mutants blocks chromosome partitioning. *Genes Cells*, 3, 209-220.
9. Hargreaves, D., Rice, D. W., Sedelnikova, S. E., Artymiuk, P. J., Lloyd, R. G. & Rafferty, J. B. (1998). Crystal structure of *E. coli* RuvA with bound DNA Holliday junction at 6 Å resolution. *Nature Struct. Biol.* 5, 441-446.
10. Tsaneva, I. R., Muller, B. & West, S. C. (1993). RuvA and RuvB proteins of *Escherichia coli* exhibit DNA helicase activity *in vitro*. *Proc. Natl Acad. Sci. USA*, 90, 1315-1319.
11. Muller, B., Tsaneva, I. R. & West, S. C. (1993). Branch migration of Holliday junctions promoted by the *Escherichia coli* RuvA and RuvB proteins. I. Comparison of RuvAB- and RuvB-mediated reactions. *J. Biol. Chem.* 268, 17179-17184.
12. Tsaneva, I. R. & West, S. C. (1994). Targeted versus non-targeted DNA helicase activity of the RuvA and RuvB proteins of *Escherichia coli*. *J. Biol. Chem.* 269, 26552-26558.
13. Parsons, C. A. & West, S. C. (1993). Formation of a RuvAB-Holliday junction complex *in vitro*. *J. Mol. Biol.* 232, 397-405.
14. Yu, X., West, S. C. & Egelman, E. H. (1997). Structure and subunit composition of the RuvAB-Holliday junction complex. *J. Mol. Biol.* 266, 217-222.
15. Mahdi, A. A., Sharples, G. J., Mandal, T. N. & Lloyd, R. G. (1996). Holliday junction resolvases encoded by homologous *ruvA* genes in *Escherichia coli* K-12 and phage 82. *J. Mol. Biol.* 257, 561-573.
16. Davies, A. A. & West, S. C. (1998). Formation of RuvABC-Holliday junction complexes *in vitro*. *Curr. Biol.* 8, 725-727.
17. Constantinou, A., Davies, A. A. & West, S. C. (2001). Branch migration and Holliday junction resolution catalyzed by activities from mammalian cells. *Cell*, 104, 259-268.
18. Wood, R. D., Mitchell, M., Sgouros, J. & Lindahl, T. (2001). Human DNA repair genes. *Science*, 291, 1284-1289.
19. Ikura, T., Ogryzko, V. V., Grigoriev, M., Groisman, R., Wang, J., Horikoshi, M. *et al.* (2000). Involvement of the TIP60 histone acetylase complex in DNA repair and apoptosis. *Cell*, 102, 463-473.
20. Shen, X., Mizuguchi, G., Hamiche, A. & Wu, C. (2000). A chromatin remodeling complex involved in transcription and DNA processing. *Nature*, 406, 541-544.
21. Tong, J. & Wetmur, J. G. (1996). Cloning, sequencing, and expression of *ruvB* and characterization of RuvB proteins from two distantly related thermophilic eubacteria. *J. Bacteriol.* 178, 2695-2700.
22. Neuwald, A. F., Aravind, L., Spouge, J. L. & Koonin, E. V. (1999). AAA+: A class of chaperone-like ATPases associated with the assembly, operation, and disassembly of protein complexes. *Genome Res.* 9, 27-43.
23. Gajiwala, K. S. & Burley, S. K. (2000). Winged helix proteins. *Curr. Opin. Struct. Biol.* 10, 110-116.
24. Iwasaki, H., Han, Y. W., Okamoto, T., Yoshikawa, M., Yamada, K., Toh, H. *et al.* (2000). Mutational

analysis of the function motifs of RuvB, an AAA+ class helicase and motor protein for Holliday junction branch migration. *Mol. Microbiol.* 36, 528-538.
25. Yamada, K., Kunishima, N., Mayanagi, K., Ohnishi, T., Nishino, T., Iwasaki, H. *et al.* (2001). Crystal structure of the Holliday junction migration motor protein RuvB from *Thermus thermophilus* HB8. *Proc. Natl Acad. Sci. USA*, 98, 1442-1447.
26. Walker, J. E., Saraste, M., Runswick, M. J. & Gay, N. J. (1982). Distantly related sequences in the α- and β-subunits of ATP synthase, myosin, kinases and other ATP-requiring enzymes and a common nucleotide binding fold. *EMBO J.* 1, 945-951.
27. Lenzen, C. U., Steinmann, D., Whitehart, S. W. & Weis, W. I. (1998). Crystal structure of the hexamerization domain of the N-ethylmaleimide-sensitive fusion protein. *Cell*, 94, 525-536.
28. Yu, R. C., Hanson, P. I., Jahn, R. & Brünger, A. T. (1998). Structure of the ATP-dependent oligomerization domain of the N-ethylmaleimide-sensitive factor complexed with ATP. *Nature Struct. Biol.* 5, 803-811.
29. George, H., Mezard, C., Stasiak, A. & West, S. C. (1999). Helicase-defective RuvB(D113E) promotes RuvAB-mediated branch migration *in vitro*. *J. Mol. Biol.* 293, 505-519.
30. Hishida, T., Iwasaki, H., Yagia, T. & Shinagawa, H. (1999). Role of Walker motif A of RuvB protein in promoting branch migration of Holliday junctions. Walker motif A mutations affect ATP binding, ATP hydrolyzing, and DNA binding activities of RuvB. *J. Biol. Chem.* 274, 25335-25342.
31. Guenther, B., Onrust, R., Sali, A., O'Donnell, M. & Kuriyan, J. (1997). Crystal structure of the δ' subunit of the clamp-loading complex of *E. coli* DNA polymerase III. *Cell*, 91, 335-345.
32. Yamada, K., Fukuoh, A., Iwasaki, H. & Shinagawa, H. (1999). Novel properties of the *Thermus thermophilus* RuvB protein, which promotes branch migration of Holliday junctions. *Mol. Gen. Genet.* 261, 1001-1011.
33. Sousa, M. C., Trame, C. B., Tsuruta, H., Wilbanks, S. M., Reddy, V. S. & McKay, D. B. (2000). Crystal and solution structures of an HslUV protease-chaperone complex. *Cell*, 103, 633-643.
34. Bochtler, M., Hartmann, C., Song, H. K., Bourenkov, G. P., Bartunik, H. D. & Huber, R. (2000). The structures of HslU and the ATP-dependent protease HslU-HslV. *Nature*, 403, 800-805.
35. Stasiak, A., Tsaneva, I. R., West, S. C., Benson, C. J., Yu, X. & Egelman, E. H. (1994). The *Escherichia coli* RuvB branch migration protein forms double hexameric rings around DNA. *Proc. Natl Acad. Sci. USA*, 91, 7618-7622.
36. Svergun, D. I., Volkov, V. V., Kozin, M. B. & Stuhrmann, H. B. (1996). New developments in direct shape determination from small angle scattering. 2. Uniqueness. *Acta Crystallog. sect. A*, 52, 419-426.
37. Mitchell, A. H. & West, S. C. (1994). Hexameric rings of *Escherichia coli* RuvB protein. Cooperative assembly, processivity and ATPase activity. *J. Mol. Biol.* 243, 208-215.
38. Marrione, P. E. & Cox, M. M. (1995). RuvB protein-mediated ATP hydrolysis: functional asymmetry in the RuvB hexamer. *Biochemistry*, 34, 9809-9818.
39. Yu, X. & Egelman, E. H. (1997). The RecA hexamer is a structural homologue of ring helicases. *Nature Struct. Biol.* 4, 101-104.
40. Singleton, M. R., Sawaya, M. R., Ellenberger, T. & Wigley, D. B. (2000). Crystal structure of T7 gene 4 ring helicase indicates a mechanism for sequential hydrolysis of nucleotides. *Cell*, 101, 589-600.
41. Karata, K., Inagawa, T., Wilkinson, A. J., Tatsuta, T. & Ogura, T. (1999). Dissecting the role of a conserved motif (the second region of homology) in the AAA family of ATPases. *J. Biol. Chem.* 274, 26225-26232.
42. Noel, J. P. (1997). Turning off the Ras switch with the flick of a finger. *Nature Struct. Biol.* 4, 677-680.
43. Zhang, B., Zhang, Y., Collins, C. C., Johnson, D. I. & Zheng, Y. (1999). A built-in arginine finger triggers the self-stimulatory GTPase-activating activity of Rho family GTPases. *J. Biol. Chem.* 274, 2609-2612.
44. Nadanaciva, S., Weber, J., Wilke-Mounts, S. & Senior, A. E. (1999). Importance of F_1-ATPase residue α-Arg-376 for catalytic transition state stabilization. *Biochemistry*, 38, 15493-15499.
45. Marrione, P. E. & Cox, M. M. (1996). Allosteric effects of RuvA protein, ATP, and DNA on RuvB protein-mediated ATP hydrolysis. *Biochemistry*, 35, 11228-11238.
46. George, H., Kuraoka, I., Nauman, D. A., Kobertz, W. R., Wood, R. D. & West, S. C. (2000). RuvAB-mediated branch migration does not involve extensive DNA opening within the RuvB hexamer. *Curr. Biol.* 10, 103-106.
47. Hiom, K. & West, S. C. (1995). Branch migration during homologous recombination: assembly of a RuvAB-Holliday junction complex *in vitro*. *Cell*, 80, 787-793.
48. Adams, D. E. & West, S. C. (1995). Unwinding of closed circular DNA by the *Escherichia coli* RuvA and RuvB recombination/repair proteins. *J. Mol. Biol.* 247, 404-417.
49. Muller, B., Tsaneva, I. R. & West, S. C. (1993b). Branch migration of Holliday junctions promoted by the *Escherichia coli* RuvA and RuvB proteins. II. Interaction of RuvB with DNA. *J. Biol. Chem.* 268, 17185-17189.
50. Nishino, T., Iwasaki, H., Kataoka, M., Ariyoshi, M., Fujita, T., Shinagawa, H. & Morikawa, K. (2000). Modulation of RuvB function by the mobile domain III of the Holliday junction recognition protein RuvA. *J. Mol. Biol.* 298, 407-416.
51. Gonzalez, S. & Wetmur, J. G. (2000). Holliday junction branch migration and resolution. RuvA, RuvB, and RuvC from the hyperthermophile *Thermotoga maritima*. *Methods Mol. Biol.* 152, 107-118.
52. Gonzalez, S., Rosenfeld, A., Szeto, D. & Wetmur, J. G. (2000). The Ruv proteins of *Thermotoga maritima*: branch migration and resolution of Holliday junctions. *Biochim. Biophys. Acta*, 1494, 217-225.
53. Otwinowski, Z. (1993). Data collection and processing. In *Proceedings of the CCP4 Study Weekend* (Sawyer, L., Isaacs, N. & Bailey, S., eds), pp. 56-62, Science and Engineering Research Council, Warrington.
54. Collaborative Computational Project Number 4 (1994). The CCP4 suite: programs for protein crystallography. *Acta Crystallog. sect. D*, 50, 760-763.
55. McRee, D. E. (1999). XtalView/Xfit - a versatile program for manipulating atomic coordinates and electron density. *J. Struct. Biol.* 125, 156-165.
56. Brünger, A. T., Adams, P. D., Core, G. M., Delano, W. L., Gros, P., Grosse-Kunstleve, R. W. *et al.* (1998). Crystallography & NMR system: a new software

suite for macromolecular structure determination. *Acta Crystallog. sect. D*, 54, 905-921.
57. Brünger, A. T. (1993). Assessment of phase accuracy by cross validation: the free *R* value. Methods and applications. *Acta Crystallog. sect. D*, 49, 24-36.
58. Svergun, D. I. (1993). A direct indirect method of small-angle scattering data treatment. *J. Appl. Crystallog.* 26, 258-267.
59. Svergun, D. I. & Stuhrmann, H. B. (1991). New developments in direct shape determination from small angle scattering. 1. Theory and model calculations. *Acta Crystallog. sect. A*, 47, 736-744.
60. Svergun, D. I., Barberato, C. & Koch, M. H. J. (1995). CRYSOL - a program to evaluate X-ray solution scattering of biological macromolecules from atomic coordinates. *J. Appl. Crystallog.* 28, 768-773.
61. White, A., Ding, X., van der Spek, J. C., Murphy, J. R. & Ringe, D. (1998). Structure of the metal-ion-activated diphtheria toxin repressor/*tox* operator complex. *Nature*, 394, 502-506.
62. Ariyoshi, M., Vassylyev, D. G., Iwasaki, H., Nakamura, H., Shinagawa, H. & Morikawa, K. (1994). Atomic structure of the RuvC resolvase: a Holliday junction-specific endonuclease from *E. coli*. *Cell*, 78, 1063-1072.

Edited by T. Richmond

(Received 14 March 2001; received in revised form 11 June 2001; accepted 11 June 2001)

THE JOURNAL OF BIOLOGICAL CHEMISTRY
© 1998 by The American Society for Biochemistry and Molecular Biology, Inc.

Vol. 273, No. 43, Issue of October 23, pp. 27786–27793, 1998
Printed in U.S.A.

An Eukaryotic RuvB-like Protein (RUVBL1) Essential for Growth*

(Received for publication, April 8, 1998, and in revised form, July 17, 1998)

Xiao-Bo Qiu, Yi-Ling Lin, Kelly C. Thome, Phillip Pian, Brian P. Schlegel, Stanislawa Weremowicz, Jeffrey D. Parvin, and Anindya Dutta‡

From the Division of Molecular Oncology, Department of Pathology, Brigham and Women's Hospital, Harvard Medical School, Boston, Massachusetts 02115

A human protein (RUVBL1), consisting of 456 amino acids (50 kDa) and highly homologous to RuvB, was identified by using the 14-kDa subunit of replication protein A (hsRPA3) as bait in a yeast two-hybrid system. RuvB is a bacterial protein involved in genetic recombination that bears structural similarity to subunits of the RF-C clamp loader family of proteins. Fluorescence *in situ* hybridization analysis demonstrated that the RUVBL1 gene is located at 3q21, a region with frequent rearrangements in different types of leukemia and solid tumors. RUVBL1 co-immunoprecipitated with at least three other unidentified cellular proteins and was detected in the RNA polymerase II holoenzyme complex purified over multiple chromatographic steps. In addition, two yeast homologs, scRUVBL1 and scRUVBL2 with 70 and 42% identity to RUVBL1, respectively, were revealed by screening the complete *Saccharomyces cerevisiae* genome sequence. Yeast with a null mutation in scRUVBL1 was nonviable. Thus RUVBL1 is an eukaryotic member of the RuvB/clamp loader family of structurally related proteins from bacteria and eukaryotes that is essential for viability of yeast.

Genetic recombination plays a critical role in maintaining gene diversification through chromosomal rearrangement and also genome stability through the repair of DNA damage. The activities of many proteins are required for recombination. In bacteria, for instance, RecA protein with the assistance of single-stranded DNA-binding protein promotes strand exchange with a homologous duplex and creates a four-strand intermediate or Holliday junction. The latter is then translocated by RuvA and RuvB proteins through branch migration and resolved by RuvC protein to yield recombinant DNA products (1). RuvB protein is a DNA-dependent ATPase and helicase that forms hexameric rings and has a low intrinsic affinity for DNA. RuvA is a structure-specific DNA-binding protein that has a high affinity for Holliday junctions and interacts with RuvB to form specific complexes with Holliday junctions. The presence of RuvA facilitates RuvB-mediated ATP hydrolysis and branch migration (2, 3).

Recombination activity has also been identified in eukaryotes and may be related to cell cycle progression. The Holliday intermediates in yeast accumulate to the highest level and become detectable during S phase (4). A yeast homolog of bacterial RecA, Rad51, is essential for spore formation during meiosis (5). Rad51 mRNA is significantly increased during meiosis and is also regulated during the mitotic cell cycle, with the highest levels found at the G_1/S boundary (6, 7). Homologs of bacterial RecA are also found in other eukaryotes, including *Xenopus laevis*, *Lilium longiflorum*, *Neurospora crassa*, *Arabidopsis thaliana*, mouse, chicken, and man (8), suggesting that the machinery involved in recombination is highly conserved among all organisms from bacteria to man. Consistently, single-stranded DNA-binding protein is also functionally conserved through evolution. Human single-stranded DNA-binding protein, also known as human replication protein A (hsRPA),[1] is a heterotrimer of 70, 32, and 14 kDa subunits. In both man and yeast, RPA serves as an important accessory factor in pairing and strand exchange carried out by Rad51 (9, 10).

Recent evidence suggests that recombination proteins may be physically associated with proteins involved in transcription. Tumor suppressor p53, a transcriptional activator for many important genes, has been demonstrated to interact with hsRPA (11) and with hRad51 to inhibit the activities of hRad51 in recombination (12). Tumor suppressor BRCA1 co-localizes at nuclear foci with hRad51 during S phase and co-immunoprecipitates with the same (13). However, BRCA1 is also a component of the RNA polymerase II holoenzyme (14) and has been implicated in transcriptional activation (15). Thus proteins like Rad51 and RPA, likely involved in recombination, physically interact with proteins involved in transcription.

In this paper, we report the identification of a human protein (RUVBL1) related in sequence to bacterial RuvB by using the 14-kDa subunit of human RPA (hsRPA3) as bait in a yeast two-hybrid system. The RUVBL1 gene is mapped to 3q21, a region with frequent rearrangements in different types of leukemia and solid tumors (16, 17). About 30% of the total cellular RUVBL1 co-purifies with the RNA polymerase II holoenzyme over multiple chromatographic steps. In addition, two yeast homologs scRUVBL1 (GenBank™ accession number S52968) and scRUVBL2 (GenBank™ accession number S61029) with 70 and 42% identity to RUVBL1, respectively, are revealed by screening the complete *Saccharomyces cerevisiae* genome sequence. Knockout of scRUVBL1 demonstrates that scRUVBL1 is essential for growth. Thus, RUVBL1 is an essential protein (in yeast) and is partly present in the RNA polymerase II holoenzyme complex.

* This work was supported in part by Grant GM53504 from the National Institutes of Health, Junior Faculty Research Award from the American Cancer Society (to J. D. P.), and Grant VM161 from the American Cancer Society (to A. D.). The costs of publication of this article were defrayed in part by the payment of page charges. This article must therefore be hereby marked "*advertisement*" in accordance with 18 U.S.C. Section 1734 solely to indicate this fact.

‡ To whom correspondence should be addressed: Brigham and Women's Hospital, Harvard Medical School, 75 Francis St., Thorn 630, Boston, MA 02115. Tel.: 617-278-0468; Fax: 617-732-7449; E-mail: adutta@rics.bwh.harvard.edu.

[1] The abbreviations used are: RPA, replication protein A; hs, *Homo sorpiens*; pol II, RNA polymerase II; kb, kilobase pair(s); DTT, dithiothreitol; PMSF, phenylmethylsulfonyl fluoride; PAGE, polyacrylamide gel electrophoresis; GAPDH, glyceraldehyde-3-phosphate dehydrogenase; GST, glutathione *S*-transferase; CBP, CREB-binding protein; bp, base pair(s).

EXPERIMENTAL PROCEDURES

Cloning and Sequencing—pAS-hsRPA3 was constructed by transferring the *Eco*RI-*Xho*I fragment of pEGRPA3 (18) to pAS2 (CLONTECH). hsRPA3 was expressed as a fusion protein containing a Gal4 DNA-binding domain in yeast Y190 (19). A human lymphocyte MATCHMAKER cDNA library (CLONTECH) was used for yeast two-hybrid interaction with hsRPA3. The transformation and selection procedures were performed according to the CLONTECH manual with slight modifications. The library plasmids harboring RUVBL1 cDNA were extracted from the screened yeast and sequenced. RUVBL1 cDNA sequence has been deposited in the GenBank™ (accession number AF070735).

Fluorescence in Situ Hybridization—An ~4.8-kb human genomic clone containing RUVBL1 was identified by screening a human placenta genomic library (CLONTECH) using the RUVBL1 cDNA as probe. The genomic clone was labeled with digoxigenin-11-dUTP as described (20). Hybridization of metaphase chromosome preparations from peripheral blood lymphocytes obtained from normal human males was performed with the RUVBL1 gene at 15 μg/ml in Hybeisol VI according to a previously described method (21).

Cell Culture—Human WI38 fibroblasts, 293T transformed embryonic kidney cells, or HeLa cells were grown in Dulbecco's modified Eagle's medium supplemented with 10% fetal bovine serum.

Anti-RUVBL1 Antibody, Immunoprecipitation, and Immunoblotting—Anti-RUVBL1 antiserum was raised in a rabbit using a recombinant His_6-tagged fragment of RUVBL1 containing amino acids 61–456 created by cloning the fragment of RUVBL1 cDNA into the *Xho*I site of pRSETC (Invitrogen). The antibody was further immunopurified from the antiserum using purified RUVBL1 as antigen. Immunoblotting was performed according to standard protocols.

293T cells were labeled with [^{35}S]methionine for 6 h in methionine-free Dulbecco's modified Eagle's medium following a 4-h starvation and lysed in RIPA buffer (150 mM NaCl, 0.1% SDS, 0.5% sodium deoxycholate, 1% Nonidet P-40, 50 mM Tris-HCl, pH 8.0, 1 mM DTT, and 0.1 mM PMSF). The lysate was precleared with preimmune serum bound to protein A-Sepharose for 1 h followed by a 1-h incubation with anti-RUVBL1 antiserum in the above lysis buffer. The precipitated complex was loaded on a 12% SDS-PAGE gel, and detected by autoradiography. To ensure that co-immunoprecipitating proteins were not a result of cross-reacting antibody, interactions were disrupted by lysing cells in 1% SDS at 100 °C. Samples were then diluted to RIPA buffer conditions and immunoprecipitated with the same antibodies.

Northern Blot (RNA) Analysis—Total RNA was extracted from HeLa cells as described (22). 10 μg of RNA/lane was separated on a formaldehyde-agarose gel and blotted to a nylon membrane. The blot was hybridized at 42 °C with a fragment of RUVBL1 cDNA encoding amino acids 61–456. The membranes were also hybridized with a 1.3-kb *Hin*dIII-*Pst*I cDNA fragment of glyceraldehyde-3-phosphate dehydrogenase (GAPDH) and cDNA fragments of 1.7 and 1.4 kb containing the entire open reading frames of cyclins B and E, excised out of RcCyclin B and RcCyclin E plasmids with *Hin*dIII and *Xba*I (23).

Purification of RUVBL1 Expressed in Insect Cells—Full-length RUVBL1 coding sequence was cloned into *Bam*HI/*Xho*I sites of pFastBac 1 (Life Technologies, Inc.) and transposed into a bacmid following the transformation of DH10 Bac (Life Technologies, Inc.). Then baculovirus bearing RUVBL1 was harvested from Sf9 insect cells transfected with the bacmid and employed to infect High 5 insect cells in Grace's insect medium supplemented with 10% heat-inactivated fetal bovine serum. The infected High 5 cells were harvested and lysed in lysis buffer (50 mM Tris acetate, pH 8.0, 150 mM KOAc, 1 mM EDTA, 10% glycerol, 1 mM DTT, 0.5% Nonidet P-40, and 0.1 mM PMSF). The lysate was first passed through phosphocellulose column equilibrated with TEGD buffer (20 mM Tris acetate, pH 7.7, 1 mM EDTA, 10% glycerol, 1 mM DTT, and 1 mM PMSF). The flow-through (fraction 1) was directly loaded onto a Q Sepharose column equilibrated with 50 mM KOAc in TEGD buffer and eluted with a 50–600 mM KOAc gradient in TEGD buffer. RUVBL1 was in the 200–350 mM KOAc fraction. Following overnight dialysis in TEGD buffer plus 50 mM KOAc, the above fraction containing RUVBL1 (fraction 2) was loaded onto a Mono Q fast protein liquid chromatography column equilibrated with 50 mM KOAc in TEGD buffer and eluted with a 50–350 mM KOAc gradient in TEGD buffer. RUVBL1 was eluted with ~260 mM KOAc and precipitated with 50% saturated ammonium sulfate for 1 h. The precipitate was dissolved in RUVBL1 storage buffer (20 mM Tris acetate, pH 7.7, 50 mM KOAc, 10% glycerol, 0.02 mM EDTA, 1 mM DTT, and 1 mM PMSF), dialyzed in the same buffer at 4 °C, and stored at −70 °C. RUVBL1 was followed in the above different steps by SDS-PAGE of fractions and Western blot with αRUVBL1 antibodies. The RUVBL1 protein purified over these steps was at least 95% pure.

ATPase Assays—Two assays, a TLC assay and a coupled spectrophotometric assay, have been used to measure ATPase activity of bacterial RuvB. They are suitable for measuring ATP hydrolysis rates at ATP concentrations below and above 125 μM, respectively. In the TLC assay (24, 25), reactions were carried out at 37 °C in the absence or presence of various DNAs including single-stranded or double-stranded linear DNAs, circular plasmid or phage DNAs, and synthetic Holliday junction DNAs at 20–200 μM (nucleotides). The reaction mixtures contained 20 mM Tris-HCl at pH 6.8–8.0, 1–32 mM $MgCl_2$, 1 mM DTT, 100 μg/ml bovine serum albumin, 25–1300 μM ATP, 40 μCi/ml [α-^{32}P]ATP, 0–0.5 μM hsRPA (18), and 0.6–4.0 μM purified RUVBL1. The reactions were stopped by addition of EDTA to 40 mM. Aliquots (1 μl) of reaction were spotted at various time points (1–60 min) onto polyethyleneimine-cellulose TLC plates, which were developed in 1 M formic acid/0.5 M LiCl. Hydrolysis of [α-^{32}P]ATP into [α-^{32}P]ADP was determined by autoradiograhpy.

The coupled spectrophotometric assay in which ATP hydrolysis was coupled with oxidation of NADH (24) employed pyruvate kinase and lactate dehydrogenase as an ATP regeneration system in addition to the reaction components supplemented in TLC assay. Because the oxidation of NADH can be detected at 380 nm by spectrophotometer, [α-^{32}P]ATP was omitted from the reaction mixture. An NADH extinction coefficient of $\epsilon_{380} = 1.21\ mM^{-1}\ cm^{-1}$ was used to calculate the rate of ATP hydrolysis.

Branch Migration and DNA Helicase Assays—Two assays using synthetic Holliday junctions and primer/template duplexes as substrates, respectively, were employed to measure branch migration and helicase activity of RUVBL1. Synthetic Holliday junctions were prepared essentially as described previously (26). The asymmetric Holliday junction was constructed from four oligonucleotides (oligos 1–4) with 88 or 89 bases. Oligo-1 was 5′-^{32}P-labeled prior to annealing using T4 polynucleotide kinase and [γ-^{32}P]ATP. Annealed junctions were purified by gel electrophoresis. The partial duplex markers used in the experiment shown in Fig. 4*B* were prepared by annealing 200 ng of ^{32}P-labeled oligo-1 with excess oligo-2 or -4. To determine the activity of RUVBL1, the reaction mixture (20 μl) contained ~2.5 ng of ^{32}P-labeled synthetic Holliday junction DNA in 20 mM Tris-HCl, pH 7.5, 10 mM $MgCl_2$, 1 mM dithiothreitol, 100 μg/ml bovine serum albumin, 1 mM ATP, and 0.6–4.0 μM RUVBL1 (26). Reactions lasted for 15–60 min at 37 °C and were stopped and deproteinized by the addition of 2 μl of 10× stop buffer to a final concentration of 20 mM Tris-HCl, pH 7.5, 25 mM EDTA, 0.5% SDS, and 2 mg ml^{-1} proteinase K. The samples were analyzed using a 6% polyacrylamide gel with a Tris borate buffer system. ^{32}P-Labeled DNAs were detected by autoradiography.

For simple helicase assays two primer/template duplexes were prepared in the same manner as the synthetic Holliday junctions. Two template oligonucleotides, 5′ to 3′ template and 3′ to 5′ template were used with their 3′ and 5′ ends, respectively, annealed to the ^{32}P-labeled primer. The DNA sequences for these oligonucleotides are the followings: primer, 5′-TGGTATGGTCAGCACTGCAGCCAGGATCAT-3′; 5′ to 3′ template, 5′-TCTCCCTATAGTGAGTCGTATTTTTGATCC-TGGCTGCAGTGCTCACCATACCA-3′; 3′ to 5′ template, 5′-ATGATC-CTGGCTGCAGTGCTCACCTTACCTTCTCCCTATACTGAGTCGTAT-TT-3′. Reaction mixtures contained 10 mM Tris-HCl, pH 8.0, 6 mM $MgCl_2$, 1 mM DTT, 2 mM ATP, 2 mM dATP or GTP or dNTP or NTP, 400 μg/ml bovine serum albumin, 2.5 nM of the annealed duplexes, and 1 μM RUVBL1. Following 2 h of incubation at 30 °C, the reactions were stopped by addition of stop buffer to a final concentration of 0.33% SDS, 17 mM EDTA, 14% glycerol, and 0.01% bromphenol blue. The samples were analyzed on an 18% polyacrylamide gel with a Tris borate buffer system. ^{32}P-Labeled DNAs were detected by autoradiography.

Purification of RNA Polymerase II Holoenzyme—pol II holoenzyme was purified from HeLa whole cell extracts through Bio-Rex 70 column, sucrose step gradient, and nickel nitrilotriacetate as described previously (14, 27). Pull-down of RNA polymerase holoenzyme from cell extracts by GST-CBP (containing amino acid residues 1805–1890 of CBP fused to glutathione *S*-transferase) or GST-BRCA1 (containing amino acid residues 1560–1863 of the familial breast cancer susceptibility gene product, BRCA1) has also been described in detail (27, 28).

scRUVBL1 Knockout and Rescue in Yeast—scRUVBL1 was amplified from yeast genomic DNA using polymerase chain reaction primer 1 (5′-CATGCCATGGTCGCTATCAGTGAAGTCA-3′; the ATG corresponding to the initiator methionine of scRUVBL1, GenBank™ accession number S52968) and primer 2 (5′-GGGGGATCCTTACAAA-TAATTTGCCGAAGTT-3′; the TTA is antisense to the termination codon TAA of the scRUVBL1 sequence). The 1.4-kb product containing

the entire open reading frame of scRUVBL1 was blunted at the *Nco*I site (by polymerase fill-in reaction) and inserted into pKS$^+$ (Stratagene) between the *Eco*RV and *Bam*HI sites in the polylinker. To knockout scRUVBL1, pKS$^+$-scRUVBL1 was digested with *Bgl*II and *Eco*RV, removing a 420-bp internal segment of the scRUVBL1 gene. This internal segment was replaced by a 1.2-kb *Hin*dIII fragment carrying the URA3 gene such that it was flanked by 630 bp of the 5′ and 330 bp of the 3′ end of scRUVBL1. The entire scRUVBL1-URA3 cassette was removed from the plasmid with *Sal*I and *Bam*HI and transformed into the diploid *S. cerevisiae* strain YSB455 (MATa/MATα ura3–52/ura3–52 leu2Δ1/leu2Δ1 trp1Δ63/trp1Δ63 his3Δ200/his3Δ200 lys2Δ202/lys2Δ202). Several URA$^+$ transformants were selected. Restriction digest and Southern analysis of genomic DNA identified several colonies with successful deletion of one copy of the scRUVBL1 gene. Sporulation and tetrad dissection was conducted for two independently derived yeast strains with a deletion of scRUVBL1 according to standard protocols.

To rescue the above yeast strains bearing a heterozygous deletion of scRUVBL1, a cDNA fragment containing scRUVBL1 open reading frame was inserted into an ectopic expression vector Yep51 (18) between *Sal*I and *Bam*HI sites. Following transformation of the strains with Yep51-scRUVBL1, the tetrads were sporulated and dissected. The strains were also transformed with Yep51 or Yep51-RUVBL1 instead of Yep51-scRUVBL1. To confirm the results of dissection, each haploid was tested by patch-mating with tester strains MAT a *met* and MAT α *met*, respectively.

RESULTS

Cloning of RUVBL1 Using Yeast Two-hybrid System—The yeast two-hybrid system is a sensitive *in vivo* method for identifying genes encoding proteins that interact with a protein of interest. Using hsRPA3 (the 14-kDa subunit of hsRPA) as a bait in the yeast two-hybrid system to screen a human cDNA library, we identified several cDNAs that encode potential hsRPA3-interacting proteins including one for RPA1 (the 70-kDa subunit of hsRPA) and a 1.8-kb novel cDNA. The latter encodes a protein of 456 amino acids (50 kDa), referred to as RUVBL1, and is a human homolog of the recently identified rat TBP-interacting protein (TIP49) (29). Amino acid sequences of RUVBL1 and TIP49 proteins are identical except that Ile^{291} in RUVBL1 is replaced by Val in TIP49. As reported previously (29), TIP49 shares high homology with RuvB proteins from different bacteria including *Thermus aquaticus thermophilus* (Ref. 30; GenBank™ accession number U38840), *Thermotoga maritima* (30), *Mycobacterium leprae* (GenBank™ accession number U00011) and *Borrelia burgdorferi* (GenBank™ accession number Y08885). As shown in Fig. 1, two regions of RUVBL1 (amino acids 26–88 and amino acids 277–425) are homologous to the RuvB sequence of *T. thermophilus* (30). *T. thermophilus* RuvB consists of 324 amino acids, and its amino acids 1–226 were aligned with the two regions of RUVBL1 in Fig. 1 (*A* and *B*). The two homologous regions between the two proteins are 25 and 38% identical, respectively, and 46 and 54% similar, respectively. The regions of homology contain Walker A and B motifs but are not restricted to just those motifs. Walker A (GxxGKT) and B (4 hydrophobic-DExH/N) motifs are involved in ATP binding and/or ATP hydrolysis of DNA/RNA helicases (31, 32). RUVBL1 contains an insertion of approximately 190 amino acids between the two regions. In a recent paper the bacterial RuvB protein was suggested to be structurally similar to subunits of RF-C and other clamp loader protein complexes associated with replicative DNA polymerases from multiple species (33). In support of this, we note a moderate sequence homology between RUVBL1, RuvB, and DNA polymerase III γ and τ subunits (GenBank™ accession number g580914) of *Bacillus subtilis* (Fig. 1*B*). Interestingly, like RUVBL1, the subunits of clamp loader protein complexes have insertions of different sizes between the regions containing the Walker A and B motifs (Ref. 33 and Fig. 1*B*). Taken together, we suggest that RUVBL1 is structurally a part of the RuvB/clamp loader subunit family of proteins.

Two putative yeast genes were identified in the *S. cerevisiae* genome encoding proteins scRUVBL1 and scRUVBL2 with 70 and 42% identity to RUVBL1, respectively. They are highly homologous to RUVBL1 over both the regions containing the Walker A and B motifs and over the third inserted region between the two motifs (Fig. 1, *A* and *B*). Because protein complexes involved in DNA repair and replication are remarkably well conserved in sequence and subunit composition between mammals and yeast, we anticipate that there are likely to be at least two related RUVBL proteins in humans. The human gene identified is more similar to scRUVBL1 than scRUVBL2 leading us to tentatively identify it as RUVBL1.

The human RUVBL1 gene was mapped to chromosome 3 in band q21 (3q21) using fluorescence *in situ* hybridization. Map position was determined by visual inspection of the fluorescent hybridization signals on 4,6-diamidino-2-phenylindole-dihydrochloride-stained metaphase chromosomes. In 18 of 20 metaphase preparations analyzed, hybridization signal was found to be present on the long arm of chromosome 3 in band q21; in 12 metaphase spreads both copies of chromosome 3 were labeled; and in 6 metaphase spreads signal was detected on one chromosome 3.

RUVBL1 mRNA Expression Is Constant through the Cell Cycle—Because Rad51 mRNA is regulated during the cell cycle (6, 7), it was interesting to determine whether the expression of RUVBL1 is similarly regulated. RUVBL1 mRNA levels were examined by Northern blot analysis of RNA from synchronous HeLa cells released from an M phase block by nocodazole (Fig. 2). The progressive decrease in cyclin B and increase in cyclin E mRNA levels indicates that the cells passed through G_1 and S synchronously. However, RUVBL1 mRNA was detected at a constant level during the cell cycle in comparison with the GAPDH control. Thus, unlike Rad51, which shows increased expression in S phase (6, 7), RUVBL1 mRNA is not cell cycle-regulated.

A 50-kDa RUVBL1 Protein Is Detected in Human Cell Lines—Antiserum against RUVBL1 was raised from a rabbit immunized with the His-tagged fragment of RUVBL1 (amino acids 61–456) overexpressed in *Escherichia coli*. Western blot with this antiserum detected a 50-kDa protein of the expected size in the following human cell lines: 293T (embryonic kidney cells transformed with adenovirus and SV40 T antigen), MCF7 (breast cancer cells), HeLa (cervical cancer cells), and WI38 (primary fibroblasts) (Fig. 3*A*, *lanes 1* and *2* and data not shown).

Because bacterial RuvB alone promotes branch migration and hydrolyzes ATP, we asked if the same was true for RUVBL1. RUVBL1 protein was overexpressed in High 5 insect cells infected with a recombinant baculovirus. In comparison with uninfected cells, a protein of 50 kDa matching the predicted size of intact RUVBL1 and three smaller breakdown products were detected in the infected cells by immunoblotting with anti-RUVBL1 antibody (Fig. 3*A*, *lanes 3–6*). Intact RUVBL1 was purified by conventional chromatography to >95% purity as shown in Fig. 3*B* (*lane 2*).

Unexpectedly, the purified RUVBL1 expressed in the insect baculovirus system did not hydrolyze ATP. Fig. 4*A* shows that RUVBL1 did not have any ATPase activity detected with TLC assay in the presence of 25 μM ATP. The results were still negative in the presence of higher concentrations of ATP up to 1.3 mM using both the TLC and the coupled spectrophotometric assays under the different buffer conditions described under "Experimental Procedures" despite the addition of different types of DNA substrates. There was no eukaryotic RUVB protein to be used as a positive control, and the conditions required for a prokaryotic RUVB protein may well be different from

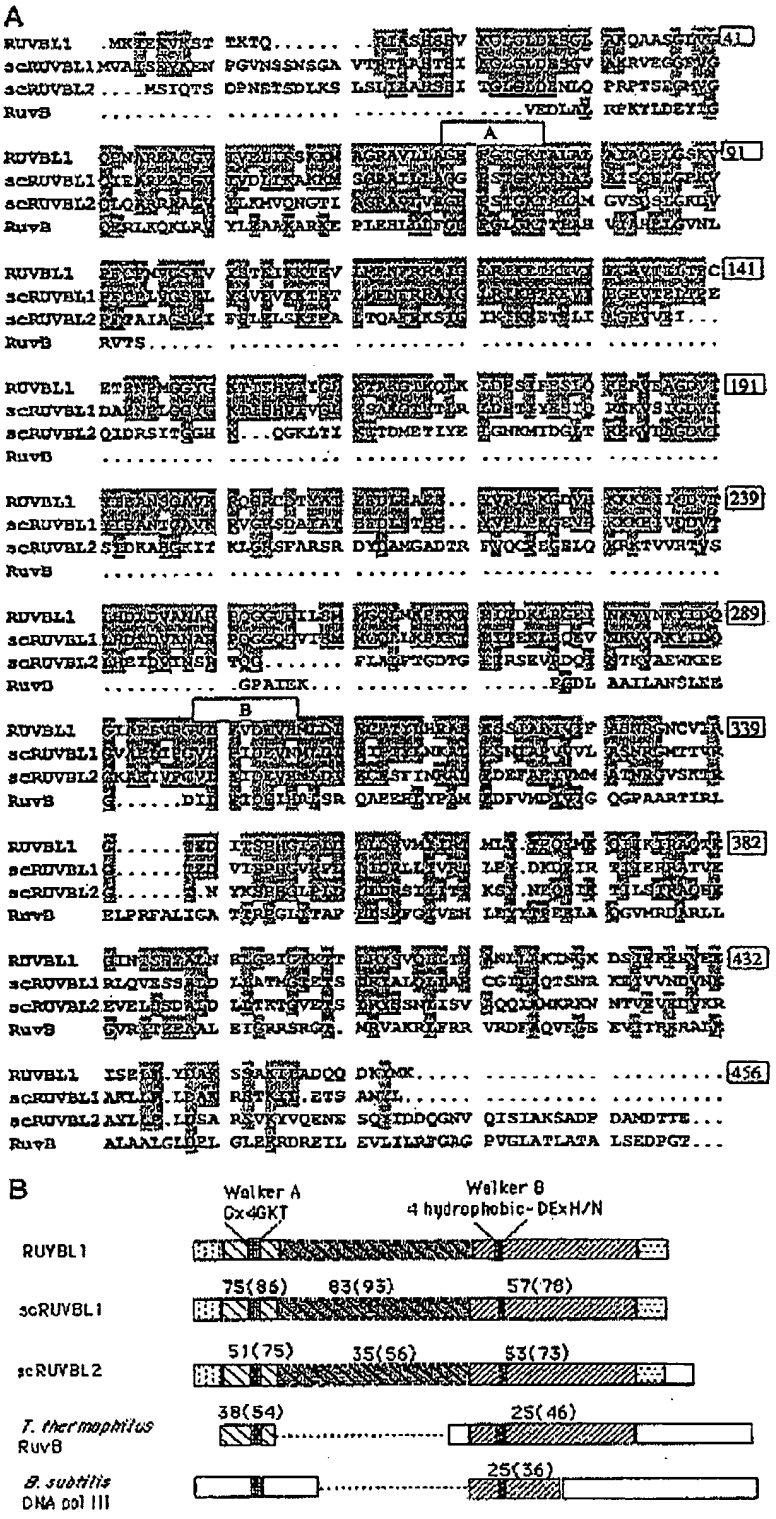

FIG. 1. *A*, the full-length sequence of RUVBL1, aligned by GCG Pileup program to show the identities with full-length scRUVBL1 (YDR190C on chromosome IV from coordinates 842032 to 840641) and scRUVBL2 (YPL235W on chromosome XVI from coordinates 103232 to 104647) as well as amino acids 1–280 of eubacteria *T. thermophilus* RuvB. The *shaded boxes* indicate the matches between RUVBL1 and any other sequences. The *dots* indicate gaps introduced in the sequences for optimal alignment. The sequences marked A and B are the Walker A and B motifs. *B*, a schematic representation of the eukaryotic RUVBL proteins, bacterial *T. thermophilus* RuvB protein and one example of a bacterial DNA polymerase clamp loader protein (*B. subtilis* DNA polymerase III; Ref. 42). The percentages of identity and similarity (in parenthesis) between each of the regions and the corresponding *shaded regions* of RUVBL1 are indicated.

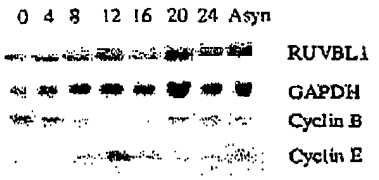

FIG. 2. **Expression of RUVBL1 mRNA through the cell cycle.** Levels of RUVBL1 mRNA in HeLa cells were examined by Northern blot analysis following the indicated hours of release from nocodazole block. The levels of cyclin B (expressed in G_2/M) and cyclin E (G_1) are shown as a reference of the cell cycle stage. GAPDH is a reference of the amount of RNA loaded. The 20-h sample is overloaded (see GAPDH control).

those that are optimal for the eukaryotic RUVBL1. Thus, High 5 cell lysate was utilized as a positive control to determine the sensitivity of the assays in detection of ATP hydrolysis (*lane 2* in Fig. 4*A*, and data not shown).

In the case of bacterial RuvBs, ATPase activity is required for helicase or branch migration activities. Therefore, it was unlikely that the purified RUVBL1 should possess any helicase activity. Indeed, the purified RUVBL1 failed to cause branch migration in a synthetic Holliday junction substrate (Fig. 4*B*). The RUVBL1 protein also failed to displace the primer strand on the primer-template duplexes described under "Experimental Procedures," suggesting that it did not have 5′-3′ or 3′-5′ helicase activities (data not shown).

RUVBL1-associated Cellular Proteins—We asked whether RUVBL1 was associated with any other cellular proteins. Immunoprecipitation of human cell lysate showed that RUVBL1 was associated with at least three other unidentified proteins. 293T cells were metabolically labeled with [^{35}S]methionine, and cellular proteins immunoprecipitated with anti-RUVBL1 antiserum. At least four bands of 160, 70, 50, and 45 kDa, respectively, were identified following immunoprecipitation (Fig. 5, *lane B*). To determine which band was from the direct interaction with anti-RUVBL1 antibodies, the cell lysate was prepared in parallel by lysing cells in 1% SDS and denatured by heating at 100 °C for 10 min. As shown in *lane D* of Fig. 5, only a 50-kDa band was detected from the denatured lysate, indicating that the 50-kDa peptide itself is RUVBL1, and the other three are RUVBL1-associated polypeptides.

Although RUVBL1 interacted with hsRPA in the yeast two-hybrid system, none of the RUVBL1 co-precipitated proteins were recognized by antibodies against hsRPA1, hsRPA2, or hsRPA3. Therefore, we have not been able to detect a stable complex between RUVBL1 and hsRPA. No ATPase or helicase activity was detected from the immunoprecipitates.

RUVBL1 Copurifies with RNA Polymerase II Holoenzyme Complex—It is possible that RUVBL1 is present in a larger complex of proteins and that the immunoprecipitation conditions disrupted such a complex. Gentler chromatographic conditions were employed to examine this issue. HeLa whole cell extract was applied to a Bio-Rex 70 column and eluted with increasing concentrations of potassium acetate. RUVBL1 was found in all fractions, although most was detected in the flow-through and the 0.6 M potassium acetate elute; the latter also contained about a half of pol II (Fig. 6*A*).

Because the 0.6 M Bio-Rex 70 fraction contains RNA pol II, we tested whether RUVBL1 was in the RNA polymerase holoenzyme complex. The 0.6 M Bio-Rex 70 column protein fraction was centrifuged through a sucrose gradient and analyzed by Western blotting (Fig. 6*B*). RUVBL1 and pol II appeared in a major peak centering on fractions 13–19. The holoenzyme-specific polypeptides cyclin C and cdk 8 are associated in these fractions (27). Thus, RUVBL1 co-eluted with the RNA pol II holoenzyme.

Holoenzyme peak fractions from the sucrose gradient were then subjected to metal chelate chromatography, and RUVBL1 again co-eluted with pol II (Fig. 6*C*). About 50% of RUVBL1 bound to the metal chelate matrix and co-eluted with pol II in fractions 11–13. As determined before (14), following the metal chelate chromatography, the holoenzyme was purified about 400-fold. About 30% of the total cellular RUVBL1 co-purified with the pol II holoenzyme.

Affinity matrices containing either residues 1805–1890 of CBP or residues 1560–1863 of BRCA1 have been demonstrated to specifically bind the pol II holoenzyme (27). As shown in Fig. 6*D*, RUVBL1 was also detected in the complex pulled down by either CBP or BRCA1, further suggesting that RUVBL1 is present in the pol II holoenzyme.

scRUVBL1 Is Essential for Growth—To test the biological importance of RUVBL1, one copy of *scRUVBL1* was deleted in diploid yeast by homologous recombination (Fig. 7*A*). Diploid yeast were transformed with a 2.2-kb linear DNA fragment containing the URA3 gene partially replacing scRUVBL1 sequence in open reading frame (Fig. 7*A*, *panel b*). Genomic DNA from transformed diploids was digested with *Bgl*II and probed on a Southern blot with a 630-bp fragment of *scRUVBL1*. Homologous recombination at the *scRUVBL1* locus removes a *Bgl*II site in the gene so that the probe should detect a fragment of 4230 bp instead of a fragment of 1770 bp from the wild type gene. In several of the diploids two bands of 4.2 and 1.8 kb were detected, indicating that the *URA3* gene was successfully integrated in one allele of *scRUVBL1* (Fig. 7*A*, *panel c*). Sporulation of these diploids and subsequent dissection of 12 tetrads resulted in a segregation of 2:2 for viability following meiosis (Fig. 7*B*, *panel 1*). All viable spores consistently lack URA3, which marked the deleted scRUVBL1 allele. Microscopic examination of the spores that failed to grow up into visible colonies revealed only four or five large budded cells from each spore, suggesting that scRUVBL1$^-$ yeast are nonviable. To further confirm this result, the yeast strain with heterozygous deletion of scRUVBL1 was transformed with a vector expressing ectopic scRUVBL1. 10 of 20 dissected tetrads grew into four viable colonies in the strains expressing ectopic scRUVBL1 (Fig. 7*B*, *panel 2*). Colonies from the dissected tetrads were verified as haploids by mating and segregated 2:2 for URA3 markers. In contrast, the strains transformed with the one containing human RUVBL1 (Fig. 7*B*, *panel 3*) or the empty vector (Fig. 7*B*, *panel 4*) produced only two viable colonies for each of 20 tetrads. Thus, the defect in scRUVBL1$^-$ yeast was rescued by extragenic scRUVBL1 under the control of a heterologous promoter but not by human RUVBL1. These data indicate that scRUVBL1 is essential for viability of yeast *S. cerevisiae*.

DISCUSSION

In the studies reported here, we identified a human protein RUVBL1 that interacts with hsRPA3 in a yeast two-hybrid system and is structurally similar to bacterial RuvB. The RUVBL1 gene was mapped to 3q21, a region with frequent rearrangements in different types of leukemia and solid tumors (16, 17). Thus, the assignment of the RUVBL1 gene to 3q21 encourages us to investigate in the future whether this gene is close to the rearrangement breakpoint and whether the gene or its expression is altered in tumors with this cytogenetic anomaly. In addition, two yeast homologs scRUVBL1 and scRUVBL2, which are 70 and 42% identical to RUVBL1, respectively, were revealed by screening the complete *S. cerevisiae* genome. Furthermore, we showed that RUVBL1 is present in the RNA polymerase II holoenzyme and that its yeast homolog scRUVBL1 is essential for growth.

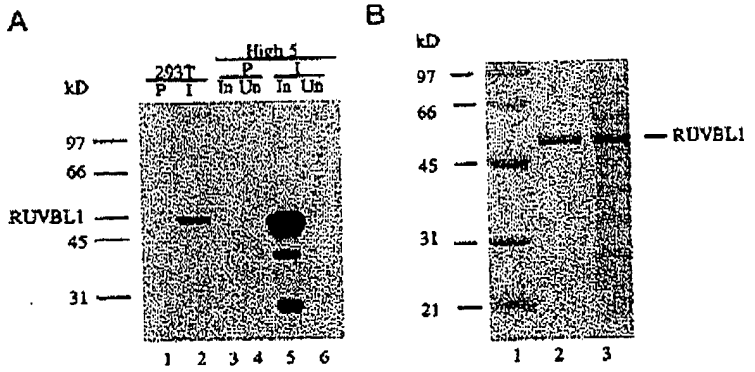

FIG. 3. **Identification and purification of RUVBL1.** *A*, identification of RUVBL1 by Western blot. S100 extract of human 293 cells and the lysate from High 5 insect cells infected (*In*) or uninfected (*Un*) with baculovirus bearing RUVBL1 cDNA were separated on 10% SDS-PAGE and blotted with rabbit preimmune serum (*P*) or immune antiserum against RUVBL1 (*I*). *B*, identification of purified RUVBL1 by SDS-PAGE and Coomassie Blue staining. *Lane 1*, protein marker; *lane 2*, purified RUVBL1; *lane 3*, the lysate of High 5 cells infected with baculovirus bearing RUVBL1 cDNA.

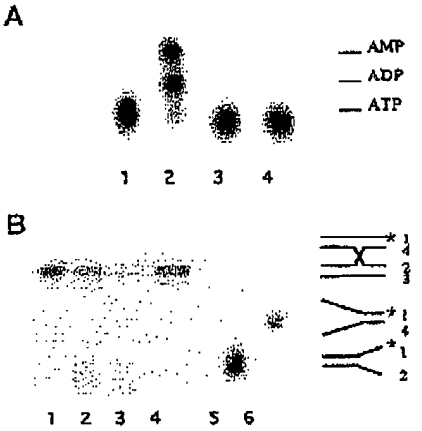

FIG. 4. **Purified RUVBL1 had no ATPase and helicase activities.** *A*, ATPase activity of RUVBL1 was tested with TLC in the reaction mixtures containing 20 mM Tris-HCl, pH 8.0, 20 mM $MgCl_2$, 1 mM DTT, 100 μg/ml bovine serum albumin, 25 μM ATP, 40 μCi/ml [α-^{32}P]ATP, 0.5 μM hsRPA, and either 0 μM (*lane 1*) or 1.2 μM of RUVBL1 (*lanes 3* and *4*) in the absence (*lane 1*) or presence of 100 μM (nucleotides) λ phage DNA (*lane 3*) or 20 μM (nucleotides) synthetic Holliday junctions (*lane 4*). *Lane 2* was a positive control in which RUVBL1 was replaced with High 5 cell lysate containing 0.5 mg/ml protein in the absence of DNAs. Reactions were carried out for 30 min at 37 °C, and the hydrolysis of ATP was assayed as described under "Experimental Procedures." *B*, branch migration assays were carried out using ^{32}P-labeled synthetic Holliday junctions as substrates in the reaction mixtures without (*lane 1*) or with the purified RUVBL1 at 1.2 μM (*lane 4*) or the RUVBL1-containing fraction 1 (*lane 2*; 0.24 mg/ml protein) or fraction 2 (*lane 3*; 0.23 mg/ml protein) as described under "Purification of RUVBL1 Expressed in Insect Cells" under "Experimental Procedures." After 30 min, the products were analyzed by gel electrophoresis and autoradiography. *Lanes 5* and *6* were the markers for partial duplexes, the products expected following complete branch migration.

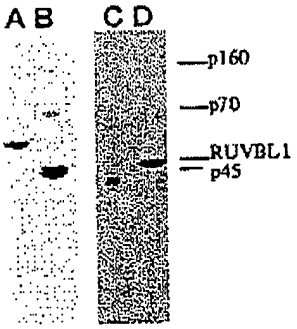

FIG. 5. **Determination of RUVBL1-associated proteins.** ^{35}S-Labeled proteins in undenatured (*lanes A* and *B*) or denatured (*lanes C* and *D*) 293T cell lysates were immunoprecipitated by preimmune serum (*lanes A* and *C*) or immune anti-RUVBL1 anti-serum (*lanes B* and *D*), separated on 12% SDS-PAGE gel, and detected by autoradiography. The polypeptides seen in the preimmune lanes were nonspecific and variable between different experiments.

Despite the sequence similarity between RUVBL1 and bacterial RuvB, we have not been able to detect ATPase and helicase activities using purified RUVBL1 expressed in baculovirus. This failure could result from inactivation of the protein during its purification from insect cells. Alternatively, the absence of these activities may reflect a requirement for additional reaction partners. One candidate partner is a RUVBL2 protein. It is interesting that biochemical studies of the bacterial RuvB hexamer have shown that only two of the six subunits bind ATP (34), indicative of a functional asymmetry in the RuvB hexamer. It is conceivable that a heteromer of RUVBL1 and RUVBL2 is necessary for ATP hydrolysis and strand displacement activity. Ongoing biochemical studies on yeast RUVBL proteins will test this hypothesis. As discussed earlier, the conservation of DNA replication and repair factors between yeast and humans make it likely that there is a human RUVBL2. Indeed, we have identified partial human cDNA sequences that appear to encode a related protein with more similarity to scRUVBL2 than to scRUVBL1. Whether these sequences truly represent human RUVBL2 will become evident once we have isolated full-length cDNA clones.

RUVBL may require partners unrelated to RuvB for its ATPase and helicase activities. Even though bacterial RuvB alone has weak ATPase and helicase activities *in vitro*, its *in vivo* activities require RuvA as a partner (35). A good candidate of a RuvA homolog is not obvious in the *S. cerevisiae* genome based on sequence analysis alone. However, this does not preclude the existence of such an eukaryotic RuvA-like molecule. As demonstrated in Fig. 5, RUVBL1 is associated with at least three other unidentified metabolically labeled proteins. Perhaps one of these RUVBL-associated proteins will emerge as an eukaryotic RuvA homolog, and our failure to observe ATPase or helicase activities in the immunoprecipitates may be caused by antibody inhibition or substoichiometric amounts of the part-

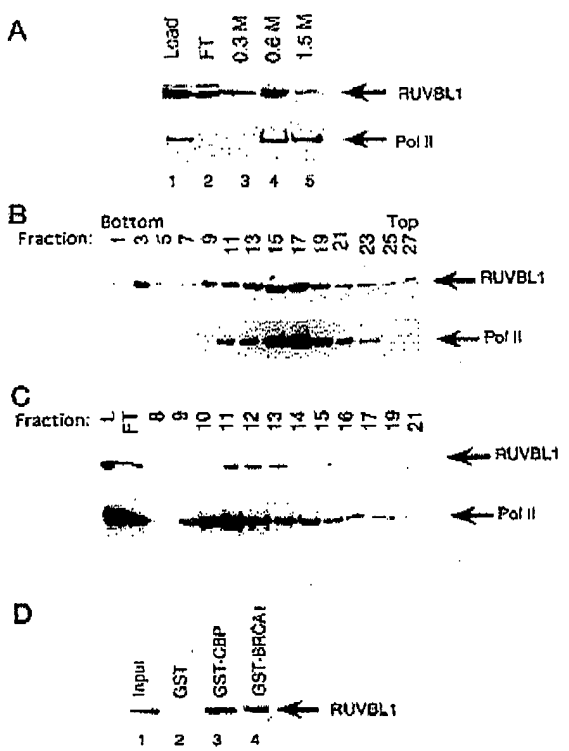

FIG. 6. **RUVBL1 copurified with RNA pol II holoenzyme.** *A*, HeLa whole cell extracts were chromatographed on Bio-Rex 70 matrix, and bound proteins were step-eluted at 0.3, 0.6, and 1.5 M KOAc. Protein samples from each fraction were subjected to SDS-PAGE, and blots were probed with RUVBL1 and pol II antibodies. *B*, the Bio-Rex 70 0.6 M fraction was subjected to centrifugation through a 10–60% sucrose gradient. After centrifugation, samples were collected and examined by Western blot with antibodies against RUVBL1 and pol II large subunit. *C*, fractions from sucrose sedimentation step were pooled and subjected to metal chelate chromatography. Fractions were eluted with a linear 5–130 mM gradient of imidazole. The indicated fractions were subjected to immunoblot analysis and probed with antibodies specific to RUVBL1 and pol II large subunit. *D*, GST fusion proteins GST-CBP (1805–1890) and GST-BRCA1 (1560–1863) were prebound to glutathione-agarose beads and then incubated with the fractions from Bio-Rex70 0.6 M elution step. Following washing in buffer containing 0.25 M KOAc and 0.5% Nonidet P-40, bound proteins were subjected to Western blotting and probed with immunopurified anti-RUVBL1 antibodies.

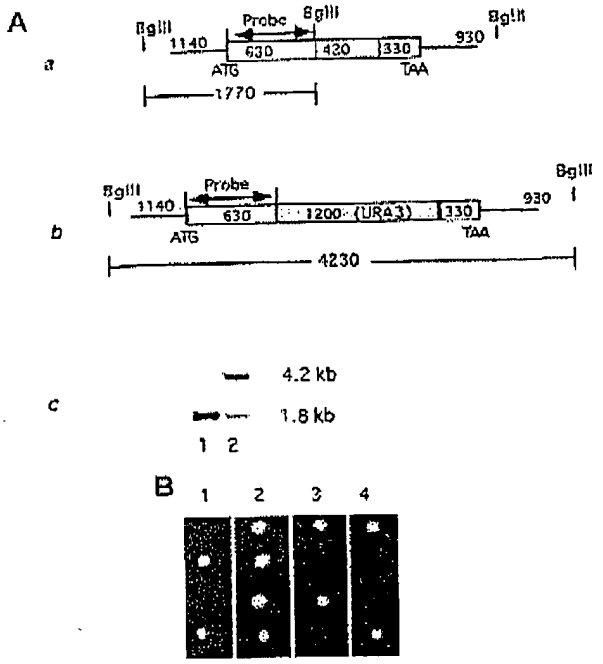

FIG. 7. **scRUVBL1 was essential for growth of yeast.** *A*, deletion of one allele of scRUVBL1. *Panels a* and *b* describe schematically wild type and partially replaced scRUVBL1 sequences, respectively. A deletion of one allele of *scRUVBL1* was detected by Southern blot of genomic DNA from scRUVBL1$^{+/-}$ (*panel c*, *lane 1*) or scRUVBL1$^{+/-}$ (*panel c*, *lane 2*) diploids with indicated probe according to standard protocols. *B*, diploid yeast with heterozygous knockout at the scRUVBL1 locus were either sporulated and dissected directly (*panel 1*) or following transformation with Yep51-scRUVBL1 (*panel 2*), Yep51-RUVBL1 (*panel 3*), or Yep51 (*panel 4*).

ner proteins. Additional proteins are also associated with RUVBL1 under gentler conditions of extraction (*e.g.* the polypeptides of the RNA polymerase II holoenzyme complex). ATPase and helicase activities have been reported in the RNA polymerase holoenzyme (36), and some of this may be due to RUVBL1 and its partners. Finally, RUVBL1 was shown to interact with hsRPA3 by the yeast two-hybrid assay but not by immunoprecipitation, indicating that low level or transient interactions of RUVBL1 with functional partners may be disrupted under conditions where the protein is extracted from cells. It may then be impossible to identify ATPase and helicase activity of RUVBL1 until the functional complex is reconstituted from recombinant proteins. Because we have a phenotype from the deletion of scRUVBL1, genetic complementation experiments in yeast will answer whether the Walker A and B motifs of scRUVBL1 are essential for the normal function of this protein. If the Walker A and B motifs prove essential genetically, biochemical experiments to demonstrate ATP binding (and hydrolysis) by scRUVBL1 (with or without putative partners) may be more successful.

BRCA1, which co-localizes and co-immunoprecipitates with hRad51 (13), is also a component of the RNA polymerase II holoenzyme (14), suggesting that DNA recombination repair proteins may be loosely associated with complexes involved in transcription. In this vein, it has also been noted that hRad51 and hsRPA, both of which are involved in DNA recombination repair, are present in RNA polymerase II holoenzyme under certain conditions (37). Recombination has been shown to be involved in the repair of mistakes ensuing from DNA replication and may be required for the completion of DNA replication. For example, mutations in DNA polymerases, ligases, topoisomerases, and DNA helicases all lead to increased mitotic recombination. The viability of some replication mutants also depends on recombination (4). These lines of evidence suggest that recombination plays a critical role in protecting genomic DNA from damage or mistakes. Genomic DNA in somatic cells is exposed to exogenous and endogenous damaging species throughout life. It is very important to have mechanisms to repair damaged DNA prior to transcription. Nucleotide excision repair has been linked to transcription. Proteins involved in nucleotide excision repair are found physically associated with transcription factors like TFIIH, facilitating the efficient repair of transcriptionally active areas of the genome (38–40). Based on its homology to RuvB, RUVBL1 is expected to be involved in recombination repair. As discussed above, BRCA1 is implicated in recombination repair because of its association with hRad51. Thus, the association of RUVBL1 and BRCA1 with the pol II holoenzyme complex may indicate that some aspects of recombination repair is similarly linked to transcription.

We did not expect a cellular component involved in recombination to be essential for viability. Although targeted disruption of the Rad51 gene leads to lethality in embryonic mice (41), a Rad51 null mutant of *S. cerevisiae* survives (5). Of course, other proteins in yeast may substitute for an essential function of Rad51. It is possible that recombination repair and scRUVBL1 are essential for accurate replication of the genome. The absence of scRUVBL1 may cause incomplete replication and result in cell death. Alternatively, if the co-purification of RUVBL1 with RNA polymerase holoenzyme implies that RUVBL1 has an essential function in transcription, the nonviability of scRUVBL1$^-$ yeast could be due to a global failure in transcription. Finally, there are other helicases in the RNA polymerase holoenzyme, including subunits of TFIIH and RNA helicase A, that facilitate the activation of transcription of specific promoters (35, 38). Thus, RUVBL1 may be essential for activation of transcription of certain essential genes. In conclusion, the sequence homology and biochemical fractionation data on RUVBL1 suggest that it is involved in recombination repair and/or transcription. Whether or not these or other unknown activities of RuvB make scRUVBL1 essential for viability remains to be determined.

Acknowledgments—We thank members of the Dutta Laboratory for helpful discussions, Nikhil Wagle for technical assistance, Laifong Lee and Dr. David Pellman for advice, and Dr. Cynthia C. Morton for critically reading the manuscript.

REFERENCES

1. Eggleston, A. K., Mitchell, A. H., and West, S. C. (1997) *Cell* 89, 607–617
2. Tsaneva, I. R., Muller, N., and West, S. C. (1992) *Cell* 69, 1171–1180
3. Muller, B., Tsaneva, I. R., and West, S. C. (1993) *J. Biol. Chem.* 268, 17179–17184
4. Zou, H., and Rothstein, R. (1997) *Cell* 90, 87–95
5. Shinohara, A., Ogawa, H., and Ogawa, T. (1992) *Cell* 69, 457–470
6. Flygare, J., Benson, F., and Hellgren, D. (1996) *Biochim. Biophys. Acta* 1312, 231–236
7. Yamamoto, A., Taki, T., Yagi, H., Habu, T., Yoshida, K., Yoshimura, Y., Yamamoto, K., Matsushiro, A., Nishimune, Y., and Morita, T. (1996) *Mol. Gen. Genet.* 251, 1–12
8. Gupta, R. C., Bazemore, L. R., Bulub, E. I., and Radding, C. M. (1997) *Proc. Natl. Acad. Sci. U. S. A.* 94, 463–468
9. Sung, P., and Robberson, D. L. (1995) *Cell* 82, 453–461
10. Baumann, P., and West, S. C. (1997) *EMBO J.* 16, 5198–5206
11. Dutta, A., Ruppert, J. M., Aster, J. C., and Winchester, E. (1993) *Nature* 365, 79–82
12. Sturzbecher, H. W., Donzelmann, B., Henning, W., Knippschild, U., and Buchhop, S. (1996) *EMBO J.* 15, 1992–2002
13. Scully, R., Chen, J., Plug, A., Xiao, Y., Weaver, D., Feunteun, J., Ashley, T., and Livingston, D. M. (1997) *Cell* 88, 265–275
14. Scully, R., Anderson, S. F., Chao, D. M., Wei, W., Ye, L., Young, R. A., Livingston, D. M., and Parvin, J. D. (1997) *Proc. Natl. Acad. Sci. U. S. A.* 94, 5605–5610
15. Sumasundaram, K., Zhang, H., Zeng, Y. X., Houvras, Y., Peng, Y., Zhang, H., Wu, G. S., Licht, J. D., Weber, B. L., and El-Deiry, W. S. (1997) *Nature* 389, 187–190
16. Kashuba, V. I., Gizatullin, R. Z., Protopopov, A. I., Allikmets, R., Korolev, S., Li, J., Bulden, F., Tory, K., Zabarovska, V., Maracek, Z., Sumegi, J., Klein, G., Zabarovsky, E. R., and Kisselev, L. (1997) *FEBS Lett.* 419, 181–185
17. Rynditch, A., Pekarsky, Y., Schnittger, S., and Gardiner, K. (1997) *Gene (Amst.)* 193, 49–54
18. Lin, Y.-L., Chen, C., Keshav, K. F., Winchester, E., and Dutta, A. (1996) *J. Biol. Chem.* 271, 17190–17198
19. Harper, J. W., Adami, G. R., Wei, N., Keyomarsi, K., and Elledge, S. J. (1993) *Cell* 75, 805–816
20. Zhao, Y., Bjorbaek, C., Weremowicz, S., Morton, C. C., and Moller, D. E. (1995) *Mol. Cell. Biol.* 15, 4353–4363
21. Ney, P. A., Andrews, N. C., Jane, S. M., Safer, B., Purucker, N. E., Weremowicz, S., Morton, C. C., Goff, S. C., Orkin, S. H., and Nienhuis, A. W. (1993) *Mol. Cell. Biol.* 13, 5604–5612
22. Chomczynski, P., and Sacchi, N. (1987) *Anal. Biochem.* 162, 156–159
23. Hinds, P. W., Millbrandt, S., Dulic, V., Arnold, A., Reed, S. I., and Weinberg, R. A. (1992) *Cell* 70, 993–1006
24. Marriane, P. E., and Cox, M. M. (1995) *Biochemistry* 34, 9809–9818
25. Mitchell, A. H., and West, S. C. (1996) *J. Biol. Chem.* 271, 19497–19205
26. Hiom, K., and West, S. C. (1995) *Cell* 80, 787
27. Neish, A. S., Anderson, S. F., Schlegel, B. P., Wei, W., and Parvin, J. D. (1998) *Nucleic Acids Res.* 26, 847–853
28. Anderson, S. F., Schlegel, B. P., Nakajima, T., Wolpin, E. S., and Parvin, J. D. (1998) *Nat. Genet.* 19, 254–256
29. Kanemaki, M., Makino, Y., Yoshida, T., Kishimoto, T., Koga, A., Yamamoto, K., Yamamoto, M., Moncollin, V., Egly, J.-M., Muramatsu, M., and Tamura, T. (1997) *Biochem. Biophys. Res. Commun.* 235, 64–68
30. Tung, J., and Wetmur, J. G. (1996) *J. Bacteriol.* 178, 2695–2700
31. Gorbalenya, A. E., Koonin, E. V., Donchenko, A. P., and Blinov, V. M. (1989) *Nucleic Acids Res.* 12, 4713–4730
32. Koonin, E. V. (1993) *Nucleic Acids Res.* 11, 2541–2547
33. Guenther, B., Onrust, R., Sali, A., O'Donnell, M., and Kuriyan, J. (1997) *Cell* 91, 335–345
34. Marriane, P. E., and Cox, M. M. (1996) *Biochemistry* 35, 11228–11238
35. Friedberg, E. C., Walker, G. C., and Siede, W. (1995) *DNA Repair and Mutagenesis*, p. 451, American Society for Microbiology, Washington, D. C.
36. Nakajima, T., Uchida, C., Anderson, S. F., Lee, C. G., Hurwitz, J., Parvin, J. D., and Montminy, M. (1997) *Cell* 90, 1107–1112
37. Makimoto, E., Shiekhattar, R., Sheldon, M., Cho, H., Drapkin, R., Rickel, P., Lees, E., Anderson, C. W., Linn, S., and Reinberg, D. (1996) *Nature* 381, 86–89
38. Lin, C. L. G., Kovalsky, O., and Grossman, L. (1998) *Nucleic Acids Res.* 26, 1466–1472
39. Winkler, G. S., Vermeulen, W., Coin, F., Egly, J. M., Hoeijmakers, J. H., and Weeda, G. (1998) *J. Biol. Chem.* 273, 1092–1098
40. Ali, R. B., Teo, A. K., Oh, H. K., Chuang, L. S., Ayl, T. C., and Li, B. F. (1998) *Mol. Cell. Biol.* 18, 1660–1669
41. Tsuzuki, T., Fujii, Y., Sakumi, K., Tominaga, Y., Nakao, K., Sekiguchi, M., Matsushiro, A., Yoshimura, Y., Morita, T. (1996) *Proc. Natl. Acad. Sci. U. S. A.* 93, 6236–6240
42. Struck, J. C., Vogel, D. W., Ulbrich, N., and Erdmann, V. A. (1988) *Nucleic Acids Res.* 16, 2720

Proc. Natl. Acad. Sci. USA
Vol. 96, pp. 7398–7402, June 1999
Genetics

Stimulation of homologous recombination in plants by expression of the bacterial resolvase RuvC

GIL SHALEV*†, YARON SITRIT*, NAOMI AVIVI-RAGOLSKI*, CONRAD LICHTENSTEIN‡, AND AVRAHAM A. LEVY*§

*Department of Plant Sciences, The Weizmann Institute of Science, Rehovot 76100, Israel; and ‡School of Biological Sciences, Queen Mary and Westfield College, University of London, London E1 4NS, United Kingdom

Edited by Nina Fedoroff, Pennsylvania State University, University Park, PA, and approved April 26, 1999 (received for review March 24, 1999)

ABSTRACT **Targeted gene disruption exploits homologous recombination (HR) as a powerful reverse genetic tool, for example, in bacteria, yeast, and transgenic knockout mice, but it has not been applied to plants, owing to the low frequency of HR and the lack of recombinogenic mutants. To increase the frequency of HR in plants, we constructed transgenic tobacco lines carrying the *Escherichia coli RuvC* gene fused to a plant viral nuclear localization signal. We show that *RuvC*, encoding an endonuclease that binds to and resolves recombination intermediates (Holliday junctions) is properly transcribed in these lines and stimulates HR. We observed a 12-fold stimulation of somatic crossover between genomic sequences, a 11-fold stimulation of intrachromosomal recombination, and a 56-fold increase for the frequency of extrachromosomal recombination between plasmids cotransformed into young leaves via particle bombardment. This stimulating effect may be transferred to any plant species to obtain recombinogenic plants and thus constitutes an important step toward gene targeting.**

Gene targeting (GT) involves the disruption or replacement of an endogenous allele by one manipulated *in vitro*. This replacement requires that after transfection into the target cell the transgene recombines with the target allele by homologous recombination (HR) by virtue of sharing extensive sequence similarity, rather than integrating randomly by illegitimate recombination. As HR occurs efficiently in many lower eukaryotes such as budding yeast and in bacteria, GT has proved to be a very powerful reverse genetic tool to study gene function. The GT technology is also now routine, if not still laborious in the generation of transgenic knockout mice, and has provided models for human genetic disease and the role of homeotic genes in development (1).

The mechanism of HR has long been an elusive, yet fascinating, problem. Studies in prokaryotes and lower eukaryotes have provided much insight into the nature of this process, the recombination intermediates, the genes, and the proteins involved (2–4). The basic steps of HR are listed below together with the proteins required in *Escherichia coli*: (*i*) initiation of HR by a DNA double-strand break and/or single-strand DNA formation by the RecBCD complex; (*ii*) exchange of DNA strands, including homology recognition and strand displacement, done by RecA-like proteins; (*iii*) heteroduplex extension, with branch or bubble migration, performed by RuvA plus RuvB or RecG to yield a recombination intermediate, a four-way DNA junction named the Holliday junction; and (*iv*) resolution of this heteroduplex Holliday junction by the endonuclease RuvC. Steps *iii* and *iv* have only very recently been elucidated: in *E. coli* the RuvA and RuvB proteins (encoded on one operon) have been shown to form a complex promoting ATP-dependent branch migration of Holliday junctions, a process of high importance for the formation of heteroduplex DNA. A second operon encodes *RuvC* and the *orf-26* gene; RuvC is the endonuclease that binds specifically, as a dimer, to Holliday junctions and promotes a subsequent resolution of Holliday junctions. Mutations in *RuvA*, *RuvB*, or *RuvC* result in defects in recombination and DNA repair. Genetic and biochemical studies indicate that branch migration and resolution are coupled by direct interactions between these three Ruv proteins, possibly by the formation of a RuvABC complex (4). A RuvC homolog, CCE1 (cruciform cutting endonuclease), has been reported for mitochondria of *Saccharomyces cerevisiae* (5) and for the fission yeast *Schizosaccharomyces pombe* (6). No plant homolog has yet been found.

In plants, the frequency of HR is low, as evidenced in the Kb/centiMorgan ratio, which is typically much higher than in lower eukaryotes or prokaryotes (7). However, GT has been demonstrated after direct delivery of DNA (8, 9) or by *Agrobacterium*-mediated infection (10, 11) using engineered genomic targets, albeit at a frequency 10^{-4}- to 10^{-5}-fold lower than illegitimate integration. There are two recent reports of GT in *Arabidopsis* via *Agrobacterium* infiltration *in planta* (12, 13). Unfortunately, the number of events was so small that it is not possible to obtain good GT frequency estimates. Low frequencies of HR also have been reported when quantification was done for intrachromosomal recombination (ICR) in tobacco and *Arabidopsis* (14–16). Similarly, the rate of somatic crossover between homologous chromosomes was shown to be very low (17, 18). Although low frequencies of HR are probably important to maintain stability of the repetitive plant genome, they are nonetheless a major hindrance to the implementation of the powerful GT technology in plants.

Why HR is inefficient in plants remains obscure. The recent isolation of *Arabidopsis* mutants affected in somatic and/or meiotic HR (19) might help identify the components of the plant recombination machinery and reveal how HR is regulated in plants. An alternative approach to overcoming the problem of low rates of HR is to overexpress well-characterized HR-related genes from heterologous species in plants and test how this affects HR in plants. By using this approach, (20) it was shown that the overexpression of the bacterial *RecA* gene in plants is associated with a 10-fold increase in the rate of intrachromosomal HR, suggesting that expression of the plant RecA homologs partially limits the rates of HR. Additional components must be tested to obtain a more comprehensive understanding of the control of HR in plants.

The publication costs of this article were defrayed in part by page charge payment. This article must therefore be hereby marked "*advertisement*" in accordance with 18 U.S.C. §1734 solely to indicate this fact.

PNAS is available online at www.pnas.org.

This paper was submitted directly (Track II) to the *Proceedings* office.

Abbreviations: HR, homologous recombination; GT, gene targeting; ICR, intrachromosomal recombination; GUS, β-glucuronidase; WT, wild type; NLS, nuclear localization signal; ECR, extrachromosomal recombination.

†Present address: Department of Human Genetics and Molecular Medicine, Sackler School of Medicine, Tel Aviv University, 69978, Israel.

§To whom reprint requests should be addressed. e-mail: Lplevy@weizmann.weizmann.ac.il.

Here, we constructed transgenic tobacco plants expressing *RuvC* and show that it is associated with a 12-fold increase in somatic crossover between genomic sequences, with an 11-fold increase in ICR, and with a 56-fold increase in extrachromosomal recombination (ECR) between plasmids cotransformed into leaves via particle bombardment. We discuss possible mechanisms leading to this increase as well as the possible applications for GT improvement.

MATERIALS AND METHODS

We built a series of constructs for studying the effect of RuvC on HR in tobacco plants. Plasmid pJD330, kindly provided by V. Walbot (Stanford University, Stanford CA), is a Bluescript derivative carrying the β-glucuronidase (*GUS*) reporter gene driven by the cauliflower mosaic virus 35S promoter fused to the tobacco mosaic virus translational enhancer Ω (21). Recombination partners were constructed, each with a different deletion in the *GUS* gene as described (22): one partner, 3′Δ *GUS*, (pGS001) carries a 700-bp (*SspI–EcoRI*) deletion in the 3′ region of *GUS*. The second partner, 5′Δ *GUS* (pGS003) carries a 12-bp 5′ deletion including the ATG initiation codon of *GUS*. Neither plasmid partner alone showed any GUS activity in transient assays. The *RuvC* sequence was obtained by PCR using two primers C5′ and C3′: 5′-GTCGACCATG-GCTATTATTCTCGGC-3′, 5′-GCATGCTAAGATCTAC-GCAGTCGCCCTCTCGC-3′, which carry *SphI* and *BglII* sites, respectively for use in further cloning. After amplification, a 520-bp amplified fragment was isolated, cloned, and subsequently fully sequenced to confirm that no amplification errors occurred. A *SalI–SphI* fragment of the *RuvC* gene was subcloned into identical sites of the pCd vector (a Bluescript derivative vector), giving rise to plasmid pGS021, which contains the RuvC ORF under the control of the 35S promoter and with termination sequences of *Octopine synthase (ocs)*. A 230-bp *SphI–BglII* fragment carrying a nuclear localization signal (NLS) (kindly given to us by Vitally Citovsky, State University of New York, Stony Brook) allowing protein targeting to the nucleus and taken from the *Nla* gene of tobacco etch virus (23) was subcloned into the same sites of plasmid pGS021, giving rise to plasmid pGS022, consisting of the 35S-*RuvC*-NLS-*OCS* 3′ components. A 2,050-bp *Asp718–SpeI* fragment including the four components was subcloned into the *Asp718–XbaI* sites of the pPZP111 binary vector (24), giving rise to plasmid pGS023.

Tobacco Transformation. The binary vector mentioned above was introduced by electroporation into the *Agrobacterium tumefaciens* LB4404 strain (25). The transformed *Agrobacterium* strains were used to infect leaf discs of two *Nicotiana tabacum* cultivars (cv. Samsun-NN and cv. Xanthi) and regenerate transgenic plants as described by Horsch (26). All of the plants [wild type (WT) and transgenic] in the Xanthi background were heterozygote for the *Sulfur* chlorophyll mutation (*Su/su*). All transgenic plants carried transformation markers that confer resistance to kanamycin (100 mg/liter). The number of T-DNA copies was determined on the basis of kanamycin resistance frequency in T_2 self-pollinated seedlings and by Southern blot analysis (data not shown).

For the ICR assay, transgenic tobacco plants transformed with a construct that enables us to monitor HR through reactivation of the GUS gene were used. These plants were kindly provided by Barbara Hohn (Friedrich Miescher Institute, Basel, Switzerland) and are described by Puchta *et al.* (16). GUS activity was determined by histochemical staining of 3-week-old seedlings as described (22).

Biolistic Transformation and the ECR Assay. The 3′Δ *GUS* plasmid (pGS001), with and without the 5′Δ *GUS* (pGS003) plasmid linearized at its unique *SpeI* restriction site, was transformed into leaves of WT and *RuvC*-expressing plants through biolistic bombardment, using the helium-driven PDS-1000/He system (Bio-Rad), according to the manufacturer's instructions. Seven leaves, 3–4 cm long taken from WT Samsun-NN or from RuvC-expressing plants in the same Samsun-NN background, were biolistically transformed, and after 30 hr of recovery, GUS activity was determined by histochemical staining as described (22). Monitoring of HR was done by counting the number of blue spots per bombarded leaf, as seen under a binocular microscope.

RNA Extraction and Northern Blotting. Plant RNA samples were isolated from young leaves of WT Xanthi plant and transgenic lines expressing RuvC in the Xanthi background with the Tri Reagent-RNA/DNA/protein isolation reagent kit (Molecular Research Center, Cincinnati). Northern blot analysis was performed with a nylon membrane following the manufacturer's instructions.

RESULTS

Expression of RuvC in Plants. To overproduce the bacterial RuvC protein in plant nuclei, an expression vector carrying the *RuvC* ORF downstream of the 35S promoter with a translational fusion to the carboxyl terminus of a NLS was cloned in a T-DNA binary vector (Fig. 1*A*). This vector was transformed into tobacco plants by agroinfection, and expression of *RuvC* was tested by Northern blot analysis in T1 plants and WT. As shown in Fig. 1*B*, an 800-nt fragment was detected from five independent transformation events. The size of this fragment is, as expected for the pGS022 construct, suggesting that RuvC mRNA is properly processed, and the band intensity (out of the total RNA) suggests that *RuvC* transcript is relatively abundant in the transgenic plants. These transgenic lines did not show any indication of retarded growth, suggesting that the transformation procedure and the expression of the *RuvC*-NLS transcript did not interfere with the normal pattern of plant development. Similarly, there was no decrease in pollen fertility, and cytogenetic analyses performed at different stages of meiosis did not provide evidence for chromosomal loss or breakage (data not shown). This finding suggests that overall these plants are relatively genetically stable.

Increased ECR in RuvC-Expressing Plants. A rapid assay to test the recombinogenicity of *RuvC*-expressing plants is to quantify the frequency of homologous recombination between extrachromosomal molecules: two plasmids, pGS001 and pGS003, were cotransformed, via particle bombardment, into leaves of transgenic plants expressing *RuvC* and WT control plants. RuvC-expressing plants were kanamycin-resistant progeny of T1 plants and therefore segregate for *RuvC* homozygous and heterozygous plants. Both WT and transgenic plants are of the same Samsun-NN genetic background. Each of these plasmids contains a different mutation that prevents GUS expression (Fig. 2*A*): pGS001 has a deletion in the 3′ end (3′ΔGUS in Fig. 2), and pGS003, a deletion in the 5′ end (5′ΔGUS in Fig. 2). The two plasmids share 1,800 bp of identical sequences, and GUS activity can be restored upon HR between the two plasmids and can be quantified by the number of blue spots (Fig. 2). Linearization of pGS003 at the *SpeI* site, located between the 35S promoter and the GUS gene (Fig. 2), was done to increase the efficiency of HR in the assay, in accordance with findings of various labs (27). This assay is similar in principle to the previously described ECR bombardment assay (28) with different recombination substrate molecules. Both the 3′ and the 5′ deleted GUS plasmids were found to be GUS negative when transformed separately either in WT tobacco or RuvC-expressing plants (Fig. 2*A*). However, after cotransformation of the two plasmids, blue spots were detected in leaves of *RuvC*-expressing plants and leaves of the WT line (Fig. 2 *C* and *D*). Blue spots were counted for each bombarded leaf under a binocular microscope. An average of two spots per leaf was detected in the WT (Fig. 2*C*), whereas an average of 111 spots was detected in leaves of the RuvC-

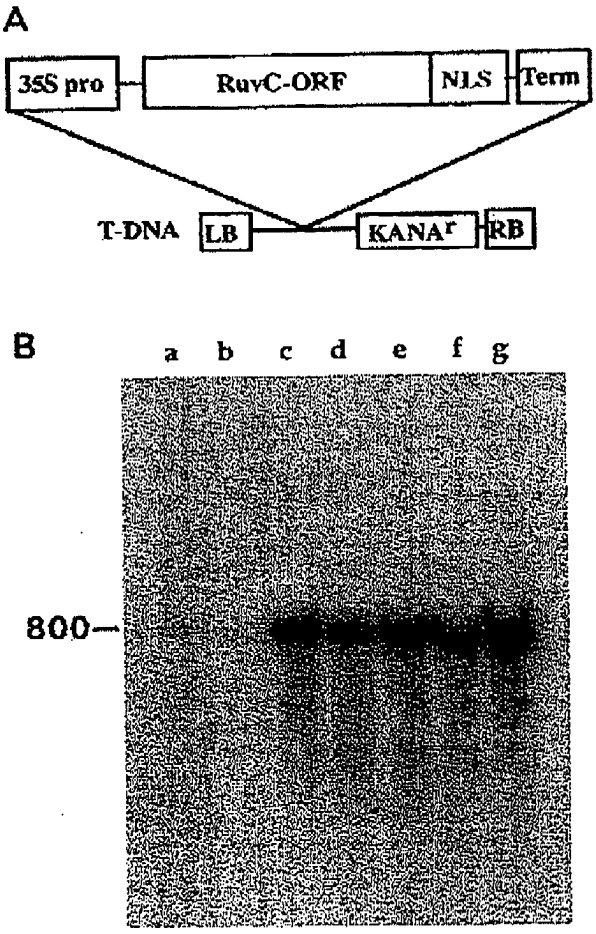

FIG. 1. Expression of RuvC in transgenic plants. (*A*) The expression vector contains the RuvC ORF translationally fused in the carboxyl-terminal region to the NLS derived from the tobacco etch virus (23), and cloned between the cauliflower 35S promoter (35S pro) and the transcription termination region from the octopine synthase gene (Term). This expression cassette was cloned into the pPZP111 binary vector (24), giving rise to clone pGS023, and was transformed in tobacco. (*B*) Transcription of RuvC was determined by Northern blotting of total RNA and hybridization with the RuvC ORF fragment as a probe. An 800-nt transcript was detected in five independent transgenic plants (background of *Su/su* cv. Xanthi) transformed with pGS023 (lanes c–g), but not in the nontransformed control *Su/su* Xanthi line (lanes a and b).

expressing plants treated under the same transformation conditions (Fig. 2*D*), i.e., *RuvC* expession was associated with a ≈56-fold increase in ECR. The frequency of blue spots observed with a positive 35S-GUS control was similar in RuvC-expressing plants or in the WT control (Fig. 2*B*), indicating that RuvC does not improve transformability or expression of the bombarded leaves (data not shown). The blue spots were bigger when bombardment was done with 35S-GUS than with the recombination partners (Fig. 2 *B* vs. *D*), presumably because of the larger copy number of GUS-expressing plasmid molecules transformed with 35S (all the molecules on the bead) than with the cotransformed deleted recombination substrates (only recombinant molecules).

Increased ICR in RuvC-Expressing Plants. The effect of *RuvC* on ICR was determined by using the previously described ICR "GU-US" assay. According to this assay, ICR

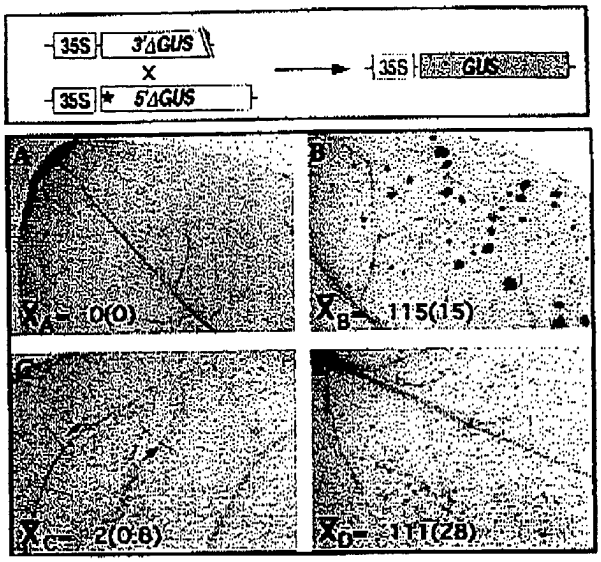

FIG. 2. ECR in RuvC-expressing plants. (*Top*) A schematic representation of the constructs used for the ECR assay is shown. Homologous recombination between two defective GUS genes, one of which is deleted in the 3′ region (3′ΔGUS) and one in the 5′ region (5′ΔGUS), gives rise to a GUS active gene (the blue box on the *Top Right* and the blue spots in the *Middle* and *Bottom*). (*Middle and Bottom*) Pictures of tobacco leaves (cv. Samsun-NN) that underwent bombardment and staining for GUS activity are shown, together with the average number of blue spots per leaf and the SEM in parenthesis. (*A–C*) Bombardment of the 3′ΔGUS or of the 5′ΔGUS plasmid alone (*A*) and of the 35S-GUS gene (*B*), and cotransformation of the 3′ΔGUS and 5′ΔGUS-containing plasmids into WT tobacco (*C*). (*D*) Cotransformation of the 3′ΔGUS and 5′ΔGUS plasmids in transgenic plants expressing RuvC.

events are recognized as blue sectors after histochemical staining of seedlings. It was shown that these sectors are obtained through the reactivation of a GUS reporter gene via HR between two directly repeated truncated GUS fragments (GU and US), which share a 0.6-kb long overlap (14). We have compared the occurrence of blue sectors in the cotyledons and in the first and second true leaves of F_1 (RuvC X GU-US) seedlings of a cross between RuvC-expressing plants [in the *N. tabacum* cv Samsun (N/N) background] and plants homozygous for the GU-US construct, versus the F_1 (Samsun X GU-US) seedlings of a cross between the *N. tabacum* cv Samsun (N/N) and plants homozygous for the GU-US construct. In both crosses the GU-US construct is in an hemizygote dose, and the genetic background is similar. Therefore, the differences in frequency of blue sectors between the two crosses, as shown in Table 1, are most probably related to the activity of *RuvC*. The expression of *RuvC* was associated with

Table 1. Frequency of blue sectors in seedlings of plants carrying the GUS ICR assay and expressing *RuvC*

Cross	No. of stained seedlings	No. of blue sectors*
F_1 (GU-US X *RuvC*)		
Cross no. 71	337	11
Cross no. 72	30	1
Cross no. 73	211	6
Cross no. 74	250	6
Total	828	24
F_1 (GU-US X Samsun)	402	1

*Blue sectors were monitored in cotyledons and in the first or second true leaf. Most sectors were from cotyledons.

an 11.4-fold increase in the frequency of blue sectors. Note that in RuvC X GU-US, the data presented in Table 1 is from four crosses (nos. 71–74), each with an independent *RuvC* transformant, and no obvious differences in ICR frequency was found between the crosses. One difference was in the size of the sectors. Cross no. 74 had small sectors (1–2 cells large), whereas the other crosses had larger sectors (1–16 cells), indicating late recombination in cross no. 74. Tobacco cotyledons can be used to determine the ICR frequency because the development (number of cells and patterns of divisions) of this organ is well understood (29). Based on the frequency and size of blue sectors in cotyledons (data not shown), we estimate that ICR occurs in the 10^{-6} range/genome in the presence of *RuvC* and in the 10^{-7} range in WT tobacco.

Increased Somatic Crossover in RuvC-Expressing Plants. The effect of *RuvC* on somatic crossover was determined by using the frequency of twin sectors in T1 *Su/su* Xanthi transgenic plants expressing *RuvC* transcript (Fig. 1). The sulfur gene (*Su*) controls chlorophyll pigmentation in tobacco. It is characterized by a pale green color in leaves and shoots of heterozygote *Su/su* plants (30). Self-pollination of *Su/su* plants gives rise to progeny that segregate for ¼ dark green *Su/Su* plants, ½ pale green *Su/su* plants, and ¼ yellow *su/su* plants that die soon after germination. *Su/su* plants occasionally give rise to simple dark green or white sectors or to twinned (contiguous dark green and white) sectors (Fig. 3*A*). These sectors can occur as a result of various genetic events, such as point mutations at the sulfur locus, chromosome loss or breakage, chromosome nondisjunction, or somatic crossover. Carlson (17) has provided direct evidence that most twinned sectors (12 of 13 sectors regenerated and cytologically analyzed) in *Su/su* tobacco plants are derived from somatic crossover (17). We found, via cytological analysis and pollen viability, that transgenic lines carrying *RuvC* did not show any evidence for chromosomal instability (data not shown). These data, in accordance with Carlson's previous analysis, suggest that twin sectors correspond to somatic crossover events rather than to chromosome loss associated with chromosome gain in the sister cell. The frequency of twinned sectors (average number per leaf) in *RuvC*-expressing plants and in the WT cultivar used for the production of the transgenic *RuvC* plants is shown in Fig. 3*B*. There is a 12-fold higher frequency of twin sectors in *RuvC* compared with WT plants, suggesting that somatic crossover is significantly increased as a result of *RuvC* expression. This effect on twin sectors was found in six different transgenic lines expressing the *RuvC* transcript, ruling out the possibilities of position effect, spontaneous mutation, or somaclonal variation. Moreover we have made several transgenic plants in the *Su/su* background with constructs that do not express RuvC, and these plants did not show increased somatic crossover. Therefore, the mere fact of being transgenic (i.e., to undergo transformation and regeneration and to express antibiotic resistance genes) does not normally increase the rate of somatic crossover.

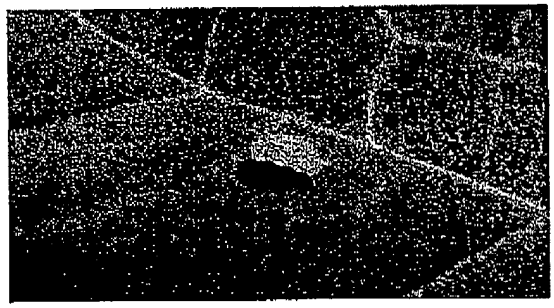

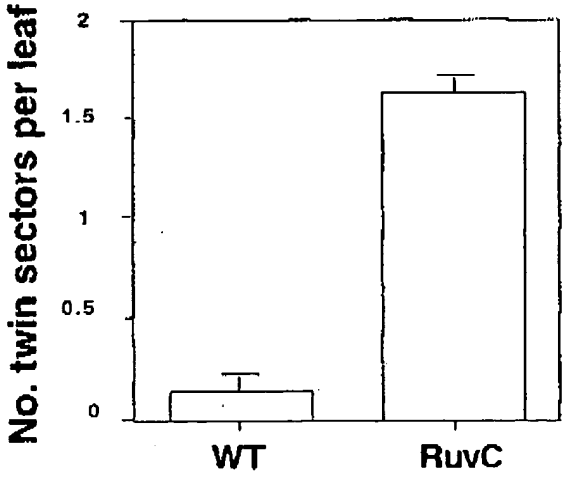

FIG. 3. Frequency of twin sectors in RuvC-expressing *Su/su* plants. A picture of a twin sector is shown on the background of a light green (*Su/su*) tobacco leaf (*Upper*). The dark green and the yellow sectors are contiguous and probably were formed as a result of somatic crossover (17). The number of twin sectors was counted in 20 leaves per plant. (*Lower*) The average number of twin spots per leaf is shown with error bars representing the SEM. This average was calculated out of six T1 transgenic plants originating from independent transformation events of *Su/su* plants with RuvC (i.e., 6 × 20 = 120 leaves) and three *Su/su* nontransformed plants (i.e., 3 × 20 = 60 leaves).

DISCUSSION

This study shows that overexpression of *RuvC* is associated with increased HR in higher eukaryotes. This effect was observed for ICR with the somatic crossing-over twin-sector assay (12-fold increase), ICR with the GU-US assay (11-fold), and extrachromosomal plasmid sequences with the ECR bombardment assay (56-fold increase) in tobacco plants.

The stimulating effect of *RuvC* on HR in plants is surprising as this protein is active at the final steps of the HR process. This effect might result from one or from a combination of the following possibilities. The increased HR frequency might result from a direct RuvC effect: plant cells might contain several heteroduplex DNA molecules, which for some unclear reasons are not efficiently resolved under normal levels of expression. In the WT, cells with unresolved heteroduplexes would stop dividing. Overproduction of RuvC could lead to RuvC-mediated cleavage of these unresolved structures and thus enable cell division to proceed and subsequent twin sector formation. Similarly, in the ECR assay, RuvC expression might enable the resolution of heteroduplexes between the transformed plasmids, which, otherwise (in the WT) would accumulate. It has been shown for mitochondrial DNA that the number of unresolved junctions increases significantly in *ccc1* (CCE1 is the yeast homolog to RuvC) yeast mutants (31). Another possible explanation for the RuvC effect is that in plants, Holliday junctions might resolve in favor of the parental configuration (with subsequent gene conversion) to avoid chromosome translocations between repeats. Maybe RuvC removes this bias and permits resolution to give crossover recombinants. RuvC overproduction also might have a nonspecific, yet nonetheless direct, effect on HR through nonspecific DNA binding, nuclease activity, and subsequent induction of the endogenous HR machinery, in a genome-wide fashion, to repair the damage. It has been found, *in vitro*, that in addition to the high affinity binding capacity to four-way DNA junctions, CCE1 is able to bind duplex DNA molecules, albeit with lower affinity (5).

The effect of RuvC on HR might be specific but indirect. It was discussed earlier that branch migration and resolution of the Holliday junctions may be coupled by direct interactions between RuvA, RuvB, and RuvC proteins, possibly by the formation of a RuvABC complex (4). If so, it is conceivable that the overexpressed RuvC protein recruits RuvA- and RuvB-like plant proteins in the cells to form the complex indispensable for branch migration and resolution of Holliday junctions. Thus, the increased HR frequency might result from increased helicase activity of RuvA and RuvB and may affect earlier steps of HR rather than the final resolution step. So far, plant homologs of RuvC, RuvA, and RuvB proteins have not been identified.

In conclusion, although we do not understand the mechanism by which RuvC stimulates both genomic and extrachromosomal HR in plants, the expression of this protein can lead to the engineering of recombinogenic plants. Such plants, in combination with the development of improved gene targeting vectors, may enable high frequencies of exogenous DNA integration into chromosomal targets via HR and thus facilitate reverse genetics in plants by gene targeting.

We thank Prof. Barbara Hohn for the ICR-GUS tobacco seeds, Dr. Shahal Abu, Dr. Dvora Aviv, and Dr. Ron Vunsh for help and discussions, and the Israeli Plant Genome Center for help with the particle bombardment experiments. This work was performed with support from a United Kingdom-Israel grant to A.A.L. and C.L.

1. Capecchi, M. R. (1997) *Cold Spring Harb. Symp. Quant. Biol.* **62**, 273–281.
2. Camerini-Otero, R. D. & Hsieh, P. (1995) *Annu. Rev. Genet.* **29**, 509–552.
3. Kowalczykowski, S. C. (1994) *Experientia* **50**, 204–215.
4. West, S. (1997) *Annu. Rev. Genet.* **31**, 213–244.
5. White, M. F. & Lilley, D. M. J. (1997) *J. Mol. Biol.* **266**, 122–134.
6. Whitby, M. C. & Dixon, J. (1997) *J. Mol. Biol.* **272**, 509–522.
7. Puchta, H. & Hohn, B. (1996) *Trends Plant Sci.* **1**, 340–348.
8. Halfter, U., Morris, P. & Willmitzer, L. (1992) *Mol. Gen. Genet.* **231**, 186–193.
9. Paszkowski, J., Baur, M., Bogucki, A. & Potrykus, I. (1988) *EMBO J.* **7**, 4021–4026.
10. Lee, K. Y., Lund, P., Lowe, K. & Dunsmuir, P. (1990) *Plant Cell* **2**, 415–425.
11. Offringa, R., De Groot, M. J. A., Haagsman, H. J., Does, M. P., Van den Elzen, P. J. M. & Hooykaas, P. J. J. (1990) *EMBO J.* **9**, 3077–3084.
12. Miao, Z.-H. & Lam, E. (1995) *Plant J.* **7**, 359–365.
13. Kempin, S. A., Liljegren, S. J., Block, L. M., Rounsley, S. D. & Yanofsky, M. F. (1997) *Nature (London)* **389**, 802–803.
14. Swoboda, P., Gal, S., Hohn, B. & Puchta, H. (1994) *EMBO J.* **13**, 484–489.
15. Tovar, J. & Lichtenstein, C. (1992) *Plant Cell* **4**, 319–332.
16. Puchta, H., Swoboda, P. & Hohn, B. (1995) *Plant J.* **7**, 203–210.
17. Carlson, P. S. (1974) *Genet. Res.* **24**, 109–112.
18. Evans, D. A. & Paddock, E. F. (1976) *Can. J. Genet. Cytol.* **18**, 57–65.
19. Masson, J. E. & Paszkowski, J. (1997) *Proc. Natl. Acad. Sci. USA* **94**, 11731–11735.
20. Reiss, B., Klemm, M., Kosak, H. & Schell, J. (1996) *Proc. Natl. Acad. Sci. USA* **93**, 3094–3098.
21. Gallie, D. R., Sleat, D. E., Watts, J. W., Turner, P. C. & Wilson, T.-M.A. (1987) *Nucleic Acids Res.* **15**, 3257–3273.
22. Shalev, G. & Levy, A. A. (1997) *Genetics* **146**, 1143–1151.
23. Carrington, J. C., Freed, D. D. & Leinicke, A. J. (1991) *Plant Cell* **3**, 953–962.
24. Hajdukiewicz, P., Svab, Z. & Maliga, P. (1994) *Plant Mol. Biol.* **25**, 989–994.
25. Hockema, A., Hirsch, P. R., Hooykaas, P. J. J. & Schilperoort, R. A. (1983) *Nature (London)* **303**, 179–180.
26. Horsch, R. B., Fry, J. E., Hoffmann, N. L., Eichholtz, D., Rogers, S. G. & Fraley, R. T. (1985) *Science* **227**, 1229–1231.
27. Puchta, H., Swoboda, P. & Hohn, B. (1994) *Experientia* **50**, 277–284.
28. Masson, J. E., King, P. J. & Paszkowski, J. (1997) *Genetics* **146**, 401–407.
29. Fridlender, M., Lev-Yadun, S., Baburek, I., Angelis, K. & Levy, A. A. (1996) *Planta* **199**, 307–313.
30. Burk, L. G. & Menser, H. A. (1964) *Tob. Sci.* **8**, 101–104.
31. Lockshon, D., Zweifel, S. G., Freeman-Cook, L. L., Lorimer, H. E., Brewer, B. J. & Fangman, W. L. (1995) *Cell* **81**, 947–955.

Arabidopsis Nucleolar Protein Database

Bioinformatics Home

Arabidopsis Nucleolar Protein Database - Table of Nucleolar Proteins

Species	Locus	Arabidopsis Gene Descriptor	Protein Class	Localisation	Image Present	Human 692 Protein	Reciprocal BLAST
arabidopsis	At5g22330	RuvB DNA helicase-related protein	snoRNP (C/D) biogenesis	nd		●	●

Images

There are no images for this particular sample.

Additional Information Resources

The following information resources may be availablefor your Locus. Click on the images below to go to that data source.

Information Resource	Description
tair	Information on At5g22330 at TAIR (The Arabidopsis Information Resource)
mips	Information on At5g22330 at MIPS (Munich Information Center for Protein Sequences)
e	Information on At5g22330 at Entrez (NCBI Cross Database Search)

Human and Yeast Orthologues

Click on the images in the 'Data Sources' column to retrieve further information.
SGD = The *Saccharomyces* Genome Database.

Species	Locus	Description	E Value to Previous	Data Sources
human	RUVBL1	RuvB-like 1 (TIP49 - TATA binding protein interacting protein 49kDa)	0	Entrez
yeast	Rvb1	No Description Available	e-160	SGD Entrez

BLASTx vs Human Nucleolar Proteome

Red highlighting of score column represents low score values.

Arabidopsis Nucleolar Protein Database

id_description	subject_name	Length	score	bits	%	p	matches	Pos	length	IPI
TATA box-bindingprotein-interacting protein-related [Arabidopsis thaliana] (458 letters)	>IPI: IPI00021187.1| SWISS-PROT: Q9Y265| REFSEQ_NP: NP_003698| TREMBL: P82276| ENSEMBL:EN SP00000318297 Tax_Id=9606 RuvB-like 1	456	1671	648	70	0.0	320	391	455	IPI00021187

Click here to return all BLAST hits

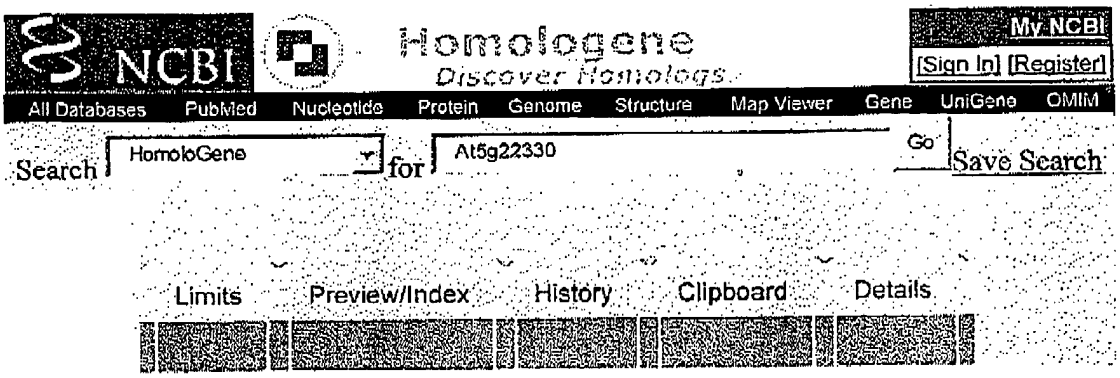

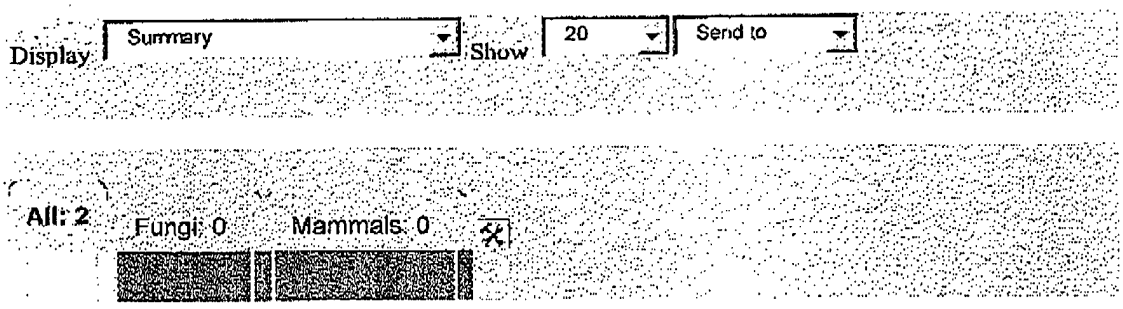

Items 1 - 2 of 2 One p

1: HomoloGene:37839. Gene conserved in Eukaryota

H.sapiens	RUVBL1	RuvB-like 1 (E. coli)
C.familiaris	LOC476512	similar to RuvB-like protein 1
M.musculus	Ruvbl1	RuvB-like protein 1
R.norvegicus	Ruvbl1	RuvB-like protein 1
G.gallus	LOC416022	similar to RuvB-like 1 (49-kDa TATA box-bi...
D.melanogaster	pont	pontin
A.gambiae	3290812	Anopheles gambiae str. PEST ENSANGG0000002...
C.elegans	5K460	RuvB-like 1 (5K460)
S.pombe	SPAPB8E5.09	Schizosaccharomyces pombe SPAPB8E5.09 gene
S.cerevisiae	RVB1	Saccharomyces cerevisiae RVB1 gene
K.lactis	KLLA0D185...	Kluyveromyces lactis NRRL Y-1140 KLLA0D185...
E.gossypii	AGL119C	Eremothecium gossypii AGL119C gene
M.grisea	MG03958.4	Magnaporthe grisea 70-15 MG03958.4 gene
N.crassa	NCU03482.1	Neurospora crassa NCU03482.1 gene

A.thaliana	At5g22330	Arabidopsis thaliana At5g22330 gene
O.sativa	OJ1014_E0...	Oryza sativa (japonica cultivar-group) OJ1...

2: HomoloGene:72366. Gene conserved in Eukaryota

P.troglodytes	LOC460670	TATA binding protein interacting protein 4...
R.norvegicus	LOC299306	similar to RuvB-like protein 1
O.sativa	P0506B12.32	Oryza sativa (japonica cultivar-group) P05...
P.falciparum	PF11_0071	Plasmodium falciparum 3D7 PF11_0071 gene

>at5g22330 Ruv DNA-helicase-like protein

General properties

Length [aa]	458
Molecular weight [Da]	50323.7
Isoelectric point	5.7
Manually edited	no
Contig name	chr5:chromosome5_v181103
Position	[7449818] 7449818-7449729, 7449155-7448967, 7448846-7448715, 7448623-7448474, 7448267-7448112, 7447954-7447820, 7447734-7447669, 7447572-7447466, 7447374-7447275, 7447196-7447105, 7447022-7446953, 7446862-7446773 [7446773]
GC content [%]	43.7

Protein function

Closest homologue (BLASTP)	TREMBL|AB007651_11 product: "Ruv DNA-helicase-like protein"; Arabidopsis thaliana genomic DNA, chromosome 5, P1 clone:MWD9. 0.0
Functional categories	04 transcription 04.05 mrna transcription 04.05.01 mrna synthesis 04.05.01.01 general transcription activities
Automatically derived functional categories	63.03 nucleic acid binding 1e-137 - H.sapiens_exp 40.10 nucleus 1e-137 - H.sapiens_exp 04 TRANSCRIPTION 1e-137 - H.sapiens_exp 03.01.05.03 DNA recombination 1e-137 - H.sapiens_exp 03.03.02 meiosis 1e-137 - H.sapiens_exp 25.05.25 gametogenesis 1e-137 - H.sapiens_exp 63.19 nucleotide binding 1e-137 - H.sapiens_put 63.01 protein binding 1e-134 - D.melanogaster_put 03.01.03 DNA synthesis and replication 1e-126 - A.thaliana_put 03.01.05 DNA recombination and DNA repair 1e-126 - A.thaliana_put 06.01 protein folding and stabilization 1e-123 - H.sapiens_exp 40.03 cytoplasm 1e-123 - H.sapiens_exp 03.01.05.01 DNA repair 1e-123 - H.sapiens_exp 05 PROTEIN SYNTHESIS 1e-123 - H.sapiens_exp 62.01.07 binding / dissociation 1e-123 - H.sapiens_exp
COGs 1e-62	COG1224 DNA helicase TIP49, TBP-interacting protein COG0465 ATP-dependent Zn proteases 1e-39
PFAM domains	PF06068 TIP49 C-terminus 1.5e-217
BLOCKS	IPB001984 ATP-dependent serine proteases, Lon family PR00819 CbxX/CfqX superfamily signature PR00918 Calicivirus non-structural polyprotein
family signature	IPB002648 Isopentenyl transferase IPB003442 Uncharacterised P-loop hydrolase UPF0079
PROSITE motifs	ATP_GTP_A (1)
Automatically derived PIR superfamilies	PIR|JC5521 JC5135 0.0 PIR|JC5521 trehalose trehalohydrolase 0.0

1121D At5g22330 MIPS report.txt
PIR|JE0334 hydrolase 0.0
PIR|T19534 n MJ1163 1e-135
PIR|T40697 ein MJ1163 2e-97
PIR|F75150 63 5e-96
PIR|S61029 se 1e-94
PIR|D71191 RY ah1827 1e-94
PIR|T46049 conserved hypothetical protein MJ1163 2e-93
PIR|D69476 se trehalohydrolase 2e-90
Automatically derived keywords PIR|JC5521 atp 0.0

Protein structure

Known3D PDB|1njg mol:protein length:250 DNA Polymerase III Subunit Gamma
PDB|1ixz mol:protein length:254 ATP-Dependent Metalloprotease Ftsh
PDB|1lv7 mol:protein length:257 Ftsh
PDB|1d2n mol:protein length:272 N-Ethylmaleimide-Sensitive Fusion Protein
PDB|1nsf mol:protein length:273 N-Ethylmaleimide Sensitive Factor
PDB|1iy2 mol:protein length:278 ATP-Dependent Metalloprotease Ftsh
PDB|1ofh mol:protein length:310 ATP-Dependent Hsl Protease ATP-Binding Subun
PDB|1hqc mol:protein length:324 Ruvb
PDB|1iqp mol:protein length:327 Rfcs
PDB|1in5 mol:protein length:334 Holliday Junction DNA Helicase Ruvb
PDB|1jr3 mol:protein length:373 DNA Polymerase III Subunit Gamma
PDB|1do0 mol:protein length:442 Heat Shock Locus U
PDB|1g4a mol:protein length:443 ATP-Dependent Hsl Protease ATP-Binding Subun
PDB|1kyi mol:protein length:444 ATP-Dependent Hsl Protease ATP-Binding Subun
PDB|1g3i mol:protein length:444 ATP-Dependent Hslu Protease ATP-Binding Subu
PDB|1g41 mol:protein length:444 Heat Shock Protein Hslu
PDB|1e32 mol:protein length:458 P97
PDB|1ksf mol:protein length:758 ATP-Dependent Clp Protease ATP-Binding Subun
PDB|1oz4 mol:protein length:806 Transitional Endoplasmic Reticulum Atpase
PDB|1qvr mol:protein length:854 Clpb Protein
PDB|1im2 mol:protein-het length:444 ATP-Dependent Hsl Protease ATP-Binding S

SCOP domains d1d2na_ c.37.1.13 (A:) Hexamerization domain of N-ethylmalemide-sensitive fusion (NSF) protein {Chinese hamster (Cricetulus griseus)}
d1g41a_ c.37.1.13 (A:) Hslu {Haemophilus influenzae}
d1in4a2 c.37.1.13 (A:17-254) Holliday junction helicase RuvB {Thermotoga maritima}
d1iqpa2 c.37.1.13 (A:2-232) Replication factor C {Archaeon Pyrococcus furiosus}
d1e32a2 c.37.1.13 (A:201-458) Membrane fusion atpase p97, D1 domain {Mouse (Mus musculus)}
Structural class Alpha_Beta

Low complexity 3.7 %

Structural summary

```
Sequence        MEKVKIEEIQSTAKKQRIATHTHIKGLGLEPTGIPIKLAAGFVGQLEAREAAGLVVDMIK
Structure       ........hhhhhhhhhhhh............hhhhhhh..hhhhhhhhhhhhhhhhhh
Low complexity  ................................................................
Non-globular    ..NNNNNNNNNNNNNNNNNNNNNNNNNNNNNNNNNNNNNNNNNNNNNNNNNNNNNNNN

Sequence        QKKMAGKALLLAGPPGTGKTALALGISQELGSKVPFCPMVGSEVYSSEVKKTEVLMENFR
Structure       hhhhhhheeeee......hhhhhhhhhhhh............hhhhhhhhhhhhhhhhhh
Low complexity  ................................................................
Non-globular    NNNNNNNNNNNNNNNNNNNNNNNNNNNNNNNN....NNNNNNNNNNNNNNNNNNNN

Sequence        RAIGLRIKETKEVYEGEVTELSPEETESLTGGYGKSISHVVITLKTVKGTKHLKLDPTIY
Structure       hhhhhhhhhhhhh...eee.............eeeeeeeee.....eeeee...hh
Low complexity  ..............LLLLLLLLLLLLLLLL..............................
Non-globular    NNNNNNNNNNNNNNNNNNNNNNNNNNNNNNNNNNNNNNNNNNNNNNNNNNNNNNNNN

Sequence        DALIKEKVAVGDVIYIEANSGAVKRVGRSDAFATEFDLEAEEYVPLPKGEVHKKKEIVQD
Structure       hhhhhhhhh...eeeeee....eeee....hhhhhhhhhhhh........hhhhhhhhee
Low complexity  ................................................................
Non-globular    NNNNNNNNNNNNNNNNNNNNNNNNNN.....................................

Sequence        VTLQDLDAANARPQGGQDILSLMGQMMKPRKTEITDKLRQEINKVVNRYIDEGVAELVPG
Structure       eeehhhhh.........hhhhhhhhhh....hhhhhhhhhhhhhhhhhhhh.........
Low complexity  ................................................................
Non-globular    ................................................................

Sequence        VLFIDEVHMLDMECFSYLNRALESSLSPIVIFATNRGVCNVRGTDMPSPHGVPIDLLDRL
Structure       eeee........hhhhhhhhhhh....eeeeee.....eee.............hhhhhh
Low complexity  ................................................................
Non-globular    ................................................................

Sequence        VIIRTQIYDPSEMIQIIAIRAQVEELTVDEECLVLLGEIGQRTSLRHAVQLLSPASIVAK
Structure       hhhhh.....hhhhhhhhhhhhhhhhhhhhhhhhhhhhh..hhhhhhhhhhh....eeee
Low complexity  ................................................................
Non-globular    ................................................................

Sequence        MNGRDNICKADIEEVTSLYLDAKSSAKLLHEQQEKYIS
Structure       ........hhhhhhhhhhhhhh.hhhhhhhhhhhh...
Low complexity  .....................................
Non-globular    .....................................
```

Protein Detail

Protein: AT5G22330.1

Date last modified	2004-05-05			
TAIR Accession	AASequence:4015249			
External IDs	**SwissPROT**	**PIR**	**GenPept**	**Similar Proteins in Genbank**
	Q9FMR9		15242217	NCBI BLink

Properties

Calculated MW	50306.0
Calculated PI	5.7333
Length (aa)	458

Domains

Database	Structural Class Type	Accession	Interpro	Position
tigrfam		TIGR00635	RuvB	37-175
pfam		PF00004	AAA ATPase centr	68-422
pfam		PF06068	TIP49, C-terminal	120-442
superfam	Alpha and beta proteins (a/b)	52540		37-123
superfam	Alpha and beta proteins (a/b)	52540		295-440
superfam	Alpha and beta proteins (a/b)	52540		66-148
superfam	Alpha and beta proteins (a/b)	52540		177-268

Sequence

Send to WU-BLAST

```
  1 MEKVKIEEIQ STAKKQRIAT HTHIKGLGLE PTGIPIKLAA GFVGQLEARE
 51 AAGLVVDMIK QKKMAGKALL LAGPPGTGKT ALALGISQEL GSKVPFCPMV
101 GSEVYSSEVK KTEVLMENFR RAIGLRIKET KEVYEGEVTE LSPEETESLT
151 GGYGKSISHV VITLKTVKGT KHLKLDPTIY DALIKEKVAV GDVIYIEANS
201 GAVKRVGRSD AFATEFDLEA EEYVPLPKGE VHKKKEIVQD VTLQDLDAAN
251 ARPQGGQDIL SLMGQMMKPR KTEITDKLRQ EINKVVNRYI DEGVAELVPG
301 VLFIDEVHML DMECFSYLNR ALESSLSPIV IFATNRGVCN VRGTDMPSPH
351 GVPIDLLDRL VIIRTQIYDP SEMIQIIAIR AQVEELTVDE ECLVLLGEIG
401 QRTSLRHAVQ LLSPASIVAK MNGRDNICKA DIEEVTSLYL DAKSSAKLLH
451 EQQEKYIS
```

Protein Detail

Associated Genes	**Gene Model** ?	**Locus** ?	**seqviewer link**
	AT5G22330.1	AT5G22330	Sequence Viewer

External Link The Arabidopsis Subcellular Proteomics Database (ASPD)

User Comments ?
(shows only the most recent comments by default)

Add My Comment | Hide Comments | Show All Comments

Attribution	**type**	**name**	**date**
	submitted_by	AGI-TIGR	2001-08-22

NCGR ABRC Carnegie

General comments or questions: curator@arabidopsis.org
Seed or DNA stock questions (donations, availability, orders, etc): abrc@arabidopsis.org

Arabidopsis Nucleolar Protein Database

Bioinformatics Home

Arabidopsis Nucleolar Protein Database - Table of Nucleolar Proteins

Species	Locus	Arabidopsis Gene Descriptor	Protein Class	Localisation	Image Present	Human 692 Protein	Reciprocal BLAST
arabidopsis	At5g67630	RuvB DNA helicase-related protein	snoRNP (C/D) biogenesis	nd		●	●

Images

There are no images for this particular sample.

Additional Information Resources

The following information resources may be availablefor your Locus. Click on the images below to go to that data source.

Information Resource	Description
tair	Information on At5g67630 at TAIR (The Arabidopsis Information Resource)
mips	Information on At5g67630 at MIPS (Munich Information Center for Protein Sequences)
e	Information on At5g67630 at Entrez (NCBI Cross Database Search)

Human and Yeast Orthologues

Click on the images in the 'Data Sources' column to retrieve further information.
SGD = The *Saccharomyces* Genome Database.

Species	Locus	Description	E Value to Previous	Data Sources
human	RUVBL2	RuvB-like 2 (TIP48 - TATA binding protein interacting protein 48kDa)	0	Entrez
yeast	Rvb2	No Description Available	e-157	SGD Entrez

BLASTx vs Human Nucleolar Proteome

Red highlighting of score column represents low score values.

Arabidopsis Nucleolar Protein Database

id_description	subject_name	Length	score	bits	%	p	matches	Pos	length	IPI
DNA helicase, putative [Arabidopsis thaliana] (469 letters)	>IPI: IPI00009104.1| SWISS-PROT: Q9Y230| REFSEQ_NP: NP_006657| ENSEMBL: ENSP00000221413 Tax_Id=9606 RuvB-like 2	463	1650	640	71	0.0	321	383	450	IPI00009104

Click here to return all BLAST hits

Protein Detail

Protein: AT5G67630.1

Date last modified 2004-05-05

TAIR Accession AASequence:4012777

External IDs

SwissPROT	PIR	GenPept	Similar Proteins in Genbank
Q9FJW0		15240788	NCBI BLink

Properties

Calculated MW	52097.0
Calculated PI	5.2366
Length (aa)	469

Domains

Database	Structural Class Type	Accession	Interpro	Position
prosite		PS50150	RFCdomain	329-411
pfam		PF00004	AAA ATPase_centr	68-412
pfam		PF06068	TIP49, C-terminal	120-433
superfam	Alpha and beta proteins (a/b)	52540		40-106
superfam	Alpha and beta proteins (a/b)	52540		270-444
superfam	Alpha and beta proteins (a/b)	52540		65-231

Sequence

Send to WU-BLAST

```
  1 MAELKLSESR DLTRVERIGA HSHIRGLGLD SALEPRAVSE GMVGQVKARK
 51 AAGVILQMIR EGKIAGRAIL IAGQPGTGKT AIAMGMAKSL GLETPFAMIA
101 GSEIFSLEMS KTEALTQSFR KAIGVRIKEE TEVIEGEVVE VQIDRPASSG
151 VASKSGKMTM KTTDMETVYD MGAKMIEALN KEKVQSGDVI AIDKATGKIT
201 KLGRSFSRSR DYDAMGAQTK FVQCPEGELQ KRKEVVHCVT LHEIDVINSR
251 TQGFLALFTG DTGEIRSEVR EQIDTKVAEW REEGKAEIVP GVLFIDEVHM
301 LDIECFSFLN RALENEMSPI LVVATNRGVT TIRGTNQKSP HGIPIDLLDR
351 LLIITTQPYT DDDIRKILEI RCQEEDVEMN EEAKQLLTLI GRDTSLRYAI
401 HLITAAALSC QKRKGKVVEV EDIQRVYRLF LDVRRSMQYL VEYQSQYMFS
451 EPIKNDEAAA EDEQDAMQI
```

Associated Genes

Gene Model	Locus	seqviewer link
AT5G67630.1	AT5G67630	Sequence Viewer

Protein Detail

External Link The Arabidopsis Subcellular Proteomics Database (ASPD)

User Comments ?
(shows only the most recent comments by default)

Add My Comment | Hide Comments | Show All Comments

Attribution

type	name	date
submitted_by	AGI-TIGR	2001-11-30

NCGR ABRC Carnegie

General comments or questions: curator@arabidopsis.org
Seed or DNA stock questions (donations, availability, orders, etc): abrc@arabidopsis.org

Nucleic Acids Research, 1993, Vol. 21, No. 7 1647–1653

Two cDNAs from the plant *Arabidopsis thaliana* that partially restore recombination proficiency and DNA-damage resistance to *E.coli* mutants lacking recombination-intermediate-resolution activities

Qishen Pang, John B.Hays* and Indira Rajagopal
Department of Agricultural Chemistry and Program in Genetics, Oregon State University, Corvallis, OR 97331-6502, USA

Received August 5, 1992; Revised and Accepted March 3, 1993 GenBank accession nos M98455, M98456

ABSTRACT

Escherichia coli ruvC recG **mutants lack RuvC endonuclease, which resolves crossed-strand joint molecules (Holliday junctions) formed during homologous recombination into recombinant products, and an activity (RecG) thought to partially replace RuvC. They are therefore highly deficient in homologous recombination, and sensitive to UV light and chemical DNA-damaging agents, presumably because of inability to tolerate unrepaired DNA damage by recombinational mechanisms (Lloyd, R.G. (1991) *J. Bacteriol.* 173:5414–5418). We transformed these mutants with plasmids expressing cDNAs from the plant *Arabidopsis thaliana*. Selection for bacteria with increased resistance to methylmethanesulfonate yielded two cDNAs, designated *DRT111* and *DRT112* (DNA-*d*amage-*r*epair/*t*oleration). Expression of these plant cDNAs, especially *DRT111*, restored conjugal recombination proficiencies in *ruvC* and *ruvC recG* mutants to nearly wild-type levels. Both plant cDNAs significantly increased resistance of both mutants to UV light and several chemical DNA-damaging agents, but did not fully correct the mutant phenotypes. Drt111 activity, but not Drt112, also increased, to nearly wild-type levels, resistance of *recG* single mutants to UV plus mitomycin C. The predicted Drt111 and Drt112 polypeptides, 383 and 167 amino acids respectively, show no similarity with one another or with prokaryotic Holliday resolvases. Both appear chloroplast targeted; Drt112 is highly homologous to *Arabidopsis* plastocyanin. *DRT111* and *DRT112* probes hybridize only to DNA from closely related plants.**

INTRODUCTION

Projected depletion of the stratospheric ozone layer is expected to significantly increase terrestrial UV-B irradiation at DNA-damaging wavelengths (1,2). This has heightened interest in the mechanisms by which green plants, which will necessarily be exposed continually to increased UV fluxes, resist DNA-damaging agents. Studies with yeast and, especially with the bacterium *E.coli*, have demonstrated that removal of photoproducts and recombinational toleration of unrepaired DNA lesions are both important resistance mechanisms (3). Excision repair and photoreactivation of UV photoproducts have been described for several plant species, including the model green plant *Arabidopsis thaliana* (4). However, there has been no strong evidence for homologous-recombination-dependent toleration processes, such as daughter-strand- gap filling (5).

The *E.coli* RecA protein mediates homologous pairing and strand exchange during recombination, yielding a crossed-strand intermediate (Holliday junction). Mutants lacking this activity are highly sensitive to DNA damage, as well as recombination-deficient. Recently, we isolated four *Arabidopsis* cDNAs that partially complemented the UV-sensitivity phenotypes of *E.coli* mutants lacking all repair and toleration responses (Pang, Q., Hays, J.B., Rajagopal, I. and Schaefer, T.S., manuscript submitted). One of these, *DRT100* (DNA-*d*amage-*r*epair-*t*oleration) proved to partially complement RecA$^-$ DNA-damage-sensitivity and recombination-deficiency (Rec$^-$) phenotypes (6). The size of the predicted Drt100 protein was similar to that of bacterial RecA proteins, but there was little global homology. Simultaneously, Jagendorf and coworkers (7) isolated an *Arabidopsis* cDNA with considerable *recA* homology by a hybridization approach, but did not test it for activity in *E.coli*. Both Drt100, the putative RecA analog, and the *Arabidopsis* RecA homolog appear to be chloroplast-targeted proteins. The existence of these genes argues strongly for the importance of DNA-damage-toleration processes in plants, at least for chloroplast genomes.

Activities that resolve crossed-strand intermediates into recombinant products have been demonstrated in *E.coli* phages T4 (8) and T7 (9), in *E.coli* itself (10), and in yeast (11–13). The *E.coli* resolvase active in extracts has been identified as the product of the *ruvC* gene (14), purified to homogeneity, and

* To whom correspondence should be addressed

characterized biochemically (15). Surprisingly, *ruvC* mutants are only slightly Rec⁻, but are highly sensitive to UV light and other DNA-damaging agents (16); double mutants, *ruvC recG*, are highly Rec⁻, and even more DNA-damage-sensitive. This suggests that *recG* encodes (or controls) a resolvase-like activity, not readily detectable in crude extracts, that substitutes fairly well for RuvC in conjugal and transductional recombination, but not in DNA-damage toleration. Further evidence for the more demanding nature of the latter process is its requirement for the RuvA and RuvB proteins as well (16).

The lack of amino-acid conservation among the phage and bacterial resolvases (17) suggested that hybridization approaches were not likely to yield the corresponding plant genes. Instead, we have selected for *Arabidopsis* cDNAs that apparently complement *E.coli* RuvC⁻ RecG⁻ phenotypes. The two cDNAs isolated in this way restore recombination nearly to wild-type levels, and increase resistance to DNA-damaging agents.

MATERIALS AND METHODS

Bacteria and bacteriophages

All strains used are derivatives of *Escherichia coli* K-12. Strain AB1157 is wild-type with respect to the markers of interest here (RuvC⁺ Rec⁺ phenotype) and is also F⁻ *thi-1 his-4* Δ(*gpt-proA*) *argE3 thr-1 leuB6 kdgK1 rfbD(?) ara-14 lacY1 galK2 xyl-5 mtl-1 tsx-33 supE44 rpsL31* (18). Isogenic with AB1157, except as indicated, are the RuvC⁻ strain CS85, *ruvC53 eda-51*::Tn*10*, and the RuvC⁻ RecG⁻ strain N3398, *recG258*::Tn*10* mini-*kan ruvC53 eda-51* (19), and the RecG⁻ strain N2731 (20), *recG 258*::Tn*10* mini-*kan*. Strain EG333 is HrfC *pyrA*::Tn*10 mstB cysG303* Δ(*lac-pro*)XIII (21). The vector phage λYES is *cI857*; it incorporates a cloning/expression site and yeast-*E.coli* shuttle-vector-plasmid elements between two phage P1 *lox* sites (25). Phage λCRE *cI*(*ind*⁻) *red3 xis1* overexpresses the P1 Cre protein via a bacterial *lac* promoter (6,25). Neither λYES nor λ CRE *cI*(*ind*⁻) prophages are inducible by DNA-damaging agents.

Plasmids

Plasmid pSE936, the product excised from λYES by Cre-*lox* recombination, encodes ampicillin-resistance and plasmid *ori* elements for selection and propagation in *E.coli*, as well as *URA3* and other elements for function as a yeast plasmid (25). Depending on their orientation, cDNAs inserted at the unique *Xho*I site are transcribable via the bacterial p_{lac} or yeast p_{GAL1} promoters. In plasmids pQP1110 and pQP1120, *Arabidopsis* cDNAs *DRT111* and *DRT112* are transcribed via p_{lac}. Plasmids pQP1112 and pQP1122, in which *DRT111* and *DRT112* are inverted with respect to p_{lac}, were constructed by digestion of plasmids pQP1110 and pQP1120 with *Xho*I endonuclease and re-ligation of the products, and were identified by restriction analysis of plasmids from transformed bacteria.

Media and solutions

TBY-broth, LB-broth-plates, and M9-minimal-plates have been described (26,27). TBY-Ap broth and LB-Ap plates contain 50 μg/ml ampicillin (Ap).

Selection and isolation of *DRT111* and *DRT112* cDNA

We infected about 10^{10} RuvC⁻ RecG⁻ bacteria (strain N3398), lysogenic for λCRE *cI*(*ind*⁻) *red3 xis1*, with an aliquot (5×10^{10} plaque-forming units) of an *Arabidopsis* cDNA library in the vector λYES. This library had been obtained from R. Davis, Stanford University (25) and amplified once, as described previously (6). We grew the infected cells for one hour in TBY broth, at which point there were 5×10^9 total Ap-resistant bacteria (as determined by plating a small aliquot). We selected for cells containing excised plasmids, by growth for three hours in 100 ml TBY-Ap broth, plus 2 mM isopropylthio-β-D-galactopyranoside (IPTG), yielding about 10^{11} bacteria. These were harvested by centrifugation and resuspended in 10 ml TBY. We spread the entire culture on twenty LB plates containing 0.06% methylmethane-sulfonate (MMS) and IPTG, and incubated them 40 h at 30°C. Although none of 10^{11} bacteria in a parallel N3398(pSE936) culture survived on these plates, the cDNA-library-containing culture yielded 25 survivors. These were streaked across LB plates and tested for resistance to 5, 10, 15, and 20 J/m² of UV light. Four isolates were UV-resistant, and plasmids extracted from each of these conferred resistance upon naive RuvC⁻ RecG⁻ bacteria. When digested with *Eco*RI endonuclease, one active plasmid released insert fragments of about 1.1 kb and 0.3 kb; we designated the cDNA as *DRT111*. The other three plasmids released 0.8-kb inserts; based on their apparently identical sizes, and complementation phenotypes in preliminary experiments (data not shown), we designated all three cDNAs as *DRT112*, and arbitrarily picked one for further study. (Their identity was subsequently confirmed by DNA sequence determinations.) We designated the respective plasmids pQP1110 and pQP1120.

Measurement of bacterial resistance to DNA-damaging agents

Cells were grown to late log phase in TBY-Ap broth containing IPTG, harvested by centrifugation, and resuspended to 1.5×10^8 colony-forming units (CFU) per ml, as described (6). Cell suspensions were treated with 254-nm UV light at a rate of 1 w/m² and spread on LB-Ap plates, or spread on LB-Ap plates containing mitomycin C or methylmethanesulfonate (MMS) or 4-nitroquinoline-N-oxide (NQO). All manipulations were performed under room lighting, so that all cells were phenotypically Phr⁺. Plates were incubated overnight at 30°C.

Measurement of conjugal recombinant frequencies

Procedures were essentially as described by Miller (27). Overnight cultures of the donor strain (EG333), grown in TBY broth containing tetracycline (12.5 μg/ml), and of recipient strains harboring various plasmids, grown in TBY-Ap broth with or without 2mM IPTG, were subcultured in fresh broth, grown to about 2×10^9 cells per ml, mixed at a ratio of three donors to one recipient, and incubated at 37°C. After 1 hr we stirred mixtures vigorously, harvested the cells by centrifugation, and resuspended them in one volume of 0.01M $MgSO_4$. After 30 min at room temperature, cells were spread on LB-Ap plates and incubated overnight at 37°C, to score total recipient colony-forming units, or spread on M9-glucose-minimal plates containing ampicillin (50 μg/ml), histidine (0.5 mM), arginine (0.06 mM), and proline (2 mM), to score Ap-resistant Leu⁺ Thr⁺ recombinants, or on M9-galactose-(casamino acids) plates containing ampicillin to score Ap-resistant Gal⁺ recombinants, or on M9-glucose-minimal plates containing arginine (0.06 mM), histidine (0.5 mM), proline (2 mM), ampicillin and 13 μg per ml tetracycline (Tc) to score Ap-resistant (Leu⁺ Thr⁺) recombinants.

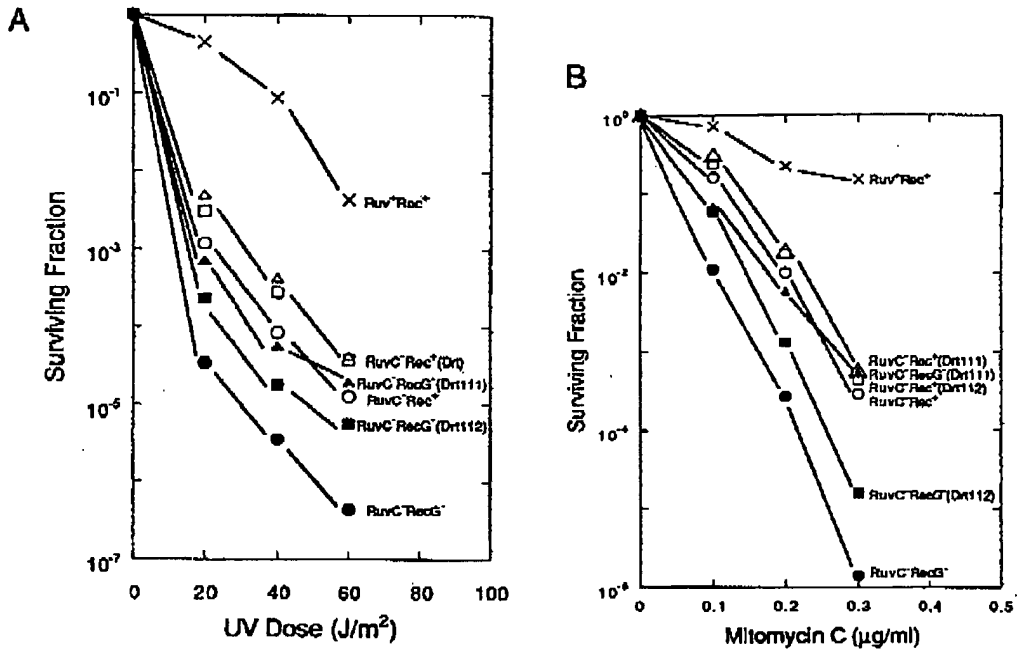

Figure 1. Resistance to DNA-damaging agents of bacteria expressing Drt111 and Drt112. Indicated bacteria were (A) irradiated with 254-nm UV light to fluences indicated, or (B) spread on plates containing indicated mitomycin C concentrations, and surviving bacteria scored, as described under 'Materials and Methods'. Surviving fraction equals CFU surviving divided by CFU on LB-Ap plates (no UV). Strains [phenotypes] employed: (×), AB1157 (pSE396) = [Ruv⁺ Rec⁺]; (○), CS85 (pSE396) [= RuvC⁻ Rec⁺]; (△), CS85 (pQP1110) = [RuvC⁻ Rec⁺(Drt111)]; (□), CS85 (pQP1120) = [RuvC⁻ Rec⁺(Drt112)]; (●), N3398 (pSE396) = [RuvC⁻ RecG⁻]; (▲), N3398 (pQP1110) = [RuvC⁻ RecG⁻(Drt111)]; (■), N3398 (pQP1120) = [RuvC⁻ RecG⁻(Drt112)]. Data correspond to averages for two trials. Standard deviations were generally less than symbol sizes and were almost always 10% of values shown or less.

Determination and analysis of DNA sequences

The Oregon State University Central Services Laboratory determined DNA sequences on double-stranded DNA by an automated technique, using an Applied Biosystems Model 373A DNA sequencer and a Taq Dye Primer Cycle Sequencing Kit, with dideoxy chain termination, thermal cycling and primer-coupled dyes, according to instructions supplied by the manufacturer (bulletin No. 237605). M13mp*lac* Universal and Reverse primers (United States Biochemical Corp.) and internal primers were employed. For each sample, sequences were determined in both directions at least once each. In some regions we also determined DNA sequences manually, by dideoxy sequencing of duplex DNA using a Sequenase kit (United States Biochemical Corp). We compared the predicted amino-acid sequences for Drt111 and Drt112 to protein sequences in the SWISSPROT data base, using Intelligenetics Suite release 5.4 programs QUEST, PEP, SEQ, and GENALIGN. The last program, developed by Dr. H. Martinez, is a copyrighted product of Intelligenetics, Inc. We searched GENBANK release 69, and NBRFPIR and EMBL protein-sequence libraries using the Intelligenetics FASTDB search program.

Hybridization analyses

DNA was extracted from *Arabidopsis*, broccoli and cabbage (*Brassica pekinensis*) tissues as described (4). DNA from bean (*Phaseolus vulgaris*) and maize (*Zea mays*) were gifts respectively of David Mok and Carol Rivin, Oregon State University. DNA digested with *Eco*RI endonuclease was analyzed by electrophoresis, blotting, hybridization with a [^{32}P]-labeled [random-primer-method (28)] *Eco*RI fragment isolated from plasmids QP1111 and pQP1121, and autoradiography, as described (29), with minor modifications. Hybridization, at 37°C, employed solutions containing 50% formamide and 0.6 M salt. Reduced-stringency hybridization employed 32% formamide. Aqueous washes (0.03 M salt) were at 37°C; filters were autoradiographed for 48 hr.

RESULTS

Selection and isolation of cDNAs

E.coli ruvC recG bacteria lack activities that resolve recombination intermediates (Holliday junctions), and therefore are deficient in homologous recombination (Rec⁻) and DNA-damage-toleration functions (19). We established an *Arabidopsis* cDNA plasmid expression library in RuvC⁻ RecG⁻ bacteria harboring a λCre prophage, by infecting 10^{10} cells of strain N3398 with a phage λYES *Arabidopsis* cDNA library, at a multiplicity of 5 phage per cell. The endogenous Cre activity expressed by the λCre prophage (25) excised plasmids from the λYES phage via site-specific recombination at the *lox* sites in λYES; plasmids were established in about 50% of the bacteria.

We amplified cDNA-plasmid-containing bacteria and plated them in the presence of 0.06% methylmethanesulfonate, a concentration which killed all non-cDNA-containing bacteria, and

Table I. Effects of Drt111 and Drt112 on resistance of *E.coli* mutants to UV light

Relevant bacterial (plasmid) phenotype[a]	Relative survival (%) after indicated UV fluences (J/m²)[b]		
	20	40	60
Ruv⁺ Rec⁺ (none)	(100)	(100)	(100)
Ruv⁺ RecA⁻ (none)	0.3	0.05	0.05
Ruv⁺ RecA⁻ (Drt111)	0.4	0.05	0.05
Ruv⁺ RecA⁻ (Drt112)	0.4	0.06	0.05
Ruv⁺ RecB⁻C⁻F⁻ (none)	0.2	0.08	0.05
Ruv⁺ RecB⁻C⁻F⁻ (Drt111)	0.2	0.08	0.08
Ruv⁺ RecB⁻C⁻F⁻ (Drt112)	0.3	0.07	0.06
RuvC⁻ RecG⁻ (none)	0.1	0.01	0.03
RuvC⁻ RecG⁻ (Drt111)	2.7	0.16	0.67
RuvC⁻ RecG⁻ (Drt112)	1.4	0.06	0.27

[a]Respective bacterial strains (plasmids) employed, lines 1 through 10, were AB1157 (pSE936), QP3070(pSE936), QP3070(pQP1110), QP3070(pQP1120), JH312(pSE936), JH312(pQP1110), JH312 (pQP1120), N3398 (pSE936), N3398 (pQP1120), N3398 (pQP1120).
[b]Fractions of bacterial suspensions surviving indicated UV doses were measured as described under 'Materials and Methods,' and divided by surviving fractions for Ruv⁺ Rec⁺ (none) bacteria. These latter values (relative survival of 100%) were 0.32 at 20 J/m², 0.043 at 40 J/m², and 0.0027 at 60 J/m². Data correspond to averages for two plates (range typically ± 10%).

we tested the 25 survivors for resistance to 10–30 J/m² UV light. All four UV-resistant isolates harbored plasmids containing putative cDNA inserts—one of 1.4 kb, three of 0.8 kb. On the basis of the apparent identity of size and correction activity (see below) of the latter three cDNAs, we identified two unique DNA-damage-repair/toleration cDNAs, *DRT111* and *DRT112*. We tested these for their effect on various DNA-damage-sensitivity and recombination-deficiency phenotypes of *E.coli ruvC*, *ruvC recG*, and *recG* mutants.

Partial correction of DNA-damage-sensitivity phenotypes by Drt111 and Drt112

We measured the effect of Drt111 and Drt112 activity on the resistances, to ultraviolet light (Fig. 1A) and to the DNA-crosslinking agent mitomycin C (Fig. 1B), of RuvC⁻ single and RuvC⁻ RecG⁻ double mutants. Drt111 and Drt112 increased the resistance to UV light of both RuvC⁻ single mutants (Fig. 1A, open symbols) and RuvC⁻ RecG⁻ double mutants (filled symbols). Although the factors by which survival was increased were greater for the double mutants, apparent correction efficiencies relative to wild-type resistance ranged from 0.1% to 1%. Resistance of RuvC⁻ and RuvC⁻ RecG⁻ bacteria to mitomycin C (Fig. 1B; open, filled symbols) was also increased by the presence of Drt111 and Drt 112. Here resistances were increased by as much as 400-fold [RuvC⁻ RecG⁻ (Drt111) at 0.3 μg/ml], and apparent correction efficiencies were as high as 10 to 40% (at 0.1 μg/ml). The two plant cDNAs also increased resistance to methylmethanesulfonate, at concentrations of 0.015 to 0.045%, by factors of about 2-fold for RuvC⁻ and up to 20-fold for RuvC⁻ RecG⁻ mutants, corresponding to complementation efficiencies of 0.1% or less; resistance of RuvC⁻ RecG⁻ mutants to 10 μM nitroquinoline oxide was increased 7-fold by Drt111 and 3-fold by Drt112 (data not shown).

Drt111 and Drt112 might partially correct the DNA-damage-sensitive phenotypes of RuvC⁻ RecG⁻ bacteria by resolving intermediates generated by normal (RecA-dependent) *E.coli* recombinational toleration processes, or suppress the phenotypes, by mediating new repair or recombinational toleration pathways that did not require RuvC or RecG function, for example. We tested the ability of plasmids expressing Drt111 or Drt112 to increase the resistance of other Rec⁻ mutants to UV light (Table I). Under conditions where Drt 111 and Drt112 significantly increased survival of RuvC⁻ RecG⁻ bacteria (Table I, lines 8–10), there was no effect on survival of RecA⁻ (lines 2–4) or RecB⁻C⁻F⁻ (lines 5–7) bacteria.

We also tested for correction of Rec G⁻ single mutations, using the UV-plus-mitomycin-C assay of Lloyd and Buckman (20) (Table II). RecG⁻ (Drt111) bacteria were about half as resistant as wild-type, but RecG⁻ (Drt112) bacteria were not significantly more resistant than RecG⁻.

Table II. Resistance of RecG⁻ mutants expressing Drt111 or Drt112 to UV light plus mitomycin C.

Relevant bacterial (plasmid) phenotype[a]	Survival (%) of bacteria treated as indicated	
	UV only	UV plus mitomycin C
Rec⁺ (none)	15 ± 2	13 ± 0.5
RecG⁻ (none)	1.7 ± 0.3	0.26 ± 0.13
RecG⁻ (Drt111)	8.5 ± 0.7	6.1 ± 0.7
RecG⁻ (Drt112)	2.7 ± 0.2	0.45 ± 0.06

[a]Respective strains (plasmids) employed, lines 1 through 4, were AB1157 (pSE936), N2731 (pSE936), N2731 (pQP1110), N2731 (pQP1120).
[b]Bacteria were grown in broth containing ampicillin and IPTG, treated with 30 J per m² UV light, as described under 'Materials and Methods,' spread on LB plates with or without 0.2 μg per ml mitomycin C (20), and incubated overnight. Data represent averages for two trials (two plates per trial), with ranges indicated.

Table III. Conjugal recombinant frequencies

Relevant bacterial (plasmid) phenotype of recipients[a]	Number of recipients (CFU/ml × 10⁻⁷)[b]	Number of Thr⁺ Leu⁺ Ap^r recombinant (CFU/ml × 10⁻⁷)[b]	Relative recombinant frequency[c]
Rec⁺ Ruv⁺ (none)	35 ± 4	5.6 ± 0.6	(1.0)
Rec⁺ RuvC⁻ (none)	32 ± 4	1.0 ± 0.4	0.21
Rec⁺ RuvC⁻ (Drt111)	21 ± 2	2.5 ± 0.2	0.75
Rec⁺ RuvC⁻ (Drt112)	24 ± 2	1.7 ± 0.2	0.44
RecG⁻ RuvC⁻ (none)	37 ± 2	0.019 ± 0.004	0.003
RecG⁻ RuvC⁻ (Drt111)	38 ± 6	0.67 ± 0.02	0.110
RecG⁻ RuvC⁻ (Drt112)	44 ± 8	0.41 ± 0.7	0.058

[a] Respective recipient bacterial strains (plasmids) employed lines 1 to 7, were: 1), AB1157 (pSE936), CS85 (pSE936), CS85 (pQP1110), CS85 (pQP1120), N3398 (pSE936), N3398 (pQP1110), N3398 (pQP1120).
[b] Conjugal matings and measurements of total recipients and Ap-resistant Thr⁺ Leu⁺ transconjugants were performed as described under 'Materials and Methods'. Hfr donor was strain EG333. Data are averages and standard deviations for two trials.
[c] Relative recombinant frequency equals ratio of recombinant frequency to recipient frequency for indicated bacteria, divided by ratio for Rec⁺ Ruv⁻ bacteria.

Correction of recombination deficiencies

Although Drt111 and Drt112 both significantly increased the resistance of both RuvC⁻ and RuvC⁻ RecG⁻ mutants to a variety of DNA-damaging agents, the apparent correction efficiencies were only several percent or less, in all but a few cases. Furthermore, these data provide no direct evidence that recombination-enhancing activities are involved. Therefore, we tested the effects of Drt111 and Drt112 on a bacterial

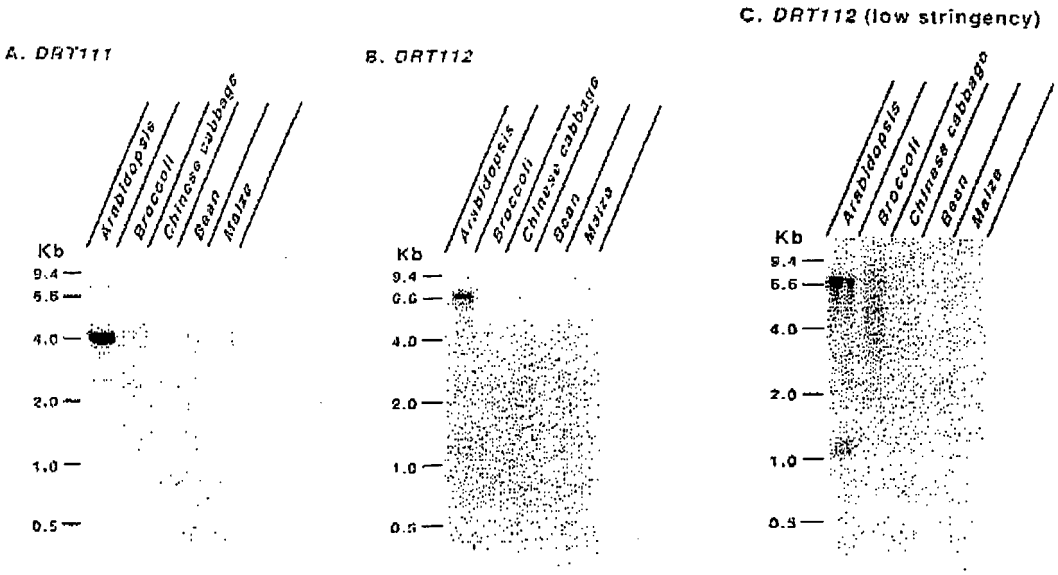

Figure 2. Hybridization of *DRT111* and *DRT112* cDNAs to plant DNA. Lanes contain DNA from *Arabidopsis* leaves and stems (5 μg), broccoli florets (10 μg), Chinese cabbage (*Brassica pekinensis*) leaves (10 μg), bean (*Phaseolus vulgaris*) seedlings (10 μg), and whole maize (*Zea mays*) plants (10 μg). Extraction of DNA, digestion with *Eco*RI endonuclease and hybridization were as described under 'Materials and Methods'. A. *DRT111* probe. B. *DRT112* probe. C. *DRT112* probe at low stringency.

recombination process. Homologous recombination is needed for formation of stable transconjugants during mating of Hfr and F⁻ bacteria. Although *recA* mutations drastically reduce conjugal recombination frequencies (30), a single *ruvC* mutation in a wild-type background reduces recombination only 5-fold [ref. (19) and Table I, line 2], perhaps because recombination intermediates are resolved in other ways. Drt111 and Drt112 corrected this RuvC⁻ phenotype, restoring recombination to nearly wild-type levels in the former case (Table III, lines 3,4). The recombinant frequency in *ruvC recG* double mutants is drastically reduced, to just 0.3% of wild-type levels (Table III, line 5). Here Drt111 increased the frequency 32-fold, to 11% of wild-type levels (about half the restoration by RecG alone), and Drt112 was slightly less effective (Table III, lines 6,7).

Neither Drt111 nor Drt112 corrected recombination deficiencies in other Rec⁻ mutants tested: The frequency of tetracycline-resistant transconjugants, in matings of the Hfr *pyrA*::Tn*10* strain EG333 with RecA⁻ and RecB⁻C⁻F⁻ recipients, were reduced respectively to 0.01% and 1% of *rec*⁺ levels, in the presence or absence of *DRT111* or *DRT112* (data not shown); in parallel experiments Drt111 and Drt112 increased recombinant frequencies in RuvC⁻ RecG⁻ bacteria from 0.17% of wild-type frequencies to 7.4% and 2.5%, respectively. Neither Drt111 nor Drt112 affected the efficiency of transfer of conjugal F′ episomes in any bacteria tested [Rec⁺, RecA⁻, RecB⁻F⁻ and RuvC⁻ RecG⁻ (data not shown)], i.e. the apparent increases in recombinant frequency are not due to increased mating efficiencies in the presence of Drt111 or Drt112.

To determine whether correction of the RuvC⁻ RecG⁻ recombination deficiency required expression of *DRT111* and *DRT112*, rather than being the result, for example, of induction of new *E.coli* activities by the presence of the plant DNA sequences themselves, we measured requirements for transcription (Table IV). Neither *DRT111* nor *DRT112*, when inverted with respect to the plasmid P_{lac} promoter, showed any correction activity (Table IV, lines 4, 6). In the absence of induction by IPTG, the activity of P_{lac}-transcribed *DRT111* and *DRT112* sequences was decreased but still significant (Table IV, lines 3, 5), presumably because multiple copies of the *lac* operator titrated out endogenous levels of even *lacI*ᵠ-expressed *lac* repressor (31).

Table IV. Effects of gene orientation and induction of expression on activity of *DRT111* and *DRT112* in recombination-deficient bacteria

Bacterial (plasmid) phenotype of recipient[a]	Frequency (%) of Ap^r Gal$^+$ transconjugants per recipient[b]	
	IPTG-induced	no IPTG
Ruv$^+$ Rec$^+$ (none)	5.0	6.2
RuvC$^-$ RecG$^-$ (none)	0.008	0.006
RuvC$^-$ RecG$^-$ (Drt111)	0.462	0.080
RuvC$^-$ RecG$^-$ (Drt111 INV)	0.008	0.008
RuvC$^-$ RecG$^-$ (Drt112)	0.180	0.060
RuvC$^-$ RecG$^-$ (Drt112 INV)	0.008	0.007

[a]Respective bacterial strains (plasmids) employed, lines 1 to 6, were AB1157 (pSE936), N3398 (pSE936), N3398 (pQP1110), N3398 (pQP1112), N3398 (pQP1120), N3398 (pQP1122).
[b]Conjugal matings, with EG333 as Hfr donor and scoring for Ap^r Gal$^+$ recombinants, were performed as described under 'Materials and Methods.' Data correspond to average for two plates; range was less than ± 10% in almost all cases.

DNA and protein sequence analyses

DNA and predicted protein sequences for *DRT111* and *DRT112* are available via GENBANK access numbers M98455 and

M98456, respectively. We used the Intelligenetics FAST DB program to search protein sequences in the GENBANK, NBRFPIR, and EMBL libraries for amino-acid-sequence similarities. The *DRT111* open reading frame predicts a 383-residue polypeptide without significant global similarity to any known protein, including the prokaryotic Holliday-junction resolvases—phage T4 gene *49* protein (32), phage T7 gene *3* protein (9), *E.coli* RuvC (17) and RecG proteins (16)—and the yeast cruciform-cutting enzyme (33). However, the Drt111 amino-acid sequence Q_{225}GqGlGKS strongly resembles the RecG sequence QGdvGsGKT (16), and thus the nucleotide binding motif (Walker box) GxxGxGKS (34) characteristic of many ATP-hydrolyzing DNA repair and recombination proteins. Surprisingly, the predicted Drt112 polypeptide, 167 amino acids, is 75% identical with *Arabidopsis* plastocyanin (35). The homology extends over most of the sequences, except for nine plastocyanin residues between Drt112 amino acids 24 and 27. Drt112 shows no significant homology with any other proteins in the data bank, or with other resolvases. The N-terminal portions of both polypeptides show features characteristic of chloroplast transit peptides (36): high frequency of serine and threonine residues, large numbers of small hydrophobic amino acids, net positive charge. We did not find a consensus chloroplast processing site (36,37) in Drt111, but the plastocyanins (35) are cleaved at a sequence that ends in Drt112 at amino acid 68. The apparent chloroplast-targeting domain of Drt111 occupies about 90 N-terminal residues.

Hybridization of *DRT111* and *DRT112* probes to plant DNA

We hybridized, at high stringency, *DRT111* and *DRT112* probes to bulk DNA from *Arabidopsis*, the closely related *Brassicaceae* broccoli and Chinese cabbage, and from bean and the monocot plant maize (Fig. 2). The *DRT111* probe hybridized strongly to DNA from *Arabidopsis* and very weakly to broccoli DNA, but not to DNA from other plants (Fig. 2A). At high stringency, the *DRT112* probe yielded only a single strong DNA signal (Fig. 2B) which presumably corresponds to *DRT112* itself. The additional two lower-molecular-weight bands that appear at lower stringency may correspond to the *Arabidopsis* plastocyanin gene (35), which encodes an *EcoRI* restriction site not in the *DRT112* sequence. Vorst *et al.* (35) detected only a single (intron-less) plastocyanin gene by hybridization analysis. Thus, despite the high degree of homology, the nucleotide differences (about 30%) apparently prevent *DRT112*-plastocyanin hybridization at high stringency.

DISCUSSION

We have isolated two *Arabidopsis* cDNAs that appear to increase recombinant progeny in conjugal crosses involving *E.coli* mutants lacking ability to resolve intermediates (Holliday structures). These cDNAs were originally selected by virtue of their ability to promote survival of *ruvC recG* mutants, on plates containing methylmethanesulfonate (MMS), but they proved to significantly increase resistance to other DNA-damaging agents as well. We have considered three explanations, other than genuine complementation—replacement of RuvC or RecG resolution activities—for these observations. Informational suppression can be ruled out: *recG258*, which is strongly corrected by *DRT111*, is an insertion mutation; the *ruvC53* allele encodes a highly temperature-sensitive but full-length protein (R. Lloyd, personal communication). Second, the requirement for P_{lac}-initiated transcription of *DRT111* and *DRT112* excludes the possibility that either DNA sequence in and of itself provokes a phenotype-suppressing response in *E.coli*. Third, the inability of Drt111 or Drt112 to promote conjugal recombination or UV-resistance in *E.coli recA* or *recB recC recF* mutants argues strongly against the notion that either activity mediates a novel recombination pathway that does not depend on resolution via RuvC or RecG activity.

Correction efficiencies, for *DRT111* and *DRT112* relative to wild-type cells, were high for conjugal recombination (9–70% and 4–25%, respectively), for resistance to lower levels of mitomycin C (10–40% and 3–10% respectively), and for complementation by Drt111 of RecG$^-$ DNA-damage sensitivity (50%). Efficiencies were less for higher degrees of damage. These trends may reflect saturation, by high amounts of DNA damage, of activities limited by lack of bacterial translation signals, poor codon usage, RNA instability or protein instability, or insolubility in *E.coli*, or the presence of activity-inhibiting chloroplast processing signals on the Drt111 and Drt112 polypeptides. In fact, in experiments in which proteins were radiolabeled in *E.coli* 'mini-cells', neither Drt111-encoding nor Drt112-encoding plasmids yielded detectable bands of the appropriate molecular weight (Q. Pang, unpublished results). The correction patterns thus suggest that activities able to efficiently resolve a few conjugal-recombination intermediates, despite low intrinsic biochemical proficiency and/or low levels of expression, may not be able to deal with large numbers of intermediates arising during DNA-damage-provoked sister-chromatid exchange.

Drt111 and Drt112 differ in the sequences and length of their polypeptides, their apparent efficiencies for complementation of RuvC$^-$ and RuvC$^-$ RecG$^-$ phenotypes, and in the ability of Drt111, but not Drt112, to efficiently complement a RecG$^-$ phenotype. The molecular weight of Drt111, 42 kDa, falls between those of RecG, 76 kD (16) and RuvC and the phage T7 and T4 resolvases, 17–19 kDa (8–10). Drt112 is highly similar to *Arabidopsis* plastocyanin (35), a nuclear-encoded chloroplast protein that participates in electron transfer between photosystem I and the cytochrome *b/f* complex. If Drt112 is processed at the same site at which plastocyanin is thought to be cleaved in the chloroplast (35), the putative nature Drt112 protein (amino acids 69–167), would have a molecular weight of only 11 kDa, significantly less than those of the RuvC/phage resolvases. The Drt112-plastocyanin similarity is reminiscent of the similarity in between respiratory-chain NADH dehydrogenase and a protein that binds to the chloroplast DNA replication origin (38).

E.coli appears to process recombination intermediates, such as Holliday structures, in two steps, by at least two pathways. The bacterial RuvA and RuvB proteins together recognize Holliday junctions and catalyze ATP-dependent branch migration (39,40,41); RecG alone efficiently accomplishes both these tasks (42). Both RuvAB and RecG activities resolve Holliday junctions in short linear model substrates, simply via branch migration out to the ends. However, resolution of such intermediates in chromosomes would require that the migrating junctions encounter preexisting DNA strand nicks, or be cleaved by resolving endonucleases. The RuvC protein is one such resolvase (10,14). Since RuvC$^-$ (and RuvA$^-$ or RuvB$^-$ mutants) are only slightly recombination-deficient (19), yet RecG does not appear to cleave Holliday junctions (42), there may another, as yet unidentified, *E.coli* resolvase that cleaves junctions recognized

by RecG. Preference of the RuvC resolvase for RuvAB-bound Holliday junctions has not been demonstrated (39,40,41). However, the indistinguishability of RuvA$^-$, RuvB$^-$, and RuvC$^-$ phenotypes (19) suggests that these proteins, which are encoded by three nearly contiguous genes (17), may act cooperatively *in vivo*. Ruv$^-$ mutants are much more sensitive to DNA damage than RecG$^-$ mutants, although both classes of mutants are only slightly recombination-deficient (19). This suggests that the Ruv and RecG pathways are nearly, but not perfectly, interchangeable for conjugal recombination, but that the Ruv proteins are designed to play the predominant role in recombinational toleration of DNA damage.

How might the *Arabidopsis* Drt activities identified here relate to these *E.coli* functions? Drt111 is slightly more than half the size of RecG. However, both proteins exhibit a nucleotide binding site, recombination frequencies in RuvC$^-$RecG$^+$ and RuvC$^-$RecG$^-$ (Drt111) bacteria are similar (Table III), and Drt111 efficiently corrects RecG$^-$ phenotypes, despite its apparently low level of expression. Although Drt111 may thus serve as a RecG analog, Drt112 does not correct RecG$^-$ phenotypes. The pattern of correction, by apparently limited amounts of Drt112, of RuvC$^-$ and RuvC$^-$RecG$^-$ phenotypes is not inconsistent with partial replacement of the RuvC endonuclease, but such an identification requires further study, *in vitro* as well as *in vivo*. The lack of extensive similarity among all proteins thus far implicated in resolution of recombination intermediates—Drt111, Drt112, the *E.coli* Ruv and RecG proteins, and the phage T4 and T7 resolvases—suggests that various organisms have recruited a wide variety of proteins to mediate this process. The validity of these speculations remains to be tested, by biochemical studies with purified Drt111 and Drt112 proteins.

The two *Arabidopsis* RecA homologs/analogs described previously (6,7), and the apparent plant resolution proteins described here, incorporate putative chloroplast transit peptides. This suggests that recombinational toleration is an important feature of resistance of chloroplasts to DNA damage.

ACKNOWLEDGEMENTS

We gratefully acknowledge automated determinations of DNA sequences by Ann-Marie Girard, OSU Gene Center Central Services Laboratory, and donation of bacterial strains by Dr. Robert Lloyd, University of Nottingham. We thank Judith Hays for preparation of drawings, Denise Pratt and Cindy Alexander for word processing, and Dr. Walt Ream for suggestions for improvement of the manuscript. This work was supported by competitive grant No. 90-37280-5597 from the U.S. Department of Agriculture. This is research report No. 10093 from the Oregon Agricultural Experiment Station.

REFERENCES

1. Brasseur, G.P. (1991) *Nature*, 352:668–669.
2. Green, A.E.S., Cross, K.R., and Smith, L.A. (1980) *Photochem. Photobiol.*, 31:59–65.
3. Friedberg, E.C. (1985), In:*DNA Repair*, W.H. Freeman and Co., New York, pp. 459–497.
4. Pang, Q. and Hays, J.B. (1991) *Plant Physiol.*, 95:536–543.
5. Rupp, W.D. and Howard-Flanders, P. (1968) *J. Mol. Biol.*, 31:291–304.
6. Pang, Q., Hays, J.B., and Rajagopal, I. (1992) *Proc. Natl. Acad. Sci. USA*, 89:8073–8077.
7. Cerutti, H., Osman, M., Grandoni, P., and Jagendorf, A.T. (1992) *Proc. Natl. Acad. Sci. USA*, 89:8068–8072.
8. Mizuuchi, K., Kemper, B., Hays, J., and Weisberg, R.A. (1982) *Cell*, 29:357–365.
9. de Massey, B., Weisberg, R.A., and Studier, F.W. (1987) *J. Mol. Biol.*, 193:359–376.
10. Connolly, B. and West, S.C. (1990) *Proc. Natl. Acad. Sci. USA*, 87:8476–8480.
11. West, S.C. and Korner, A. (1985) *Proc. Natl. Acad. Sci. USA*, 82:6445–6449.
12. Symington, L.S. and Kolodner, R. (1985) *Proc. Natl. Acad. Sci. USA*, 82:7247–7251.
13. Jensch, F., Kosuk, H., Seeman, N.C., and Kemper, B. (1989) *EMBO J.*, 8:4325–4334.
14. Connolly, B., Parsons, C.A., Benson, F.E., Dunderdale, H.J., Sharples, G.J., Lloyd, R.G., and West, S.C. (1991) *Proc. Natl. Acad. Sci. USA*, 88:6063–6067.
15. Dunderdale, H.J., Benson, F.E., Parsons, C.A., Sharples, G.J., Lloyd, R.G., and West, S.C. (1991) *Nature*, 354:506–510.
16. Lloyd, R.G. and Sharples, G.J. (1991) *J. Bacteriol.*, 173:6837–6843.
17. Sharples, G.J. and Lloyd, R.G. (1991) *J. Bacteriol.*, 173:7711–7715.
18. Bachmann, B. (1972) *Bacteriol. Rev.*, 36:525–557.
19. Lloyd, R.G. (1991) *J. Bacteriol.*, 173:5414–5418.
20. Lloyd, R.G. and Buckman, C. (1991) *J. Bacteriol.* 173:1004–1011.
21. Laufer, C.S., Hays, J.B., Windle, B.E., Schaefer, T.S., Lee, E., Hays, S.L., and McClure, M.R. (1989) *Genetics*, 123:465–476.
22. Smith, T.A.G. and Hays, J.B. (1985) *Mol. Gen. Genet.*, 201:393–401.
23. Biek, D.P. and Cohen, S.N. (1986) *J. Bacteriol.* 167:594–603.
24. Bullock, M.O., Fernandez, J.M. and Short, J.M. (1987) *Biotechniques*, 5:376–379.
25. Elledge, S.J., Mulligan, J.T., Ramer, S.W., Spottswood, M., and Davis, R.W. (1991) *Proc. Natl. Acad. Sci. USA*, 88:1731–1735.
26. Hays, J.B., Martin, S.J., and Bhatia, K. (1985) *J. Bacteriol.*, 161:602–608.
27. Miller, J.H. (1972) *Experiments in molecular genetics*, Cold Spring Harbor Laboratory, Cold Spring Harbor, New York.
28. Feinberg, A.P. and Vogelstein, B. (1983) *Anal. Biochem.*, 132:6–13.
29. Wahl, G.M., Meinkoth, J.L., and Kimmel, A.R. (1987) Northern and Southern blots, In:*Methods In Enzymology*, (Berger, S.L. and Kimmel, A.R., eds.). Academic Press, New York, pp. 580–581.
30. Clark, A.J. (1971) *Ann. Rev. Microbiol.*, 25:437–464.
31. Zagursky, R.J. and Hays, J.B. (1983) *Gene*, 23:277–292.
32. Barth, K.A., Powell, D., Trupin, M., and Mosig, G. (1988) *Genetics*, 120:329–343.
33. Kleff, S., Kemper, B., and Sternglanz, R. (1992) *EMBO J.*, 11:699–704.
34. Walker, J.E., Saraste, M., Runswick, M.J. and Gay, N.J. (1982) *EMBO J.* 1:945–951.
35. Vorst, O., Oosterhoff-Teertstra, P., Vankan, P., Smeekens, S. and Weisbeek, P. (1988) *Gene*, 65:59–69.
36. Keegstra, K., Olson, L.J., and Theg, S.M. (1989) *Annu. Rev. Plant Physiol. Plant Mol. Biol.*, 40:471–501.
37. Gavel, Y. and von Heijne, G. (1990) *FEBS Lett.* 261:455–458.
38. Wu, M., Nie, Z.Q. and Yang, J. (1989) *The Plant Cell*, 1:551–557.
39. Shiba, T., Iwasaki, H., Nakata, A. and Shinagawa, H. (1991) *Proc. Natl. Acad. Sci. USA* 88:8445–8449.
40. Parsons, C.A., Tsaneva, I., Lloyd, R.G. and West, S.C. (1992) *Proc. Natl. Acad. Sci. USA* 89:5452–5456.
41. Tsaneva, I.R., Müller, B. and West, S.C. (1992) *Cell* 69:1171–1180.
42. Lloyd, R.G. and Sharples, G.J. (1993) *EMBO J.* 12:17–22.